HAWASSA UNIVERSITY

INSTITUTE OF TECHNOLOGY, FACULTY OF BIO-SYSTEMS AND WATER RESOURCES ENGINEERING, DEPARTMENT OF WATER RESOURCES AND HYDRAULIC ENGINEERING

ASSESSMENT OF GROUND WATER POTENTIAL OF DEME WATERSHED, MIDDLE OMO-GIBE BASIN, ETHIOPIA

M Sc. THESIS

BY

YONAS HAILU WASE

HAWASSA UNIVERSITY, HAWASSA, ETHIOPIA

AUGUST, 2023

ASSESSMENT OF GROUND WATER POTENTIAL OF DEME WATERSHED, MIDDLE OMO-GIBE BASIN, ETHIOPIA

YONAS HAILU WASE

A THESIS SUBMITTED TO THE

DEPARTMENT OF WATER RESOURCES AND HYDRAULIC ENGINEERING

HAWASSA UNIVERSITY INSTITUTE OF TECHNOLOGY

SCHOOL OF GRADUATE STUDIES

HAWASSA UNIVERSITY

HAWASSA, ETHIOPIA

IN PARTIAL FULFILLMENT OF THE

REQUIREMENTS FOR THE

DEGREE OF

MASTERS OF SCIENCE IN WATER RESOURCES AND HYDRAULIC ENGINEERING.

SPECIALIZATION: HYDRAULICS AND WATER RESOURCE ENGINEERING.

AUGUST, 2023

SCHOOL OF GRADUATE STUDIES

HAWASSA UNIVERSITY

EXAMINERS APPROVAL SHEET

We the undersigned, members of the Board of Examiners of the final master's degree open defense by **Yonas Hailu Wase** have read and evaluated his/her thesis entitled **"ASSESSMENT OF GROUND WATER POTENTIAL OF DEME WATERSHED, MIDDLE OMO-GIBE BASIN, ETHIOPIA"**, and examined the candidate. This is, therefore to certify that the thesis has been accepted in partial fulfillment of the requirements for the degree of master's science.

Dr.Sirak Tekleab(Phd)		**17/08/2023**
Name of Major Advisor	Signature	Date
Dr.Miret Dananto		
Name of Internal Examiner-I	Signature	Date
Gonse Amelo(Msc)		
Name of Internal Examiner-II	Signature	Date
Dr.Sisay Demeku (PhD)		**20/08/2023**
Name of External Examiner	Signature	Date
Name of school head	Signature	Date
SGS Approval	Signature	Date

SCHOOL OF GRADUATE STUDIES

HAWASSA UNIVERSITY

ADVISORS APPROVAL SHEET

This is to certify that the thesis entitled **"ASSESSMENT OF GROUND WATER POTENTIAL OF DEME WATERSHED, MIDDLE OMO-GIBE BASIN, ETHIOPIA"** submitted in partial fulfillment of the requirements for the degree of master's sceince with specialization in **HYDRAULICS AND WATER RESOURCE ENGINEERING**, Department of department of water resources and hydraulic engineering, and has been carried out by **YONAS HAILU WASE ID NO. GPHydrR/0020/13**, under our supervision. Therefore, we recommend that the student has fulfilled the requirements and hence hereby can submit the thesis to the department.

Major Advisor:

Dr.Sirak Tekleab (PhD) _____ **17/08/2023**

Signature Date

Co-Advisor:

Lamiso.S(MSC) _____ _____

Signature Date

ACKNOWLEDGEMENT

Above all else, I give thanks and praise to the all-powerful God, who gives me the ability to accomplish tasks with his empowering arm and leads me to the full success that has been predetermined by him. My main adviser, Dr. Sirak Tekleab, and co-advisor, Lamiso Shura, have my sincere gratitude and appreciation for their important guidance and consultation during my research studies, spending the majority of their time offering me advice.

I would like to express my gratitude to all of the organizations and people that supported my research by giving me access to the data and information I needed. First, I would like to thank the South Water Works Corporation, the Ethiopian Meteorological Agency, and the Ministry of Water, Irrigation, and Electricity of Ethiopia for supplying the essential information. Finally, I want to express my gratitude to my family for helping to improve my morals and finances.

DECLARATION

I hereby declare that this MSc thesis is my original work and has not been presented for degree in any other university, and all sources of material used for this thesis have been duly acknowledged.

Name Yonas Hailu.

Signature: _____

This MSc thesis has been submitted for examination with my approval as thesis advisor.

Major advisor name Co advisor name

Dr.Sirak.T(Phd). LamisoS(MSC)

Signature: 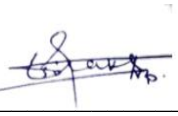 _____- Signature: _____-

Date of submission:

LIST OF ABBREVIATIONS AND ACRONMYS.

AHP	Analytical Hierarchy Process.
CI	Consistency Index.
CR	Consistency Ratio.
DD	Drainage Density
DEM	Digital Elevation Model.
DMC	Double Mass Curve.
GIS	Geographic Information System
GWP	Groundwater Potential .
GWPZ	Groundwater Potential Zone
LD	Lineament Density .
LULC	Land Use Land Cover.
MCDA	Multi-Criteria Decision Analysis Method.
MIF	Multi-Influencing Factor
MOWIE	Ministry Of Water, Irrigation and Energy
NMSA	National Meteorological Service Agency.
OLI	Operational Land Image.
R^2	Correlation Coefficient.
RF	Rainfall
RMSE	Root Mean Square Error
RS	Remote sensing.
SC	Soil Cover.
SG	Slope Gradient.
SRTM	Shuttle Radar Topographic Mission.
SWAT	Soil and Water Analysis Tool.
USDAARS	United States Department of Agriculture Agriculture Research Service .
USGS	United States Geological Survey.

VES	Vertical Electrical Sounding
Wetspass	Water Energy Transfer between Soil, Plants, and Atmosphere under a quasi-Steady-State.

Table of Contents

LIST OF ABBREVIATIONS AND ACRONMYS. V
LIST OF FIGURES X
LIST OF TABLES XI
APPENDIX-A XII
APPENDIX-B XII
ABSTRACT XIII
1. INTRODUCTION 1
1.1 Background 1
1.2. Statement of the problem 3
1.3. Objectives of the study. 4
1.3.1. General Objective. 4
1.3.2. Specific Objectives. 4
1.4. Research questions. 4
1.5. Scope of the study 4
1.6 Significance of study. 5
2. LITERATURE REVIEW 6
2.1. Groundwater resource definition and concept. 6
2.2. Review works on Groundwater potential mapping. 7
2.3. GIS and RS techniques for groundwater potential identification. 10
2.4 Comparison of GIS with other groundwater potential zone mapping methods. 11
2.5. Factors that affect groundwater resource occurrence. 13
2.5.1.Lithology 13
2.5.2 Land use land cover (LULC) 13
2.5.3 Geological formations. 14
2.5.4 Slope. 14
2.5.5. Drainage density. 14
2.5.6 Rainfall. 15
2.5.7 Soil. 15
2.6 Groundwater recharge estimation techniques. 16
2.6.1 SWAT MODEL. 17
2.6.2 SWAT-MODFLOW MODEL. 17
2.6.3 QSWAT-MODFLOW MODEL. 19
2.6.4 Model Selection Criteria. 19

2.7. Groundwater flow direction. 20
2.8 Multi-Criteria Analytical Hierarchy Process Methods. 21
2.9 Hydrologic and meteorological data analysis methods. 22
3. MATERIALS AND METHODOLOGY 24
3.1 Description of study area. 24
3.1.1. Location. 24
3.1.2. Climate of the study area. 24
3.1.3. Topography. 25
3.1.4 Land use and soil. 26
3.1.5 Geology. 27
3.2. Data Collection. 28
3.2.1 Digital elevation model. 28
3.2.2 Satellite image data. 29
3.2.3.Hydrologic data. 30
3.2.4 Meteorological data. 30
3.2.5 Soil data. 32
3.2.6 Groundwater well data. 33
3.2.7 Geology and Geomorphology data. 34
3.3 Data Analysis. 34
3.3.1 Factors influencing the potential groundwater zone. 34
3.3.2 Groundwater Recharge Estimation. 43
3.3.3 Potential Groundwater Zone Identification. 53
3.4 Methodological Framework. 60
4. RESULTS AND DISCUSSION. 61
4.1. Factors Affecting Groundwater potential occurrence. 61
4.1.1 Rainfall. 61
4.1.2. Geology 62
4.1.3 Lineament Density. 64
4.1.4 LULC 66
4.1.5 Slope. 68
4.1.6. Geomorphology. 70
4.1.7. Soil. 72
4.1.8. Drainage Density. 75
4.2. Groundwater Recharge. 78

4.2.1.Model Calibration 78
4.2.2.Model Validation. 79
4.2.3. Spatio temporal variation of recharge in Deme watershed. 80
4.3. Groundwater potential areas. 83
4.3.1. Weighted Overlay Analysis 83
4.3.2. Groundwater Potential Occurrence Area Map. 85
4.3.3. Groundwater Flow Direction. 87
4.3.4. Sensitivity analysis of Groundwater influencing Factors.. 88
4.3.5. Groundwater potential zone Validation. 89
5. SUMMARY AND CONCLUSION. 92
RECOMENDATION 94
REFERENCES 95

LIST OF FIGURES

Figure 3-1. Location map of the study area. 24

Figure3-2 Mean monthly rainfall data(mm) for 32 years from 1989 to 2020 25

Figure 3-3 Topographic map. 26

Figure 3-4. Geology map of study area. 28

Figure 3- 6. Mean annual rainfall for selected stations from 1989-2020. 32

Figure3-7.Soil map of Deme watershed 33

Figure 3- 8. Homogeneity test for the stations 36

Figure 3- 9. DMC to test consistency of meteorological station 37

Figure 4-1 Rainfall map. 61

Figure 4-2 Geology map 63

Figure 4-3. Lineament density map. 65

Figure 4-4. LULC map. 67

Figure 4-5: Slope map. 69

Figure 4-6 Geomorphology map 71

Figure 4-7 Soil map. 74

Figure 4-8.Drainage density map. 76

Figure 4- 9. Monthly Stream flow hydrograph during calibration period (1991-2001) 79

Figure 4- 10. Monthly stream flow hydrograph during validation period (2002-2006). 80

Figure 4-11. Water balance components. 81

Figure 4-13. Spatial distribution of groundwater potential zones. 86

Figure 4-14 Groundwater flow direction. 88

Figure 4-15 Validation of GWPZ in Deme Watershed. 91

LIST OF TABLES

Table3-1 Description of Landsat image to be used. 29

Table 3- 2. Description Of AOI used for LULC classification 39

Table 3- 3. Description on reference points used for accuracy assessment 41

Table 3-4 Parameters used for sensitivity analysis 51

Table 4-5 Sensitive parameters used during calibration accordingly. 52

Table 3-6 pair wise comparison matrix. 54

Table 4-1 Groundwater Potential Prospect Rainfall Map Information. 62

Table 4-2. Groundwater Potential Prospect Geology Map Information. 64

Table 4-3.Groundwater Potential Prospect Lineament Density Map Information. 66

Table 4-4.Groundwater Potential Prospect LULC Map Information. 68

Table 4-5: Groundwater Potential Prospect Slope Map Information. 70

Table 4-6.Groundwater Potential Prospect Geo morphology Map Information. 72

Table 4-7. Groundwater Potential Prospect Soil Group Map Information. 75

Table 4-8.Groundwater Potential Prospect Drainage Density Map Information 77

Table 4-9 Most Sensitive parameters used during calibration accordingly. 78

Table 4- 10. Monthly time step calibration and validation statics. 80

Table 4-11.Groundwater Potential Prospect Recharge Map Information 83

Table 4-12 Weight of parameters or normalized principal vectors. 84

Table 4-13. Ratio index for various n factors. 85

Table 4-14 GWPZ Classes. 87

Table 4-15. Sensitivity analysis of GWPZ influencing factors. 89

Table 4-16. Verification of identified groundwater potential zones with actual yield. 90

APPENDIX-A

Appendix Table-1 Mean annual Rainfall data for each station. 112

Appendix Table-2 Mean monthly stream flow data for Orata alem station(in m3/sec). 114

Appendix Table-3.Groundwater well inventory data. 115

APPENDIX-B

Appendix Figure-1. Calibration statics summary 117

Appendix Figure-2.Calibration hydrograph from SWAT CUP 117

Appendix Figure-3. Validation statics summary. 118

Appendix Figure-4.Validation hydrograph from SWAT CUP 118

ABSTRACT

The goal of this study was to assess the groundwater potential zone in a Deme watershed area of the Omo-Gibe basin, Ethiopia, where data availability was poor. In this study, a number of data from a variety of sources have been used, including climate, stream flow, and spatial thematic layers including land use maps, soil maps, drainage density maps, geology maps, slope maps, lineament density maps, and geomorphology maps. In order to estimate the recharge amount and its spatio temporal fluctuation in the watershed, Soil and Water Assessment Tool model was utilized. At the Orata Alem location within the Deme watershed, several modeling techniques, sensitivity analysis, calibration beginning from 1991 to 2001, and validation 2002 to 2006 periods, were applied. As a result, the results of the calibration and validation phases showed that the model can accurately and reasonably reproduce the stream flow pattern and the various hydrograph responses, as indicated by the Nash-Sutcliffe efficiency(ENS) values of 0.78 and 0.74 and the coefficient of determination(R^2) values of 0.81 and 0.76, respectively. The watershed's mean annual recharge rate is estimated to be 214.5 mm/y, with the northern top section of the watershed experiencing a recharge rate of 233.77 mm/y, the middle of the watershed experiencing a recharge rate of 214.72 mm/y, and the lower part of the watershed experiencing a recharge rate of 194.51 mm/y. Analytical Hierarchical Process was used to rank the various layers based on a pair-wise comparison matrix in order to estimate the final normalized weights of thematic map layers. Groundwater flow direction was determined by the Surfer model. GIS-based Multi-Criteria Decision Analysis was applied for mapping of groundwater potential zones and its results were used to identify three Groundwater Potential Zone: low, moderate and high, with area coverage of 26.3664 Km^2,744.1776 Km^2 and 271.9179 Km^2 correspondingly. Around 71.4% of the region has a moderate groundwater potential, and 26.084% has a high potential. Lastly, groundwater well inventory data for 35 wells dispersed around the region were used to validate the Groundwater Potential Zone map in order to evaluate the model's efficacy. The validation results confirmed that 84.44% the study Ground water potential zone match with ground water well points in the Deme watershed, so that the applied approach provides well reasonable results that can help in planning, management and sustainable utilization of the groundwater resources in this water-stressed area.

Keywords: Deme, GIS, Groundwater potential zone, Multi-criteria decision Analysis (MCDA), SWAT, Watershed.

1. INTRODUCTION

1.1 Background

The most important freshwater resource in arid and semi-arid regions that may be economically developed and utilised for household, industrial, and agricultural uses is groundwater (Calow et al., 2010). Groundwater is the most dependable water resource in the world due to its relative inherent significant traits, including drought reliability, low vulnerability, free from chemical and biological contamination, availability with excellent management practices, and so on (Jha et al., 2007). Although the management method is conventional, groundwater use varies throughout rural areas (Andualem and Demeke, 2019; Das, 2019).

The classic hydrogeological studies, which often involve drilling, are still used in many parts of the world, where they are expensive and time-consuming (Berehanu et al., 2017; Hussein et al., 2017; McCormack et al., 2017). Although watershed-scale models have a large amount of data requirements for calibration and validation reasons, surface water and groundwater models are significant instruments to investigate and comprehend the features and state of a watershed in as much detail as possible (Li et al., 2018).

The hydrological, lithological, atmospheric, soil, and geographic characteristics of a region influence groundwater movement (Andualem and Demeke, 2019; Das, 2019; Mallick et al., 2019); hence, the groundwater study requires multidisciplinary data. GIS tools are essential for accurately processing, comprehending, organizing, and quantifying huge amounts of data (Jha et al., 2007). The groundwater potential zone (GWPZ) has recently been mapped in several locations using GIS-based multi-criteria decision analysis (MCDA) (Arulbalaji et al., 2019; Mallick et al., 2019), including watersheds in Ethiopia (Bashe, 2017; Hussein et al., 2017; Andualem and Demeke, 2019). The capacity to identify the hydrological and hydrogeological elements of a research region in a spatial context is one of the benefits of GWPZ mapping utilizing GIS techniques and MCDA over traditional studies (Nair et al., 2017).

However, the previous studies were focused mainly on the lithology and topographic attributes and rainfall distribution of the study area (Bashe, 2017; Nair et al., 2017; Arulbalaji et al., 2019; Mallick et al., 2019). (Mallick et al., 2019) provide a thorough analysis of the use of GIS-based MCDA in GWPZ mapping and the thematic layers that

were employed; no study included groundwater recharge in GWPZ mapping. As groundwater recharge is influenced by a variety of factors, including soil type, geology, slope, and land cover (Rashid et al., 2012; Ibrahim-Bathis and Ahmed, 2016; Mallick et al., 2019), the distribution of rainfall may not accurately reflect the distribution of groundwater recharge. Consideration of rainfall distribution as the primary factor in the groundwater potential mapping may lead to false conclusions, particularly in a region with a complex topographic nature, such as Ethiopian watersheds. Understanding the spatio temporal distribution of the recharge in addition to the GWPZ in a region with limited data adds a lot to the resource's sustainable management.

According to numerous studies (Ayenew et al., 2008a, 2008b; Berhanu et al., 2013; Berehanu et al., 2017; Tegegne et al., 2017; Aga et al.,2018), many watersheds in Ethiopia have low hydrological measurements, poorly documented geomorphological characteristics, and limited hydrogeological feature research. Because of this, the groundwater potential in socioeconomically significant areas of the nation is not being explored (Ayenew, 2007; Halcrow and GIRDC, 2008; Izady et al., 2014); instead, development and abstraction are based on older studies. Water supply is mainly dependent on groundwater, though, because surface water is limited, expensive, difficult to manage, and loses water to evaporation. The search for groundwater resources is a crucial issue to address as the demand for water rises (Izady et al., 2014; Mechal et al., 2017).

In this study, to map the GWPZ in a data-scarce area of Deme Watershed a combination of Soil and Water Assessment Tool (SWAT) and GIS-based MCDA method was applied. The recharge is estimated using SWAT and then incorporated into the GIS-based MCDA together with geomorphology, geology, rainfall, soil, land use/land-cover (LULC), and DEM derived topographic characteristics. The spatio temporal distribution of groundwater recharge is also presented from the calibrated and validated SWAT model. Related to groundwater resources of the Deme watershed, it is one of the unexplored watersheds due to mainly the limited information available, in addition to the common problem of intricate geological and hydro geological nature of the region. Therefore, the procedures and conclusions from this work provide base information for policymakers, future investigation of groundwater resources in the watershed and other watersheds, which have similar nature with the current study area. Moreover, the study would also be useful input for the community and non-governmental organizations who are involving in groundwater development work.

1.2. Statement of the problem

Water is becoming more and more useful, which inevitably stresses groundwater resources (Vaux, 2011). Groundwater is a source of domestic water in both urban and rural areas, making it the only realistic way to provide for rural communities in arid and semiarid regions(Kebede, 2013). The uncontrolled population growth and poor resource management in developing nations like Ethiopia had a direct and indirect impact on the quantity and quality of groundwater (Abebe, 2021).

Due to population growth and economic development, there is a water shortage in the Deme watershed for drinking and domestic use. Some members of the community, primarily in rural areas, use untreated surface water for drinking and domestic purposes. The lack of sufficient agricultural and potable water supplies hinders the development of developing nations and causes significant hardship to human activity. However, hydro-geologic study should help establish an affordable ground water development design project to ease these hardships. Additionally, the majority of the study area facing scarcity of suitable surface water for drinking and domestic purpose, and a sizable portion of its water supply comes from groundwater (Ayano et al., 2021). In actuality, creating a map of groundwater potential has a significant impact on improving the sustainable management of groundwater resources in the study area and across the nation. According to (Nampak et al., 2014) and (Singh & Prakash, 2002), the majority of groundwater potential investigations (geophysical methods, ground-based survey, and exploratory drilling) are time and cost-intensive and require large data sets. The right platform for the analysis of massive data sets and quiet decision-making methods for groundwater exploration is provided by an integrated GIS and remote sensing study using integration of the SWAT model. The groundwater potential zones have been mapped using GIS and remote sensing data in a sizable number of prior studies (Bashe, 2017; Hussein et al., 2017; Andualem and Demeke, 2019).

Unlike these past studies the current research incorporated the hydrological model to estimate the spatio-temporal variation of recharge which supposed to improve the delineation of the potential zones (Bisrat et al., 2020). Most of groundwater potential mapping using GIS and Remote sensing (RS) did not implement combination of hydrological models to estimate recharge as influential factor to map groundwater potential zones (Benjamin et al ., 2022). However this study incorporated this key input in the analysis.

Moreover, in Deme river watershed there is no study conducted on ground water resource potential assessment, so that undertaking GIS,SWAT and Remote sensing with MCDA method will provide ground water resource potential zone to practically develop the groundwater resources primarily for domestic and other purposes.

1.3. Objectives of the study.

1.3.1. General Objective.

The primary goal of this study was to assess potential of groundwater zone in the Deme river watershed, sub basin of Omo-Gibe river in Ethiopia.

1.3.2. Specific Objectives.

- To assess factors influencing the potential groundwater zone.
- To evaluate the groundwater recharge potential zone.
- To identify the potential groundwater zones of watershed.

1.4. Research questions.

- What factors influence the presence of groundwater potential zones in the watershed?
- How much is the recharge amount spatially and temporally in the watershed?
- Are there groundwater potential zones in the watershed?

1.5. Scope of the study

This study was be limited to the Deme River catchment and which focus on the identification of groundwater resource potential areas and groundwater recharge distribution. The study area covers upstream of the gauged station at Orata-Alem. This has been in operation since 1987. The study used DEM for watershed delineation and for the generation of ground water occurrence controlling factors maps, GIS, RS, and SWAT with the multi-criteria decision analysis method to analyze the effect of ground water occurrence controlling factors and ground water recharge distribution.

1.6 Significance of study.

The most dependable and secure supply of water for domestic, agricultural, commercial, and municipal uses is groundwater. For the proper exploitation and administration of this natural resource, a systematic study of groundwater is required. Spatial data are processed and analysed as a result of the integration of RS-GIS and MCDA for groundwater potential mapping, so that which can provide useful information for water resource managers and policymakers. Subsurface studies are frequently conducted in Ethiopian when local-specific groundwater projects, such as borehole, spring, shallow, or hand-dug wells for domestic water supply, are required. According to Hussein et al. (2017), the problem of unsustainable groundwater use is growing and is a major concern for many developing nations. The lack of current geographical data on the amount and distribution of groundwater resources is one of these issues. Today, there is a critical need to use groundwater for socioeconomic development in rural regions, which necessitates knowledge of the potential assessment of groundwater resources prior to using and managing them (Tesfaye, 2015). This study should evaluate groundwater potential locations for the Deme watershed using GIS and remote sensing techniques together with a multi-criteria decision analysis method. In general, groundwater resource planners and managers will find the study valuable when creating sustainable groundwater resource project plans in the studied area.

2. LITERATURE REVIEW

2.1. Groundwater resource definition and concept.

Groundwater is a finite but replenish able resource that plays a vital role in the hydrological water cycle. Recharge and discharge of groundwater occur seasonally through rainfall and other sources, resulting in fluctuations in water levels. Below this fluctuation zone, aquifers remain consistently saturated. Excessive extraction of groundwater can lead to depletion of storage, with serious social, economic, and environmental consequences.

Groundwater is the second most important freshwater reservoir and serves as a valuable alternative to surface water for human and economic activities (Melloul and Collin, 2001; Das and Pardeshi, 2018a; Andualem and Demeke, 2019; Arabameri et al., 2019). Therefore, accurate estimation and effective management of groundwater resources are crucial, particularly in drought-prone semi-arid regions, to prevent severe water shortages (Deshmukh and Aher, 2016).

The hydrological characteristics and occurrence of groundwater in a region are primarily influenced by its geological and geomorphic features(Doke et al., 2018; Das, 2019; Adimalla, 2020). The physiographic elements control processes such as runoff, infiltration, and percolation. Various landscape, climatic, and environmental parameters, including relief, slope, drainage, lithology, geological structures, soil, lineament features, geomorphology, land use/land cover (LULC), rainfall, and distance from rivers, have been identified by researchers as important factors in determining potential groundwater zones(Das et al., 2017; Das and Mukhopadhyay, 2018; Parameswari and Padmini, 2018; Das and Pal, 2019; Maity and Mandal, 2019; Pande et al., 2019). .There is a relationship between natural streams and groundwater, where environmental flow affects groundwater occurrence and river runoff (Kuriqi et al., 2020a). Groundwater availability varies significantly across different seasons, and river runoff plays a substantial role in the recharge mechanism. (Kuriqi et al., 2020b).

2.2. Review works on Groundwater potential mapping.

Numerous studies have been conducted on mapping groundwater potential zones using GIS and remote sensing techniques. Here are summaries of a few relevant works:

In a study conducted in the Mysore Taluk basin, India, nine parameters influencing groundwater were considered, including drainage density, elevation, geology, geomorphology, land use/land cover, lineaments, rainfall pattern, slope gradient, and soil texture. These parameters were classified using the analytical hierarchical process and weighted overlay analysis in ArcGIS. The resulting GWPZ such as low, moderate, high, very high zone maps were validated with collected water inventory data to evaluate the accuracy of the findings (Ramu, 2014).

For identifying groundwater potential zones in the Thirumanimuttar basin, India an integrated approach using remote sensing and GIS was employed. Thematic maps, such as geology, drainage density, and slope, were generated using Landsat TM 30m resolution data and topographic maps. Different areas with varying groundwater availability were categorized as very high, high, medium, low, and very low potential zones. The upper, middle, and downstream areas of the basin were identified as potential zones based on the data, which were validated through field checks and observed data (AL-Ruzouq et al., 2015).

A study conducted in the trans-boundary Shatt Al-Arab basin demonstrated the feasibility of using remote sensing, GIS, and the analytical hierarchical process (AHP) for delineating groundwater potential zones. This approach provided a cost and time-effective assessment of groundwater resources compared to traditional techniques. Thematic layers derived from remote sensing and conventional data were weighted using the AHP technique. The resulting groundwater potential zones map classified the study area into five zones: very good, good, moderate, poor, and very poor. The presence of good potential zones in the southwestern areas of the basin was attributed to favorable lithology (unconsolidated sediments), geomorphology units (floodplain and pediplain), and flat terrains (Allafta et al., 2021).

In a study conducted in India, groundwater potential was identified using the weights of evidence method. The spatial database was developed using topographic sheets from the Survey of India on a 1:50,000 scale, as well as satellite data. Various thematic maps, including drainage density, contour, and stream length, were prepared using GIS and remote sensing techniques. Digital elevation model (DEM) data was used to derive slope, aspect, contour, and flow accumulation maps. Geo referencing and geometric correction of satellite data were performed through image processing. Attribute data were utilized to create buffers for agriculture and settlement areas. Overlay analysis in GIS was then applied to the thematic maps, assigning weights to each layer and determining ranks to evaluate the groundwater potential zones (Waikar & Nilawar, 2014).

In the Panipat region of the Yamuna sub-basin in India, a study was conducted to evaluate groundwater potential zones for sustainable management of groundwater stress areas. The study emphasized the usefulness of geospatial technology and the selection of multi-criteria decision-making (MCDM) techniques. Two MCDM methods, namely Analytical Hierarchy Process (AHP) and Catastrophe Theory (CT), were employed in combination with remote sensing and GIS techniques to demarcate groundwater potential zones in the region. Both models yielded similar results in terms of areal extent, but the spatial distribution of groundwater prospects differed significantly, with the CT method showing better validation results. Sensitivity analysis was also carried out to assess the effect of weights assigned to input indicators/variables in both MCDM techniques (Lakhvinder et al., 2020).

In the Ulhas basin in Western Maharashtra, India, an integrated approach utilizing GIS-based Multi-Criteria Decision Making (MCDM), Analytical Hierarchy Process (AHP), and remote sensing was used for geospatial mapping of groundwater. Various factors influencing groundwater occurrence, such as geology, distance from the river, geomorphology, slope, land use/land cover, drainage density, lineament density, soil, and rainfall, were identified from extensive literature. A pairwise comparison matrix (PCM) was formed to calculate the weight of each factor. Sub-parameter scores were assigned based on published literature. The weighted overlay analysis (WOA) tool in ArcGIS 10.1 was then employed to generate the final groundwater potential map. The methodology, techniques, and results of the study have implications for evaluating

groundwater potential zones in similar drought-prone regions worldwide (Arjun B et al., 2021).

In recent years, several researchers have adopted modern methods for groundwater exploration, including the frequency ratio method (Elmahdy, 2015) and the weights of evidence method (Masetti et al., Tahmassebipoor et al., 2016). In a study conducted in Egypt, the frequency ratio method was used to explore groundwater. A spatial database was created, incorporating various groundwater occurrence controlling factors such as topography, soil map, land use, rainfall, geology, and lineament maps obtained from different government sources in Egypt. The DEM data was utilized to calculate aspect, slope, and contour maps. The lineament map was prepared using spatial analysis in ArcGIS. All these factors, including the lineament map, slope map, geology map, and land use map, were converted into raster grids with 20x20m cells. Groundwater data, including well numbers, topography, and depth, were collected from web databases. Weights were assigned to each thematic map, and ranks were evaluated to create potential zone maps (Manap et al., 2014).

In central Eritrea, groundwater potential zone identification was conducted using GIS and remote sensing techniques (Patil, 2014). Thematic maps were generated for factors influencing groundwater occurrence and movement, such as slope, drainage density, land use/land cover, rainfall, lithology, and soil, within the GIS environment. Based on the estimated parameter results, groundwater potential zones were delineated, and areas suitable for artificial recharge were identified. The validity of the results was assessed by comparing them with borehole yield data collected from existing water supply schemes in the catchment.

The groundwater potential of the Weserbi Guto Laga Qawe Catchment in Sululta, Ethiopia, was assessed using VES (Vertical Electrical Sounding) and GIS methods (Desalegn et al., 2022). Thematic layers were generated from geophysical investigations, existing maps, and field survey results, which were then integrated into the GIS environment to delineate groundwater potential zones. Factors such as lineament density, drainage density, elevation or topography, slope gradient, aquifer resistivity, and lithology were derived, reclassified, and scaled to a common range, and appropriate weights were assigned to them. The groundwater potential zone map was produced using the multicriteria evaluation method, classifying the index into

three zones (high, moderate, and low). The resulting map was validated using eleven existing water level data points, and it showed good agreement with the model.

An attempt was made in the Bilate River catchment to delineate and classify potential groundwater zones using integrated remote sensing and GIS techniques. Thematic layers such as lithology, geomorphology, drainage density, lineament density, rainfall, soil, slope, and land use/land cover were considered (Tesfay, 2015).

In Arba Minch town, Ethiopia, groundwater potential zones were identified using geospatial and AHP tools (Muralitharan et al., 2021). Eight essential parameters, including lithology, lineament density, geomorphology, land use/land cover, slope, precipitation, drainage density, and soil type, were considered. The AHP method was adopted to derive the weights of the thematic layers and their sub-criteria, considering their varying effects on groundwater occurrence and movement.

In the Lower Omo-Gibe Watershed, Omo-Gibe Basin, Ethiopia, an integrated approach of RS, GIS, and MCDA using AHP was utilized to delineate groundwater potential zones (Eyasu, 2022). Seven thematic layers influencing groundwater potential, including lineament density, slope, soil, drainage density, land use/land cover, geology, and elevation map, were used. Scale values for the classes and thematic layers were determined using Saaty's AHP, based on expert judgment and literature. The weighted overlay spatial function tool in ArcGIS was used to integrate the thematic layers based on their weights/rates, resulting in a groundwater potential map.

2.3. GIS and RS techniques for groundwater potential identification.

The use of GIS and RS techniques for groundwater potential identification has gained prominence in hydrogeological science (Kelley, 2016). These tools offer a time and cost-effective means to gather valuable data on geology, geomorphology, lineaments, and lithological features, facilitating the delineation of groundwater potential zones (Arulbalaji et al., 2019). Given the increasing attention to groundwater issues, water resource management, and irrigation systems, modern technologies such as GIS and remote sensing play a crucial role in mapping groundwater potential zones. The integration of these advanced technologies has proven to be an effective approach in groundwater studies (Libasse, 2007).

Remote sensing has proven to be an invaluable tool for hydrologists and geologists in tackling the complex challenges associated with groundwater exploration. In recent years, satellite remote sensing data has been extensively utilized to identify groundwater potential zones. This approach not only provides efficient, reliable, and timely data but also meets the essential requirements of geographic information systems (GIS), offering current, accurate,comprehensive,and standardized information. The integration of dominant parameters is best achieved through GIS, which serves as an effective platform for storing, managing, and retrieving spatial and non-spatial data, as well as for integrating and analyzing this information to derive meaningful solutions. The combination of remote sensing and GIS has proven to be highly beneficial for groundwater studies (Arkoprovo et al., 2012). Satellite images are increasingly employed in groundwater exploration due to their ability to identify various ground features that can serve as direct or indirect indicators of groundwater presence (Jasmin and Mallikarjuna, 2011). One commonly used application of remote sensing in groundwater studies is the identification of lineaments, which are often associated with faults and fractures in hard rock formations (Salwa, 2015).

2.4 Comparison of GIS with other groundwater potential zone mapping methods.

When comparing GIS with other methods for mapping groundwater potential zones, it becomes evident that conventional techniques, such as ground surveys and geophysical methods like resistivity and ground-penetrating radar, are labor-intensive, time-consuming, and resource-demanding. In contrast, the integration of remote sensing and GIS offers an efficient, rapid, and cost-effective approach for identifying and assessing groundwater potential zones by providing valuable data on geology, geomorphology, lineaments, drainage density, and slope, as well as enabling systematic data integration for exploration and delineation purposes.

Conventional methods relying solely on ground surveys and techniques like resistivity and logistic regression models may not always be highly reliable in assessing the diverse factors influencing groundwater presence (Prosper et al., 2012). Conducting traditional field examinations to investigate subsurface water in a study area can be time-consuming, costly, and require substantial manpower. On the other hand, GIS is a fast and cost-effective tool for identifying groundwater prospective zones, while remote sensing offers the advantage of accessing large coverage areas, including

inaccessible regions. This combination enables the rapid and efficient generation of valuable information on geology, geomorphology, lineaments, slope, and other relevant factors, which are crucial for interpreting groundwater potential zones (Rajaveni et al., 2015).

Conventional methods for preparing groundwater potential zones primarily rely on ground surveys, such as the Sensitivity Analysis Method using resistivity and ground-penetrating radar, as well as probabilistic models like logistic regression. However, these conventional exploration methods may not be highly reliable due to the complex assessment of various factors that influence groundwater presence (Prosper et al., 2012). The traditional approach of conducting field examinations to seek subsurface water is time-consuming, costly, and requires significant manpower. In contrast, geographic information system (GIS) serves as a fast and cost-effective tool for identifying groundwater prospective zones, while remote sensing techniques offer the advantage of accessing extensive coverage, including inaccessible areas. These technologies efficiently generate valuable information on geology, geomorphology, lineaments, slope, and other relevant factors that aid in interpreting groundwater potential zones (Rajaveni et al., 2015).

According to (Mukherje, 2008), GIS and remote sensing techniques play a vital role in characterizing groundwater potential and recharge zones. Satellite sensors, for instance, have enabled systematic and efficient exploration of groundwater, landform mapping, geological mapping, mineral exploration, and geohazard studies. They provide valuable insights into various landforms that are not easily observed. Furthermore, Geographical Information System and remote sensing are advanced technologies that have multiple scientific applications, including monitoring natural disasters, landslides, earthquakes, volcanoes, agricultural management, mineral and groundwater exploration. These technologies allow access to extensive data, even in challenging terrains such as cliffs, mountains, and gorges (Semere, 2003).

(Salwa, 2015) compares the application of GIS and remote sensing for groundwater delineation with other methods like geospatial, numerical modeling, and geophysical methods. The author concludes that these alternative methods are expensive, laborious, time-consuming, and often destructive. In contrast, according to Tesfaye (2012), groundwater cannot be directly observed with the naked eye as it is located beneath

the ground. Various techniques, such as hydrological investigations, geophysical methods like geoelectrical or geophysical seismic refraction, provide information about groundwater and recharge potential zones, but they are costly and time-consuming. GIS and remote sensing represent the latest, cost-effective technologies for groundwater exploration as they provide comprehensive information and easy access to all the parameters and factors that control groundwater potential and recharge zone areas through the use of different software tools.

2.5. Factors that affect groundwater resource occurrence.

2.5.1.Lithology

Lithology plays an important role in the occurrence and distribution of groundwater since it is the controlling factor of infiltration rate and flow. In Ethiopia which is mainly of metamorphic rocks is considered as low yielding regional aquicludes (Chernet, 1993); nevertheless, regoliths and fractures are the main groundwater holding and transmitting media in a metamorphic terrain (Kebede, 2013). Mesozoic sediments have better productivity because they have inter-granular permeability and can have extensive aquifers (Chernet, 1993).

Lithology is a property that expresses the lineaments underlying structural features such as fractures, faults, cleavages, and discontinuity surfaces. Lineaments represent the simple and complex linear features of structures, with parts that are arranged in a rectangular or moderately curved mode, and which differ from the arrangement of the adjacent features and reflect some subsurface feature (Gogu et al., 2001). Lineaments are often used in mineral exploration studies (Bahiru and Woldia, 2016), geothermal resources (Elmahdy and Mohamed, 2016), and identification of GWPZs (Kirshna et al., 2015).

2.5.2 Land use land cover (LULC)

The land use/land cover of a certain area depends on geomorphology, agro-ecology, climate and human-induced activities. It is one of the factors affecting groundwater occurrence and availability. (Singh, 2014) stated that LULC information is an important factor in groundwater storage and recharge.

LULC includes the type of soil deposits, the distribution of residential areas, water body, and vegetation cover within a certain area. It is an important factor affecting

groundwater recharge, groundwater occurrence, and availability (Hussein et al., 2016; Kumar et al., 2016; Pande, Khadri, Moharir, & Patode, 2017; Yeh, Cheng, Lin, & Lee, 2016).

2.5.3 Geological formations.

Geological lineaments are the manifestation at the earth's surface of deeper geological structures (faults and fractures that have obvious displacement, ruptures that have no significant fracture displacement) (Han et al., 2018). It has been used to investigate the distribution of minerals (Bahiru & Woldai, 2016), determine the potential areas for runoff water harvesting (Elewa et al., 2012), the regional distribution of groundwater potential (Magesh et al., 2012), geological disasters (Yusof et al., 2011), geothermal resources, earthquakes (Elmahdy & Mohamed, 2016) and geomorphology. Moreover, identification of the weathered zones from the lineament density map is useful in soil erosion studies (Krishna, & Sarup, 2015). Areas with high lineament density denote a permeable zone so reveal good groundwater potential zones. Considering the lineament map as a baseline, lineament density (Ld) defined as the total length of lineaments per unit area (Greenbaum, 1985; Magesh et al., 2012; Yeh et al., 2016).

2.5.4 Slope.

Topography and slope gradient directly influence the infiltration of rainfall and could be considered as one of the indicators of groundwater potential accessibility (Al Saud, 2018). It can also give an indication for the general groundwater flow direction (Gupta & Srivastava, 2010). Gentle slope topography can be an indicator of the presence of high groundwater potential zones (Hussein et al., 2016). This is due to the fact that gentle slope areas have high capacity for holding rainfall and facilitate recharge to groundwater.

2.5.5. Drainage density.

Drainage density is one of the important indicators of groundwater recharge (Magesh et al., 2012) and groundwater occurrence (Sener et al., 2005). In fact, it is linked with water percolation properties of underlying lithology, consequently having close relation with groundwater mapping. The drainage density is an inverse function of permeability. Drainage density indicates rock permeability and infiltration capacity, and therefore recharges capacity. They are reflection of the rate that precipitation

infiltrated compared to surface runoff. Where rocks are highly permeable, infiltration to groundwater is high, and less water is transported in rivers as surface water; but where rocks have low permeability there is little infiltration and more surface water runoff. Low drainage density is therefore related to higher recharge and higher groundwater potential (Ramu and Vinay, 2014). The drainage density is high in the plateau and escarpment and very low in the rift floor (Nasir et al., 2018)..

An area with low permeable surface prone to high drainage density and water comes from precipitation goes to a high runoff as well and vice versa(Mageshkumar et al., 2019). As a result, high drainage density implies low groundwater potential.

2.5.6 Rainfall.

Rainfall is one of the important factors to delineate groundwater potential zones. In fact, it is the main source of natural recharge that develops groundwater resources. Several researchers reported that there is a strong positive relationship between rainfall and groundwater (Das, 2019). Rainfall is the primary water source on the earth, and it controls the surface and groundwater amount. Groundwater is a dynamic natural resource that is recharged by rainfall. Groundwater recharge is controlled by various factors with rainfall playing a key role since it represents the main source of groundwater recharge (Lee et al., 2019). Rainfall directly controls the infiltration of surface water to increase groundwater recharge (Maity and Mandal, 2019).

2.5.7 Soil.

Soil type plays a vital role in controlling the infiltration rate of precipitated water and water-holding capacity of the area and spatial variation of groundwater recharge (Mehra et al., 2016). Soil texture can be described in the ratio of sand, silt, and clay applying texture triangles which determine soil infiltration and water holding capacity. Soil type and thickness play an essential role in water recharge to the aquifer (Doke, 2019). The water infiltration and soil permeability primarily depend on the soil texture and thickness, and these factors assist the characterization of the GWPZ(Gupta & Srivastava, 2010). Groundwater recharge depends on runoff, water holding capacity, soil thickness, soil porosity, etc Consequently, it could be considered as one of the important factors for the delineation of groundwater potential zones (Kumar et al., 2016; Magesh et al., 2012).Soil has a significant control on the infiltration and percolation rates into an aquifer (Ahmad et al., 2020). Soil grain size, shape, and

arrangement and the corresponding pore system can highly affect the vertical and lateral water movement (Das and Pal, 2019).

2.6 Groundwater recharge estimation techniques.

There are many techniques available for quantifying groundwater recharge as there are different sources and processes of recharge. Each of the methods has its own limitations in terms of applicability and reliability. The objective of the recharge study should be known prior to selection of the appropriate method for determinig groundwater recharge as this may dictate the required space and time scales of the recharge estimates (Scanlon et al., 2002). According to them, techniques for estimating recharge are subdivided into various types, on the basis of the three hydrologic sources, or zones, from which the data are obtained, namely surface water, unsaturated zone, and saturated zone.

Chloride Mass Balance, Stable Isotopes (Rushton, 1991), Soil Moisture Balance Method (SMBM), Water table fluctuation method (Eilers et al., 2017) and WetSpass modeling method ((Batelaan and DeSmedt, 2001; Hasanuzzaman et al., 2017; Teklebirhan et al., 2012) are among techniques widely utilized for recharge estimation.

A groundwater study was conducted to determine the recharge,spatial distribution and potential recharge zones of groundwater at different scales in the Afram Plains region of the Volta Basin in Ghana using the Soil and Water Assessment Tool (SWAT) model and Geography Information system (GIS). approach (Benjamin et al., 2022). The SWAT model was built (1983–2016), calibrated (1983–1990), and validated (1991–1997). Digital elevation models, soil, land use, climate data and stream flow data were used. Using the GIS approach, thematic maps were created for eight contributing factors. Precipitation, Elevation, Land Cover, Land Use, Lineament, Drainage,Geology,Soil and Slope to map the recharge zones. The potential regeneration zones are categorized into very poor, poor, moderate and high zones. The potential refilling zones following validation of the drill hole and drill data indicated that the Afram Plains area was dominated by the moderate potential zone.

Study was conducted on recharge estimation and groundwater potential assessment using the SWAT model and GIS-based MCDA in a data-scarce region of Main Ethiopian Rift valley (Bisrat et al., 2020). The SWAT model was calibrated and validated using SWAT-CUP and the agreement of the observed and simulated streamflow was measured using NSE, PBIAS, R^2 , and RSR values. As the results show the SWAT model calibration and validation are reasonably acceptable. The result is categorized as low, moderate, and high GWPZs. The assessment result was cross-validated by pumping wells and springs data in the watershed; the result shows a 93% match. Important results were produced in a acceptable way using SWAT and GIS-based MCDA.

2.6.1 SWAT MODEL.

The Soil and Water Assessment Tool (SWAT) model was developed by the USDA-A RS Agricultural Research Service. SWAT (Arnold et al., 1998) is semi-distributed; A continuous-time watershed simulator that works with daily, monthly, and yearly time steps. The model is based on a semi-physical basis and allows modeling with a high le vel of spatial detail, dividing the watershed into a large number of sub-basins. SWAT can model groundwater recharge, surface and groundwater flows, sediment transport, water quality and nutrient transport, and plant growth and yield (Neitsch et al., 2002). The SWAT model can simulate the components of the hydrological water balance in a watershed. SWAT is a continuation of over 30 years of modeling work at the USDA' Agricultural Research Service. In combination with the SWAT-Arc-SWAT model,

is used to preprocess the GIS data. Arc SWAT is a SWAT model extension that runs on Arc GIS. It provides a graphical user interface that makes it easy to format GIS dat a for use in SWAT model modeling.

2.6.2 SWAT-MODFLOW MODEL.

SWATMODFLOW is a coupled groundwater–surface water model that integrates the SWAT (soil and water assessment tool) and MODFLOW (modular finite difference groundwater flow) models. It is used to simulate the hydrological and hydrogeological processes in watersheds, especially the interactions between surface water and groundwater. SWATMODFLOW can also be applied to study the potential impacts of climate change and groundwater withdrawals on water resources.

SWAT-MODFLOW is a coupled hydro geological model that combines the outputs of SWAT and MODFLOW (Sophocleous et al., 1999). SWAT-MODFLOW has been regularly improved and widely used to watersheds to mimic SW-GW interactions during the last two decades(Sophocleous and parkis, 2000:: Deb et al., 2019: Wei et al., 2019: Liu et al., 2020a: Liu et al., 2020b: Liu et al., 2020c). The restrictions necessary in each component model are covered by coupling the component models, resulting in a solution that is more accurate to real-world hydrology (Chunn et al., 2019). These SWAT-MODFLOW models, however, and coupled models in general, often are not used extensively due to the level of complexity of preparing input data, configuring model options, executing models, and interpreting results (Barthel and Banzhaf, 2016; Nielsen et al., 2017). In particular, preparing input data for coupled hydrologic models often is a slow, tedious, and error prone process.

By integrating SWAT with MODFLOW at various levels of integration, several research has been presented. SWAT-MODFLOW was used by (Eshtawi et al., 2015) to investigate the relationship between GW level and built-up area. To aid water-resources decision-making. (Izady et al., 2015)simulated flow of SWAT-MODFLOW assessed GW recharge and water budget. By defining Water transfer across the HRU-cell conversion interface,combined SWAT-MODFLOW modeling was done (Kim et al., 2008). While SWAT-MODFLOW offers many benefits for water resource management and environmental assessment, there are also some limitations to the model (C. P. Kumar, 2020).Some of the key limitations include:

Data requirements: SWAT-MODFLOW requires a significant amount of input data,including land use, soil characteristics, topography, climate data, and groundwater characteristics. Obtaining this data can be challenging, particularly in data-poor regions.

Model complexity: SWAT-MODFLOW is a complex model that requires significant expertise to set up and calibrate. This can be a barrier to entry for some users, particularly those without experience in hydrological modelling.

Computational resources: The simulation of surface water and groundwater processes at highspatial resolutions can require significant computational resources. This can be a limiting factor for some users, particularly those with limited access to high-performance computing resources.

Model uncertainty: As with any modelling approach, there is uncertainty associated with the predictions generated by SWAT-MODFLOW. This uncertainty can arise from errors in input data, model structure, and calibration.

2.6.3 QSWAT-MODFLOW MODEL.

QSWAT-MODFLOW is a coupled model that integrates SWAT (soil and water assessment tool) and MODFLOW (modular finite difference groundwater flow) to simulate the interactions between surface water and groundwater in watersheds (Guzman et al., 2015). QSWAT-MODFLOW has a graphical user interface (QSWATMOD) that facilitates the linkage of SWAT and MODFLOW models, runs simulations, and displays results within the open source Quantum Geographic Information System (QGIS) environment (C. P. Kumar, 2020). QSWAT-MODFLOW uses simplified flow equations that can yield poor results in groundwater-driven watersheds, potentially leading to erroneous results when assessing nutrient management practices, water rights, and ecosystem services. QSWAT-MODFLOW has uncertainties related to model structure, data availability, parameterization, calibration, validation, and computational efficiency. QSWAT-MODFLOW requires a lot of input data and expertise to set up and run the coupled model, which can be challenging for some users.

2.6.4 Model Selection Criteria.

Choosing the best and most relevant model is crucial in any research activity. The function specifies the type of hydrological model that must be used by the model. There are many different hydrological models that can be used to simulate the hydrological process at different spatial and temporal scales. Although there are no hard and fast rules for selecting models, there are some general principles to follow. The type of modeling approach used is usually determined by the purpose, availability of data, and easy of usage (Tassew et al, 2019). A variety of factors can be used to select the "best" hydrologic model. Because each study has its own set of objectives and needs, these criteria are research specific. There are four basic essential selection criteria that should be addressed among the research:-

1. Required model outputs are important to the study and therefore to be estimated by the model.

2. Hydrologic processes that need to be modeled to estimate the desired outputs adequately.

3. Availability of input data (Can all the inputs required by the model be provided within the time and cost constraints of the study?),

4. Price (Does the investment appear to be worthwhile for the objectives of the study?)

Therefore, Soil water analysis tool(SWAT2012) is used for this study because it is a widely used and freely available watershed model that requires climate, and Spatial data as an input and availability of suitable data to simulate the model on the study area. In general, the reasons behind selecting the SWAT2012 model for this study are:

➢ It is the public domain for free and online access.

➢ It is a Physically based model: It is based on readily observed and measured information and it attempts to simulate many hydro logical components.

➢ It was compatible with the ArcGIS interface: for ease of database management.

➢ It is suitable with data availability context for the study area.

2.7. Groundwater flow direction.

The contour lines representing the groundwater level contours (equipotential surfaces) are sketched perpendicular to the groundwater flow lines, which indicate the flow direction. Equipotential surfaces are contours lines with the same head at the same depth of the groundwater. Representative contour maps can be created for the various kinds of aquifers found within the hydrogeological basins using field measurements of the water table or piezometric surface (Tenalem and Tamiru , 2001). In order to locate new, productive wells in a certain location, contour maps of groundwater levels also known as groundwater elevation levels and flow lines are essential tools.

According to study of (Mehra et al., 2016)., diverging contour lines denote groundwater recharge zones and convergent contour lines, groundwater discharge areas. Additionally, the distance between the contour lines can be used to identify regions with good hydraulic conductivity. According to Tenalem and Tamiru (2001), increased hydraulic conductivity or permeability is actually observed in places with

homogeneous groundwater flow, particularly in locations with wide water table contour spacing and subsequently flat gradients. In other words, a dense contour map does not indicate a high level of aquifer productivity; rather, the hydraulic conductivity increases with groundwater contour distance; the closer (denser) the groundwater contour lines, the lower the hydraulic conductivity.

In order to ascertain the groundwater flow pattern of the area, a research was conducted in Utagba-Ogbe Kingdom, Ndokwa west Local Government Area of Delta State (Oseji et al., 2010). Six uniformly spaced out excavated well locations had their longitudes, latitudes, and water level elevations measured and recorded. With the help of a meter tape and a ground water level contour map, the depths to the water level in the hand-dug wells were directly measured and ground water flow direction is identified..

2.8 Multi-Criteria Analytical Hierarchy Process Methods.

According to Arulbalaji et al. (2019), multi-criteria decision analysis using Analytical HierarchicalProcess (AHP) is the most common GIS-based method for demarcating groundwater potential zones.

The Analytic Hierarchy Process (AHP) is a general theory of measurement and it is used to derive ratio scales from both discrete and continuous paired comparisons. These comparisons may be taken from actual measurements or from a fundamental scale that reflects the relative strength of preferences and feelings. The AHP has a special concern with departure from consistency, its measurement, and dependence within and between the groups of elements of its structure. It has found its widest applications in multi-criteria decision making, planning, and resource allocation and in conflict resolution (Saaty and Vargas, 1981: Saaty, 1982)

Different researchers use different weight overlay and decision-making analysis methods. from those researchers (Roy et al., 2020) adopt thematic layers of soil, slope, geology, Landuse/land cover, lineaments, and drainage gave accurate information about groundwater occurrence and generate the result from Weight Index Overlay Analysis (WIOA) by employing analytical hierarchy process methods. Finally, conclude that the analytical hierarchy process is a promising method for groundwater exploration.

The rates for the classes in a layer and weights for the thematic layers were computed based on saaty's AHP (Saaty, 1980)). Saaty's AHP is the most widely accepted method for scaling the rates/weights of factors whose entries indicate the strength with which one factor dominates over the other about the relative criteria (Tesfaye, 2010). In this method, the relative importance of individual class within the same map and thematic maps were compared to each other by pairwise comparison matrices. As such, matrices were constructed, where each criterion was compared with the other criteria, relative to its importance, on saaty's scale from 1 to 9. A score of 1 represents equal importance between the two factors, and a score of 9 indicates the extreme importance of one factor compared to the other one.

2.9 Hydrologic and meteorological data analysis methods.

A lengthy rainfall data series plays a major role in all water-related studies. Consistency and continuity of rainfall data series are very important for obtaining reliable results from such studies. However, these rainfall data series very often contain gaps or missing values due to various reasons such as the absence of observers, problems with measuring devices, loss of records, etc. The use of a rainfall data series with missing values may critically influence the statistical power and accuracy of a study (Caldera et al., 2016). Estimation of missing data is more important in mountain and forest regions where meteorological stations are scarce, and the observed data are influenced by topography and the forest microclimate. The techniques of missing data estimation can be grouped in empirical methods, statistical methods, and function fitting (Xia et al., 1999).

The empirical methods include simple arithmetic averaging, inverse distance interpolation (ID), and ratio and difference technique The statistical methods include multiple regression analysis (REG), principle component analysis and cluster analysis, Kriging method, and optimal interpolation. Most of these methods derive the missing values using observations from neighboring stations. Selecting appropriate methods for estimating missing precipitation data may improve the accuracy of hydrological models. (De Silva et al., (2007) used the aerial precipitation ratio method, the arithmetic mean method, the normal ratio (NR) method, and the inverse distance method to estimate missing rainfall data. The NR method was found to be the most accurate. The arithmetic mean method and the aerial precipitation ratio method were most appropriate for the wet zone. According to (Caldera et al., 2016) to obtain

accurate results from the Multiple Linear Regression method and the Weighted Linear Regression method, it is necessary to have a set of neighboring stations that

have fairly high correlation coefficients with the target station. And also they stated in their result that for stations that have relatively low correlation coefficients with the neighboring stations, the Inverse Distance Squared method and the Normal Ratio method performed well.

As the literature review shows that the best method for estimating missing rainfall data can vary for different areas depending on their rainfall patterns and spatial distributions and availability of the neighboring station.

3. MATERIALS AND METHODOLOGY

3.1 Description of study area.

3.1.1. Location.

Deme River has a watershed size of 1119 sq. km and is located in the southwest of Ethiopia inside the Middle Omo Gibe River sub-catchment. Additionally, it is a tributary of the Gibe3 reservoir. Deme River is situated geographically between 37031' E longitude and 6038' N latitude.

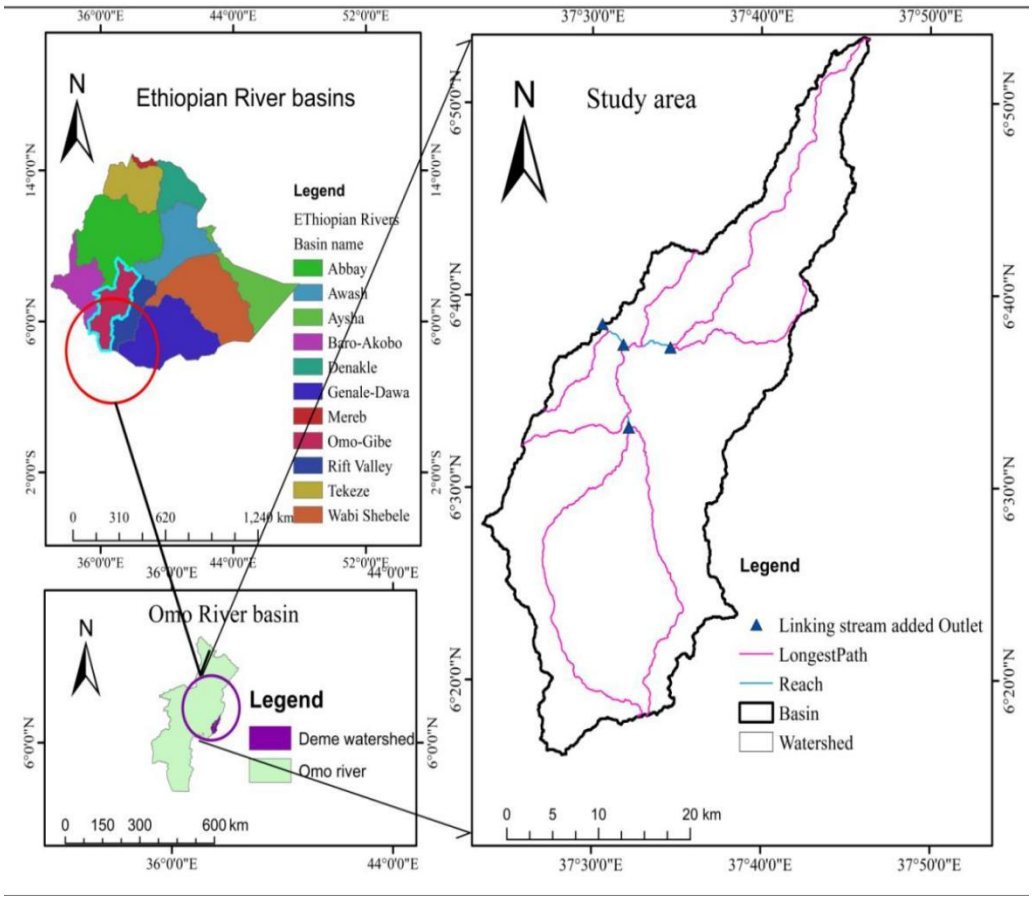

Figure 3-1. Location map of the study area.

3.1.2. Climate of the study area.

Ethiopia's climate can be categorized in a number of ways. The traditional and agroecological zones are the systems that are most frequently employed. The five climatic zones are wurch (cold climate, altitude > 3000 m), dega (temperate-like climate, altitude 2500-3000 m), woina dega (warm with altitude 1500-2500 m), kola (hot and arid with altitude 1500 m), and bereha (hot and hyper-arid type) according to traditional classification (NMSA, 2001). According to Sintayehu (2016), the research

region is located in the "Dega" (tempestuous), "Woina Dega" (sub-tropical), and "Kolla" (tropical) climatic zones, respectively. Bimodal rainfall patterns are present in the research area, as evidenced by classification according to rainfall regimes. The first round of rain occurs in April, May, and June, and the second round of rain occurs in July, August, and September.The distribution of rainfall varies seasonally and from year to year. According to data gathered from a representative station in the study area, the average annual rainfall in the area ranges from 1374 to 1197 mm. Metrological stations at Wolayta, Gesuba, Danna 2, and Dinke, mean yearly temperature ranges between 17.5 °C and 22.5 °C 2016.

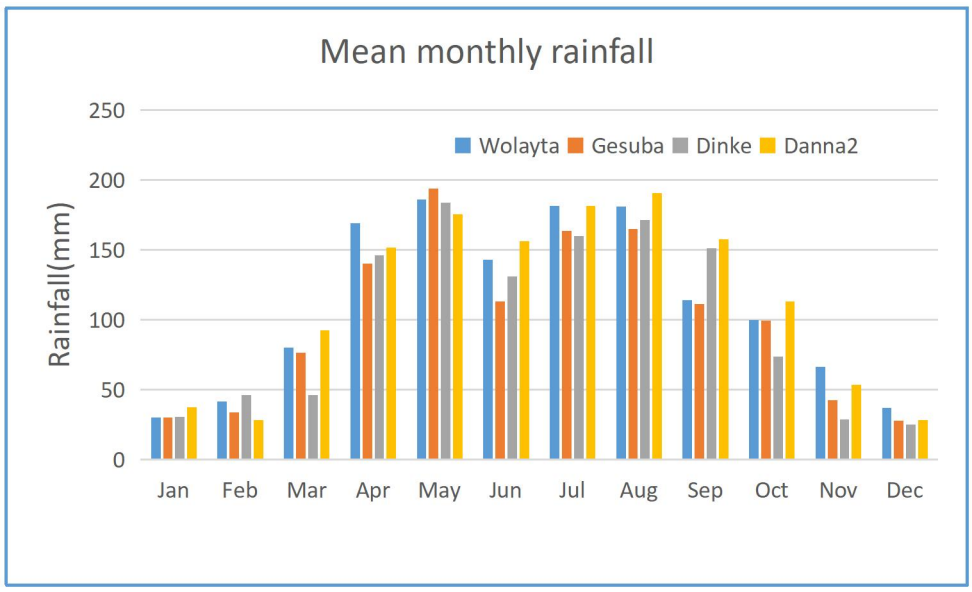

Figure3-2 Mean monthly rainfall data(mm) for 32 years from 1989 to 2020

3.1.3. Topography.

Deme Watershed's elevation ranges from 1140m to 3488masl. The plains, hills, and mountains that are flat, gently sloping to undulating, make up the majority of the watershed's landforms. The western and central portions of the watershed, which extend from Slamber town (Qucha woreda) to the outlet area of the watershed, are characterized by flat terrain. The watershed, which stretches from Selamber (northern part, eastern, southern, and south western part) to the south west of Wolayta town, is distinguished by an undulating plain and a gently sloping environment. A hilly to mountainous terrain may be found at the northern most point of Wolayta Town and the southernmost point (the mountainous part of Zara woreda) of the watershed.

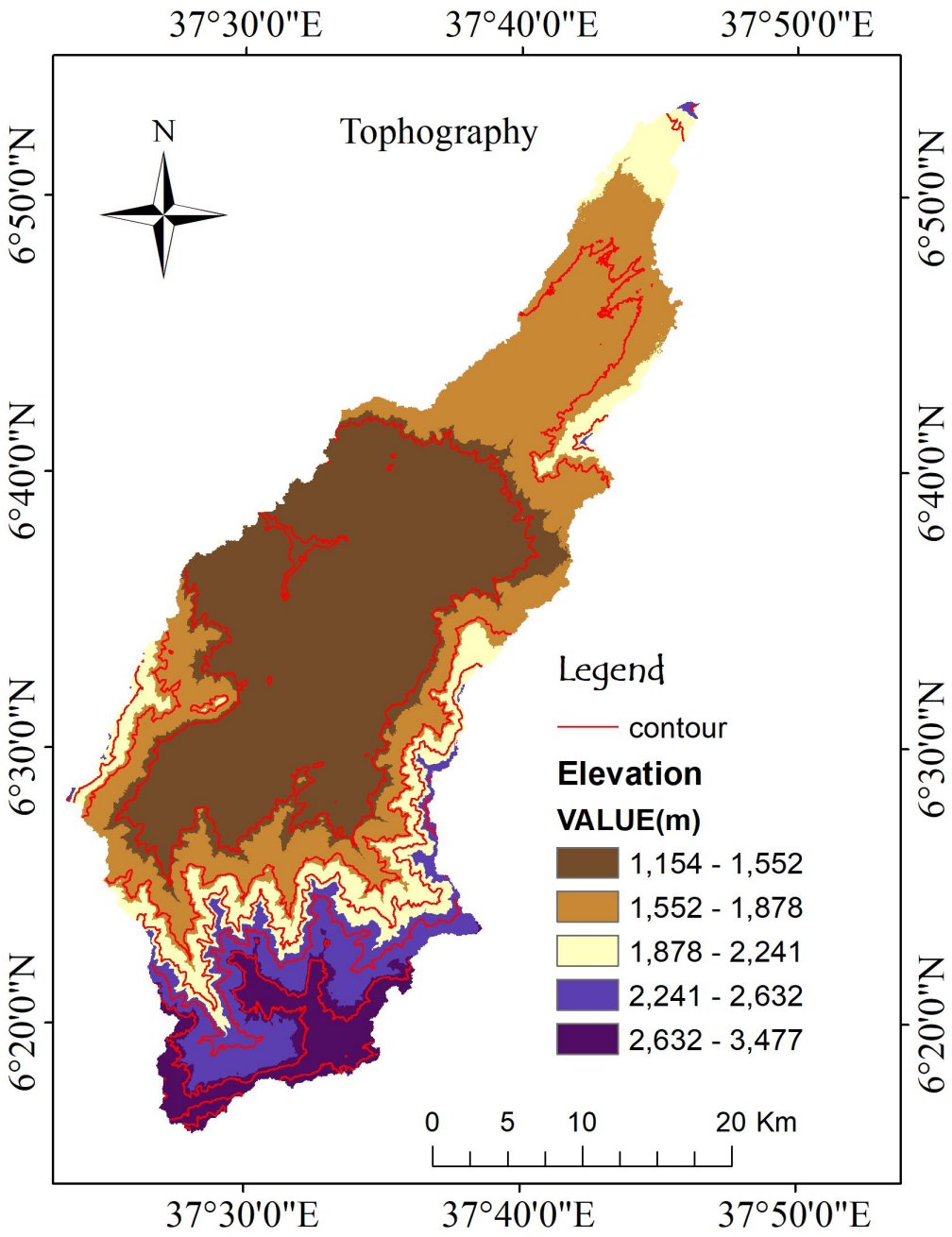

Figure 3-3 Topographic map.

3.1.4 Land use and soil.

The study region is distinguished by different agro-climate, soil, and vegetation cover because of a considerable altitudinal variation (muluken, 2021). The parts of the Omo Gibe basin's eastern catchment limit that are most heavily populated and extensively farmed are those areas (Dereje, 2015). As a result, the Deme watershed is located in the middle of the basin, where it is extensively farmed and various crops are planted. According to Richard Woodroof and companions (1996), deforested regions are now

limited to steep terrain and have been converted to agricultural use. Agriculture (73.77%), woodland (6.69%), built-up areas (1.51%), grazing land (6.09%), and waterbodies (0.4%) make up the majority of the LULC in the Deme watershed. The research region has five different types of soil, including humic alisol, lithic leptosol, chromic luvisol, humic nitisol, and eutrophic vertisol, according to the FAO soil classification system.

3.1.5 Geology.

There is limited information available on the geological formation of the study area. But according to master plan study of Omo basin the geology can be characterized by tertiary and quaternary age rhyolite and basalt volcanic in the north and middle part of the study area with quaternary alluvial overlying Precambrian basement gneisses and granite in the south. Approximately11% of the watershed area is underlain by Precambrian metamorphic gneisses and 80% of the area is underlain by Tertiary volcanic rocks. The geological domain setting of the study area is generally classified into three classes as quaternary extrusive and intrusive rock groups(Pv), tertiary extrusive and intrusive rock groups (NMn), and (NQr) Corbetti pumice flow and fall deposit as shown in figure 3-4.

Pv: quaternary extrusive and intrusive rock groups represented by lacustrine, fluvial-deltaic, and alluvial deposits and it is an aquifer with intergranular permeability.

NMn: tertiary extrusive and intrusive rock groups (NMn),which consists of ignimbrites, unwelded tuffs, ash flows, rhyolites, and trachytes. it is a jointed and faulted rock type.

NQr: Corbetti pumice flow and fall deposit (NQr), which consists of a rhyolite lava flow, pumice falls, pumice flow deposit and obsidian lava flow with fracture permeability and it has low permeability.

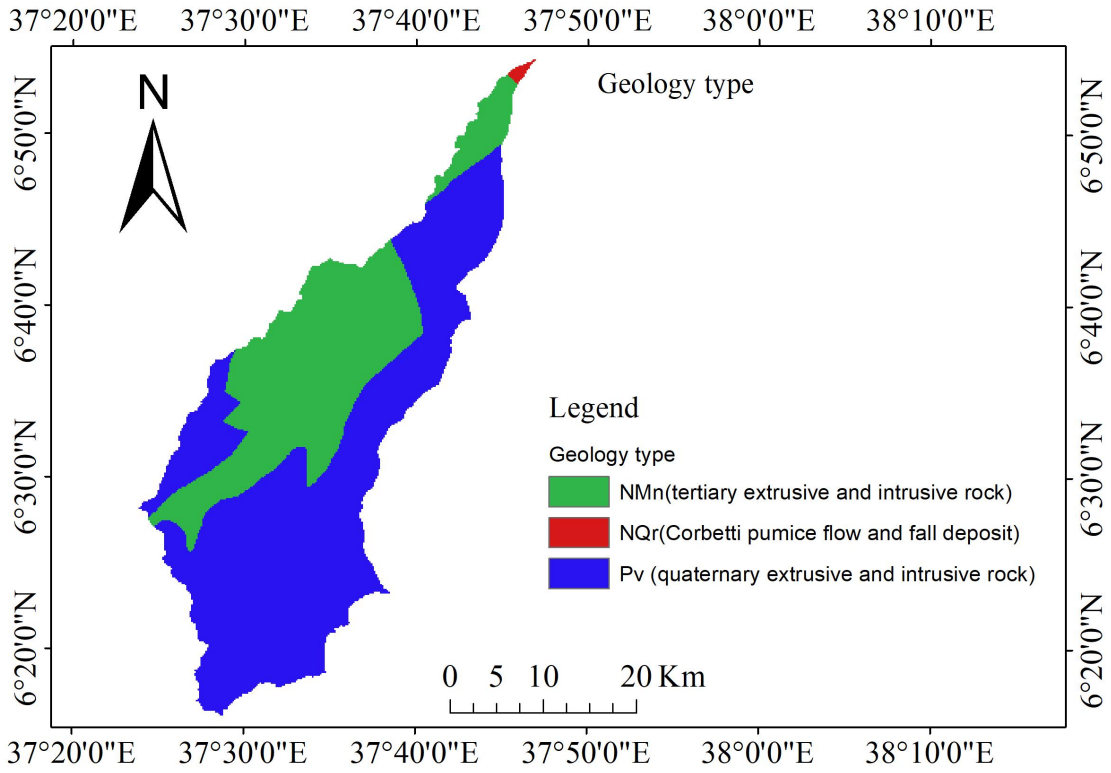

Figure 3-4. Geology map of study area.

3.2. Data Collection.

Different types of data such as meteorological, hydrological, water well inventory data and geospatial data were utilized to attain the objective of this study. These data were collected from different agencies and organizations. The DEM and satellite data were obtained from the USGS website (www.earthexplorer.usgs.gov). Geology and geomorphology data where obtained from Ethiopian geospatial institute. Soil and hydrologic data were collected from ministry of water, irrigation and electricity of Ethiopia. The meteorological data such as rainfall, temperature, humidity, and solar radiation, were obtained from the national meteorological agency of Ethiopia.

3.2.1 Digital elevation model.

DEM is digital representation of a topographic surface and specifically to a raster or regular grid of spot heights. It is the basic input for the Arc GIS integrated with Remote sensing(Erdas Emagine) model to delineate the watershed, to extract information about the topography or elevation of the watershed. It is also used to analyse the spatial extent of thematic layers of ground water influencing factors in Arc-Gis interface. For this study 30m by 30m resolution SRTM global DEM would

be obtained from USGS website. Digital elevation model (DEM) with a 30 m resolution would be used to derive a slope and drainage density map using the Arc-GIS tool (Yldrim,2021).

3.2.2 Satellite image data.

Data from remote sensing satellite images will be used to prepare thematic classes such as land use, land cover and flow density of the studied basin.

Remote sensing is the process of detecting and monitoring the physical features of an area by measuring reflected and emitted radiation from a distance (usually from satellites or aircraft). Special cameras collect remote sensing images, which help researchers "smell" everything on Earth using the DEM dataset.

Landsat 8 Operational Land Imager (OLI) satellite imagery was obtained from the United States Geological Society (USGS) website (www.earthexplorer.usgs.gov) and used to generate line densities and LULC maps. Cloud-free images of the study area was downloaded as a compressed file from the USGS website.

Table3-1 Description of Landsat image to be used.

Sensor name	Landsat 8 Operational Land Imager(OLI)	
Multi-spectral band	1 to 7 and 9	
Thermal band	10and 11	
Path and Row	169	055
	169	056
Acquisition Date	2020	
Spatial resolution	30*30	
Source	USGS (www.earthexplorer.usgs.gov)	

Automatic lineament density extraction would be performed using the line module of PCI Geomatica from land satalite image. LULC thematic maps will be prepared from land satalite image with ERDAS EMAGINE software.

3.2.3.Hydrologic data.

Water resource studies highly depend on stream flow data. Daily stream flow data for Deme river from 1989 to 2006 GC, from Oreta-alem station was collected from Ministry of Water, Irrigation and Electricity of Ethiopia. The gauging station have stream flow records from 1989 to 2006 GC. This data was used for calibration and validation purpose in SWAT CUP 5.1.6.2 to analyze the performance of SWAT2012 model.

3.2.4 Meteorological data.

Meteorological data is one of the most prerequisite parameters of SWAT and GIS mo dels to prepare grid maps of climate variables. The input data required for the SWAT simulation includes daily data on precipitation, maximum and minimum temperatures, relative humidity, wind speed, and solar radiation. These data are taken from the Ethi opian meteorologicalagency. Meteorological data used come from four stations in the Deme basin such as Wolaita sodo, Danna 2, Gesuba and Dinke meteorological station The climate data used for this study covers the period January 1989 to December 202 0. Depending on the type of station, the number of meteorological variables to be coll ected varies between stations. A detailed description of the weather station is shown

in Figure 3-5.

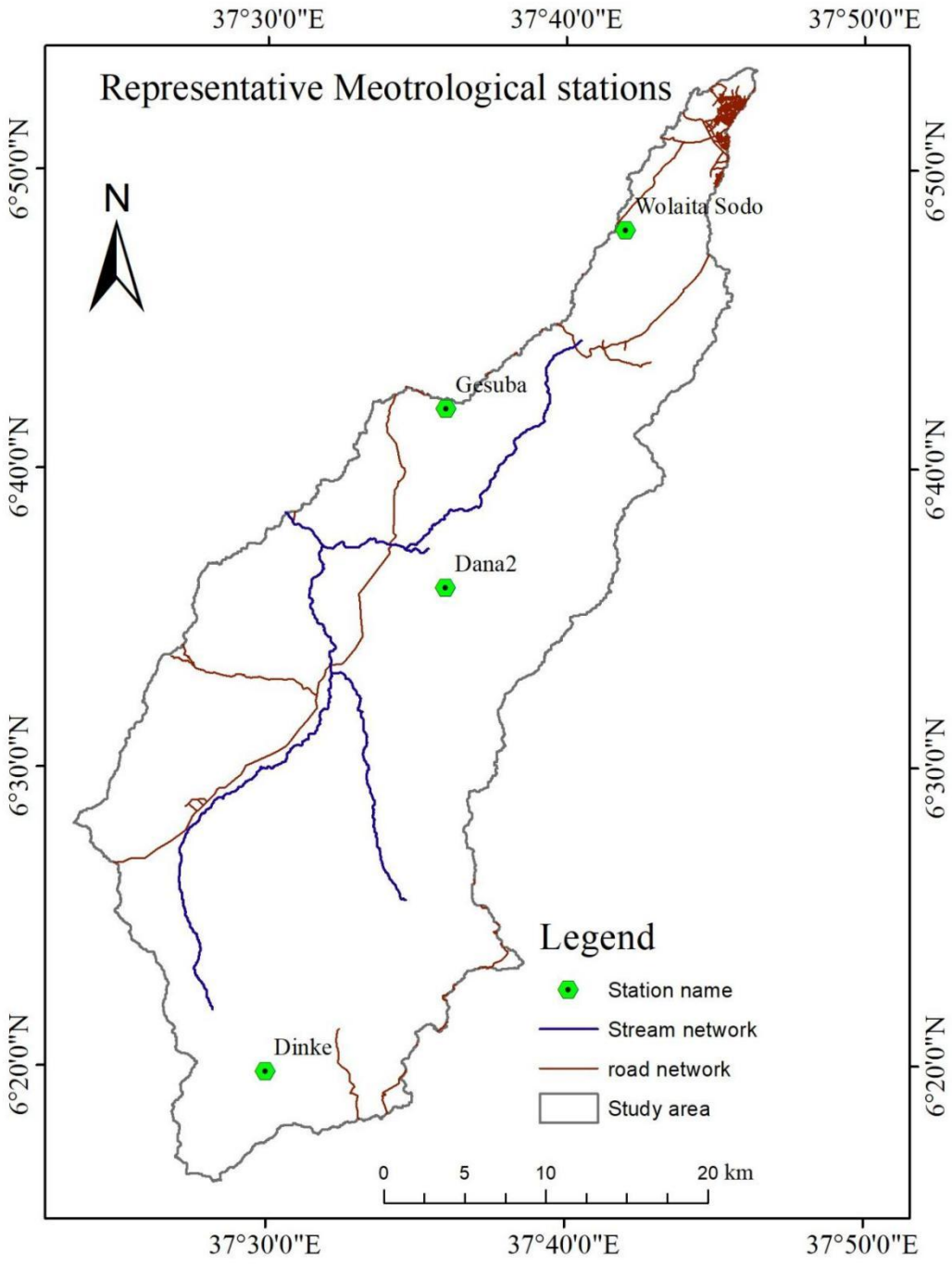

Figure3- 5. Distribution of meteorological stations in the study area.

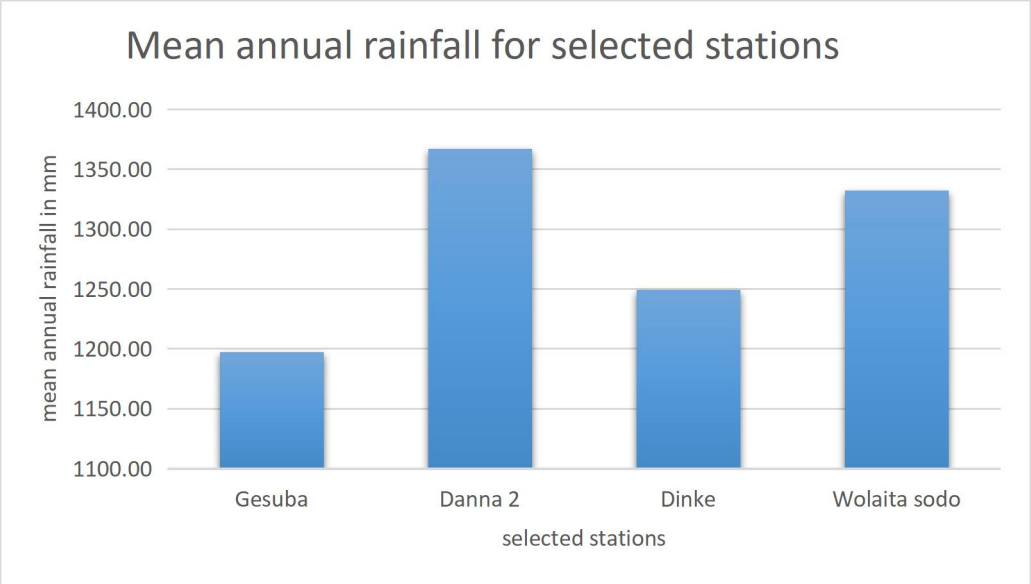

Figure 3- 6. Mean annual rainfall for selected stations from 1989-2020.

3.2.5 Soil data.

Soil data is one of the main input data of the GIS model and for making and analyzing thematic soil maps. soil map of Ethiopia in raster form taken from Ethiopia's of Ministry of Water, Irrigation and Electricity. This soil map from the FAO database has been overlaid with the study area shape file to match and obtain soil class nomenclature. This thematic soil map has been imported into the SWAT model. The SWAT model asks for physical and chemical properties of the soil such as soil texture, available water content, hydraulic conductivity, bulk density, and organic carbon content for the different layers of each soil type. A new Excel file containing the same column headings as the SWAT User Soil Table was created and these prepared soil properties were respectively populated for use in Arc SWAT2012. This prepared Excel table was then copied into the SWAT model land database.

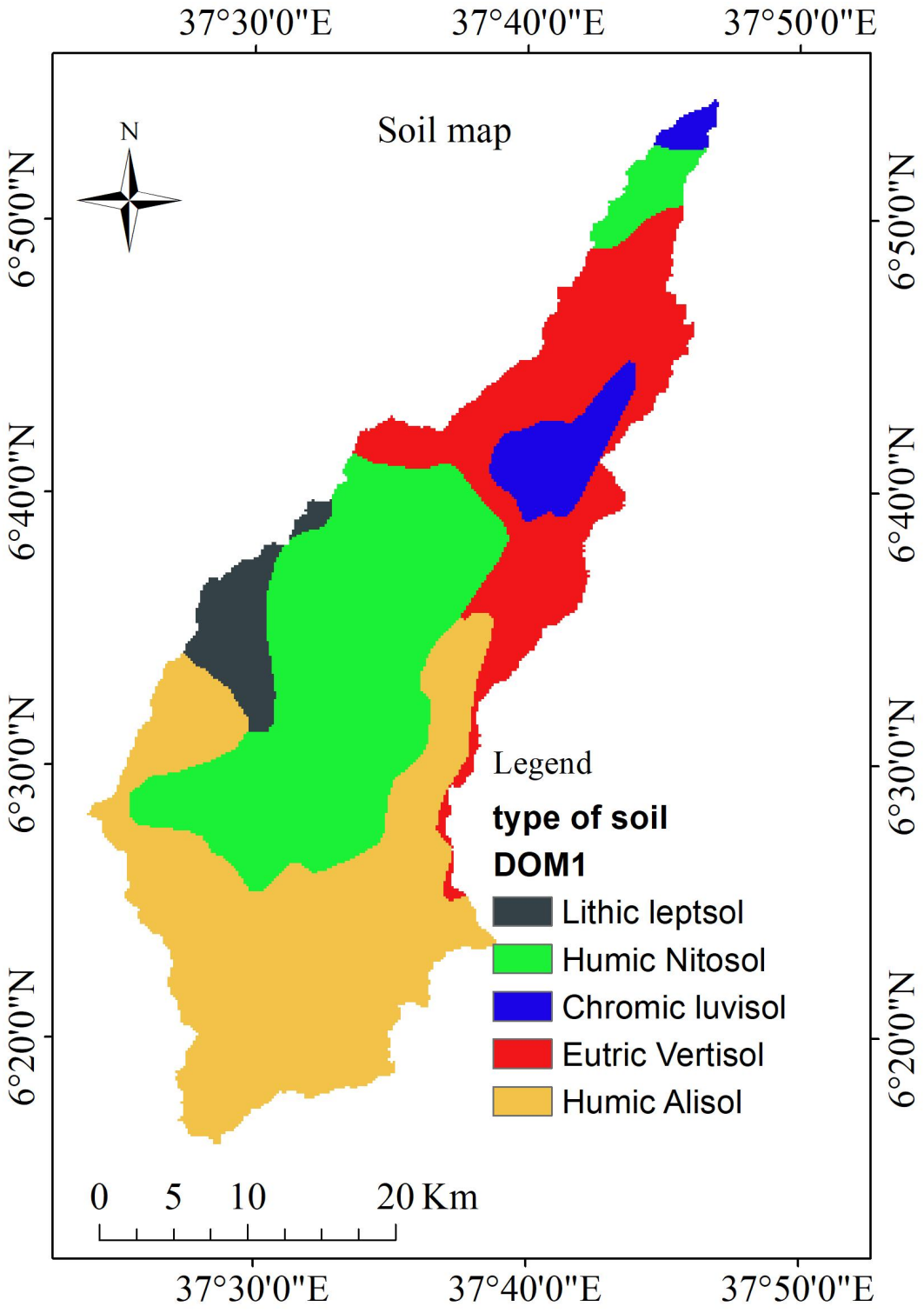

Figure3-7.Soil map of Deme watershed

3.2.6 Groundwater well data.

Ground water point data(Appendix Table-3) includes borehole, hand dug well, spring data's with information such as locations(X,Y,Z),static water level, discharge which

can be used for validation of research result with ground truth of water points on the study area. This data was obtained from Regional water, mines and energy office.

3.2.7 Geology and Geomorphology data.

Geology and Geomorphology map of Ethiopia was obtained from Ethiopian Geospatial institute to analyse and prepare thematic maps in GIS software with spatial extent of Deme watershed. The geology of the watershed is characterized by tertiary and quaternary age rhyolite and basalt volcanic rocks in the north and middle part of the study area with quaternary alluvial overlying Precambrian basement gneisses and granite in the south. These rock formations include fractured ignouse geology,aluvial, fluvial, Lacustrine alkolioviven basalt and tuffs.

Geomorphology of the watershed is characterized by undulating tophography which includes bottoms(hills), flat(flood plain), slopes of varying degree and summit(mauntainous area). The geomorphology thematic map was clipped from generalized geomorphology map of Ethiopia to the watershed for analysing ground water potential zones.

3.3 Data Analysis.

3.3.1 Factors influencing the potential groundwater zone.

To meet this objective, rainfall, geomorphology, geology, drainage density, soil, slope, landuse landcover, and lineament density data were used to develop thematic layers and to analyse their influnce on potential groundwater zones (Annesh and Paresh, 2015). The above-listed thematic layers were considered in this study as they were widely used in similar studies in various parts of the world (Waikar and Aditya, 2015: Zeinolabedinia and Esmaeily, 2015:Tesfa and Girum, 2019). The following sub-sections are provided as to show how these thematic layers were developed and how they affect potential groundwater zones.

3.2.1.1 Rainfall .

The climate data used for this study coversfrom the period January 1989 to December 2020. The data were presented in Appendix table-1.

Depending on the type of station, the number of meteorological variables to be collect ed varies between stations.

The collected data were analyzed for continuity, homogeneity, and consistency to develop areal rainfall map as described below.

I. Estimation of missed data.

Missing rainfall data can be estimated by either the arithmetic mean method or the normal ratio method. If the normal (long term mean) annual rainfall at each index station is within 10% of that for the station with the missing record, simple arithmetic mean of rainfall at index stations will provide an approximate value for the missing record, otherwise normal ratio method is applied (Subramanya, 2008). In this study, the normal ration method was used as the variation in the mean annual rainfall values were found to be more than 10%.

The equation of the Normal Ratio Method is given below

$$P_A = \frac{1}{n}\left(\frac{N_A P_B}{N_B} + \frac{N_A P_C}{N_C} + \ldots + \frac{N_A P_N}{N_N}\right) \qquad Eq.3.1$$

where, N_A, N_B, N_C…N_N=normal annual rainfall values at station A, B, C …N: P_B, P_C… P_N =rainfall records at index stations at the time of missing records and P_A= an estimated value for missing record at station A.

II. Homogeneity test.

The analysis of precipitation data is important to determine if rainfall stations in or around a watershed exhibit similar regional characteristics that would aid in further analysis. Homogeneity analysis was used to determine the variation in the statistical properties of the time series. The cause of the change can be natural or man-made. These include changes in land use and relocation of observation posts. Therefore, in order to select a representative meteorological station for the analysis of surface precipitation forecast, it is necessary to verify the uniformity of the stations in the group and to check the uniformity of rainfall data. month of the selected measuring stations. by the dimensionless parameterization method (Peterson et al., 1998) .

$$\text{Pi} = \frac{\text{over year average monthly pcp for month i}}{\text{the over years average yearly pcp of station}} \quad \ldots\ldots\ldots\ldots\ldots\ldots\ldots\ldots\ldots\ldots\ldots\ldots\text{eq3.2}$$

The selected stations were also plotted for comparison with each other in the figure below. These shows the same mode and pattern for the selected station. These assures that the selected stations were homogenous.

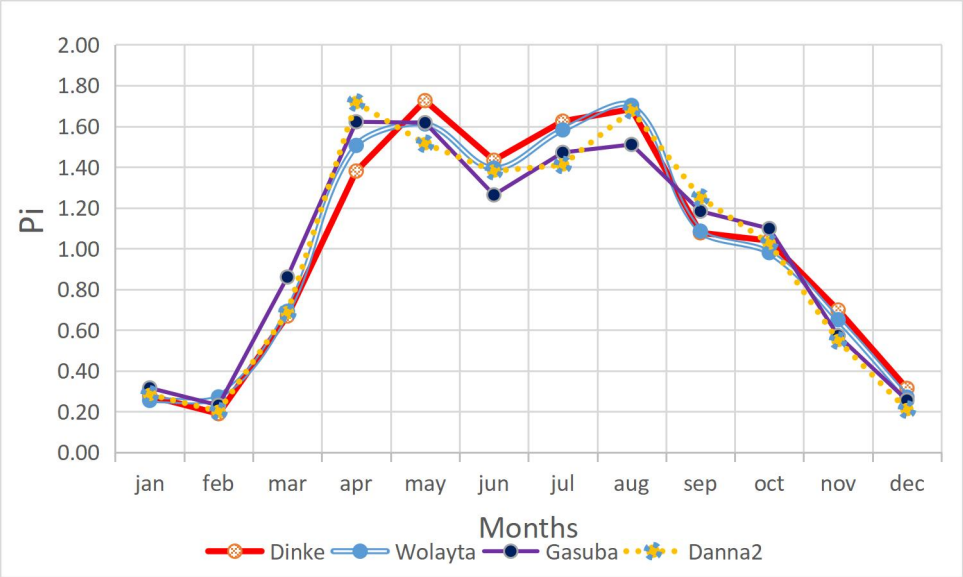

Figure 3- 8. Homogeneity test for the stations

III. Consistency test.

Double mass curves (DMC) was used to check the consistency of precipitation data to correct for inconsistent data. This technique is based on the principle that when each recorded data comes from the same original sample, it is consistent.

A consistent record is a record whose characteristics do not change over time. A double mass curve is a graph of the cumulative catch at the rain gauge of interest versus the cumulative catch of one or more gauges in more measures in an area that has been subjected to similar hydrometeorological events and is know to be consistent. The double mass curve will have a constant slope if the precipitation record of hydro meteorological events over the recording period is consistent (Giambelluca et al., 1986). A change in the slope of the double mass curve would suggest that an external factor caused the changes in the properties of the measured values. If there is a change in slope, then recording should be adjusted with the earliest or latest recording intervals undisturbed.

$$P_{cx} = P_x \frac{M_c}{M_a} \quad \text{.....eq3.3}$$

P_{cx} = corrected precipitation at any time period t1 at station

P_x = original recorded precipitation at time period t1 at station X

Correction ratio = M_c/M_a

M_c = corrected slope of the double-mass curve, M_a = original slope of the double-mass curve

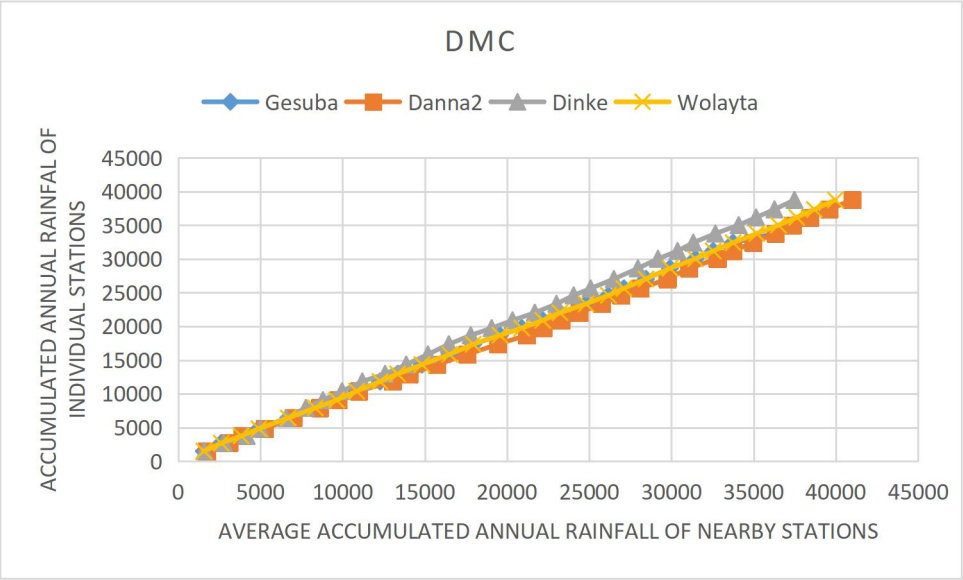

Figure 3- 9. DMC to test consistency of meteorological station

IV. Preparation of areal rainfall map.

In applying meteorological data to the whole catchment area for analysis of groundwater potential zone, it is often necessary to estimate the average areal rainfall for a catchment from rain gauge observation data. For this task inverse distance weight (IDW) interpolation techniques were applied in ArcGIS. In the IDW interpolation method, the sample points are weighted during interpolation such that the influence of one point relative to another decline with distance from the unknown point to be created weighting is assigned to sample points through the use of a weighting coefficient that controls how the weighting influence will drop off as the distance from new point increases. The greater the weighting coefficient, the less the effect points will have if they are far from the unknown point during the interpolation process. Then, the map is assigned and converted to a characteristic spatial representation format to make them suitable for analyses in GIS environments.

The prepared rainfall map is classified into five categories depending on their relation with groundwater potential zone prospects. The classes were developed as per the recommendation by (Tolche, 2021; Zeinolabedinia, and Esmaeily, 2015) .

3.3.1.2 Geology.

To develop the geology map of the study area, the geology data for this task was collected from the Geological Survey of Ethiopia and the map was prepared from this data by clipping method in the GIS environment. The geology of the study area was classified into three classes as it was extracted from ethiopian geological map. Deme watershed's geologic formation was catagorized in to three domain groups such as: quaternary extrusive and intrusive rock groups (Pv), tertiary extrusive and intrusive rock groups (NMn) and Corbetti pumice flow and fall deposit(NQr).

Then this map was resampled to suitable cell size format to develop thematic map of geology. Once the map was prepared in the required manner, a geology thematic layer was developed with classes as appropriate for groundwater potential prospective scaling as recommended by (Dainelli et al., 2001; Stefano et al., 2002).

3.3.1.3 Lineament Density

To develop the lineament density map of the study area, satellite image of the study area for the year 2020, Landsat 8 OLI images were downloaded from the USGS website(www.earthexplorer.usgs.gov). The downloaded satellite image was processed using PC Geomatics software then the line density method was used in the ArcGIS environment.

The lineament density was categorized into five classes such as 0-0.11km/km^2, 0.11-0.3km/km^2, 0.3-0.51km/km^2,0.52-0.76km/km^2, and 0.77-1.5km/km^2.

The classes were developed as per the recommendation by (Waikar and Nilawar, 2014; Tolche, 2021). Then lineament density was reclassified and resampled to with suitable cell size format in GIS to prepare thematic map of lineament density.

3.3.1.4 ULCC.

Land use/cover is one of the most important factors influencing runoff, evapo-transpiration and surface erosion in a river basin and can also be an input to the hydrologic response unit (HRU). Land use maps can be generated from satellite images using ERDAS image classification. First, the number and type of LULCs in the deme watershed were determined to perform image classification. Image

classification sets of pixels to represent LULC classes. The task of extracting information layers from multiband raster images was performed using USGS satellite imagery. Before image classification, image pre processing is performed first. It's about stacking layers, mosaiking an image, and adjusting under an image. For remote sensing image analysis, different images representing different bands are superimposed. Layer stacking allows different RGB combinations to be displayed.

After the image preprocessing is complete, the image classification is performed. For these studies, land use and land cover maps were generated based on a pixel-based supervised maximum likelihood classification. The selection of training sites that are typically representative of LULC classes is done using Google Earth. To do this, Google Earth was connected to ERDAS IMAGINE 2014 to generate AOIs for all feature class of satellite images. The number of training locations should be at least three times the number of interest categories (Khorram, 2013). After the designated training area for each class classification activity has been completed.

Table 3- 2. Description Of AOI used for LULC classification

Reference points for AOI	LULC Classes					
	Agricultural land	Built up Area	Forest land	Bush land	Grass Land	Water body
No. of AOI for 2020	200	27	100	146	72	35

In the final step, the classification of the images was then performed. Techniques used in post-processing included re-encoding and evaluating the accuracy of the classified images to verify and validate the results. The same layers with different reflectance colors are classified individually or separately and then re-encoded as a single layer.

I. Accuracy assessment

Accuracy assessment is an important step in the image classification process. The purpose of this process is to determine how effectively the pixels are grouped into the correct feature classes in the area under study. This is a process used to estimate the accuracy of image classification by comparing the classified map with the reference

map (Caetano et al., 2005). The error matrix was used to derive a series of descriptive statistics and analyzed to evaluate the accuracy (Manandhar et al., 2009). The columns of the matrix represent the number of pixels per layer for the reference data, and the rows show the number of pixels per layer for the classified image. From this error matrix, an accuracy number measures overall accuracy, user accuracy, and manufacturer accuracy.

An assessment of the accuracy of the classified map is made by comparing the classified image and the sampling points of the Google Earth image and/or knowledge of the study area. Various sampling designs were applied to evaluate the accuracy, such as the simple randomization method, the stratified randomization method, and the systematic method (Stehmn, 2000). Stratified random sampling was used in this study. For stratified random sampling, the following sample size formula is provided (Cochran 1977). These formulas are used to determine the sample size to perform the accuracy assessment.

$$N = \left(\frac{\sum WiSi}{So}\right) \text{.....3.4}$$

Where Wi = is mapped proportion of area of class i

$Si = \sqrt{U_i} * \sqrt{(1-U_i)}$

So = is the standard error of estimated over all accuracy

U_i= is for user's accuracy

Table 3- 3. Description on reference points used for accuracy assessment

Reference points for Accuracy assessment	LULC Classes					
	Agricultural land	Built up area	Forest land	Bush land	Grass land	Water body
No.of (X,Y) coordinates for 2020	141	36	78	87	44	29

3.3.1.5 Slope Factor.

To generate the slope map of the study area, the DEM of the study area was downloaded from the USGS website (www.earthexplorer.usgs.go). The downloaded DEM was processed using ArcGIS, then slope (spatial analyses tools) was used and finally it was processed in the ArcGIS environment for further analyses. Once the developed map was prepared in the required manner, a slope thematic layer was developed with five classes appropriate groundwater potential mapping.

The classes were developed as per the recommendation by (Daniel et al.., 2018; Waikar and Nilawar, 2014) have reported Slope gradient and category. The identified slope of the study area category varies from (0-65^0) and the area was classified into five classes like (0-13^0) flat, (14-26^0) gently sloping, (27-39^0) moderately sloping, (40-52^0) steeply sloping, and (53-65^0) strongly steeply sloping.

3.3.1.6 Geomorphology.

Geo morphology map of Ethiopia was obtained from Ethiopian Geospatial institute to analyse and prepare thematic maps in GIS software with spatial extent of Deme watershed. Geo morphology of the watershed is characterized by undulating tophography which includes bottoms(hills), flat(flood plain), slopes of varying degree and summit(mauntainous area). The geomorphology thematic map was clipped from generalized geomorphology map of Ethiopia to the watershed for analysing ground water potential zones. Then this map was reclassified and resampled to appropraite cell size in ArcGIS to develop thematic maps for groundwater potential prospective analysis. The classes were developed as per the recommendation by (On, 1768; Arnot & Grant, 1981) description of landform classification.

3.3.1.7 Soil.

Soil data is one of the main input data of the GIS model for making and analyzing thematic soil maps. soil map of Ethiopia in raster form taken from Ethiopia's of Ministry of Water, Irrigation and Electricity. This soil map from the FAO database has been overlaid with the study area shape file to match and obtain soil class nomenclature. To develop the soil map of the study area, Geospatial clipping process , to determine soil spatial data with watershed boundary from Ethiopia's soil spatial map in the GIS environment.

It was found that the study area soil type is categorized as humic alisol, lithic leptosols, chromic luvisol, humic nitosol, and eutric vertisol according to FOA soil classification, with the soil texture of each soil type being clay-loam, clay loam, silt-clay-loam, clay, and clay soil type, respectively based on their grain size using the United States Department of Agriculture (USDA) textural classification methods.

Spatial soil map was reclassified and adjusted to appropriate cell size to develop thematic map of soil in GIS software. Once the developed map was prepared in the required manner, a soil thematic layer was developed with classes for groundwater potential prospective as recommended by (Tolche, 2021).

3.3.1.8 Drainage Density.

To develop the drainage density map of the study area, a digital elevation model (DEM) of the study area was downloaded from the USGS website. The downloaded DEM was processed using ArcGIS environment by applying line density method that included different processes like filling sinks, creating flow direction, creating flow accumulation, creating stream order, and finally converted stream order to features then drainage density map was obtained.

Drainage density of the study area was classified into five categories which were 0.0-0.68 km/km2, 0.69-1.32km/km2, 1.33-1.96km/km2, 1.97-2.61Km/Km2 and 2.62-3.26km/km2. Once the obtained map was prepared in the required manner, a drainage density thematic layer was developed with classes for appropriate groundwater potential mapping. The classes were developed as per the recommendation by (Tolche, 2021; Waikar, and Nilawar, 2014).

3.3.2 Groundwater Recharge Estimation.

To achieve this objective climate, hydrological, soil, slope, landuse landcover, DEM data were used to develop grid layers, and for further analyses using hydrologic simulation based method with SWAT2012 model and to evaluate the performance of SWAT model with SWAT CUP5.1.6.2 software..

The SWAT2012 mode model requires all grid maps should be represented by the same row and column as well as similar cell size. In terms of this, the inputs of satellite data and meteorological data grid maps have similar cell size. All meteorological grid maps were prepared on monthly basis. The rest of the necessary maps were as analyzed in the above section 3.2.1.1 and assumed to be constant. Therefore, soil, slope, DEM, and landuse/land cover maps used were the same through the study.

Recharge is the primary means by which water reaches the aquifer and therefore its qu antification is important for the integrated and sustainable management and use of sur face and groundwater resources (Githui et al., 2012). ; Jin et al., 2015). The SWAT m odel has been applied to estimate the amount of replenishment (general water balance) worldwide (Awan and Ismaeel, 2014; Githui et al., 2012; Jin et al., 2015; Eshtawi et al., 2016; Putthividhya et al., Laonamsai, 2017).

3.3.2.1 Hydrological data analysis.

Records of Stream flow in deme watershed is obtained from MOWE with dailly data time series starting from 1989 up to 2006 of Orata alem station**.** Before using the hydrological record data of station, it is necessary to check the data for continuity. To do these the missing data should be filled by using the data of the neighbor stations such as Gogora and Mazie river with inverse distance weighted method.

1.Inverse Distance Weighting (IDW) method**.**

Inverse distance (ID) method is the most commonly used for estimation of missing data. In this method, it is based on the distance between target station and nearby station. The closer stations are better correlated with the target station compared to further stations(Wan,2019).

The estimated missing value is given by

$$P = \frac{\sum_{i=1}^{n} {}^{x_i}/_{d_{it}}}{\sum_{i=1}^{n} {}^{1}/_{d_{it}}} \qquad \text{……..eq3.5.}$$

Where:- p is Stream flow value at target station in m^3/s.

d_{it} is the distance between target station and the i^{th} nearby station in m.

X_i is stream flow value at surrounding station in m^3/s

Finally the adjusted stream flow records of Deme river(Appendix Table-2) was utilized for sensitivity, calibration, and validation process in SWATCUP5.1.6.2 to evaluate SWAT2012 model performance.

3.3.2.2 Water balance of SWAT.

The SWAT model has been applied to estimate the amount of replenishment (general water balance) worldwide (Awan and Ismaeel, 2014; Githui et al., 2012; Jin et al., 20 15; Eshtawi et al., 2016; Putthividhya et al., Laonamsai, 2017). SWAT is a physical m odel of watershed hydrological response units (HRUs) (Abbaspour et al., 2007; Arnol d et al., 2012).

SWAT uses data to simulate soil and groundwater flows, erosion, nutrient cycling, an d more. (Arnold et al., 1998). There are different versions of SWAT with different int erfaces; here 2012 version with GIS interface (SWAT) was used. HRU is the smallest segment of a watershed representing different LULC, land and landscape features in t he sub-basins. The discharge is calculated separately for each segment of the basin. T he general equation of the SWAT model is as follows (Arnold et al., 1998):

$$Sw_t = Sw_o + \sum \left(R_{day} - Q_{surf} - E_a - W_{seep} - Q_{gw}\right) \ldots\ldots\ldots\ldots eq3.6$$

Where SW_t = the final soil water content (mm).

SW_o = the initial soil water content on day i (mm).

t = the time (days).

R_{day} = the amount of precipitation on day i (mm).

Q_{surf} = the amount of surface runoff on day i (mm).

E_a= the amount of evapotranspiration on day i (mm)

W_{seep}= the amount of water entering the vadose zone from the soil profile on day i (mm).

Q_{gw} =the amount of return flow on day i (mm).

Water balance is the driving force behind all the process in SWAT model. Weather data such as daily precipitation, maximum/minimum air temperature, solar radiation, wind speed and relative humidity are required to do the water balance by SWAT model. SWAT can read directly these observed data from files from excel. In SWAT, Physical characteristics, such as slope, reach dimension and climatic data are considered for each sub watershed. For climate data, SWAT uses the data from the station nearest to the centric of each sub watershed. The water in each HRU in SWAT is stored in soil profile, shallow aquifer and deep aquifer.

Surface runoff from daily rainfall is estimated using SCS curve number method, which estimates the amount of runoff based on local LULC, soil type and antecedent moisture condition. The watershed concentration time is based on manning's formula, considering both overland and channel flow. Potential evapotranspiration can be estimated by the Penman Monteith, Priestley-Tylor or Hragreaves methods.

I.Hydrologic Water balance equation of swat model.

The Simulation of the hydrology of a watershed is done in to two separate divisions. One is the land phase of the hydrological cycle that controls the amount of water, sediment, nutrient and pesticide loadings to the main channel in each sub-basin. The second division is routing phase of the hydrologic cycle that can be defined as the movement of water, sediments, nutrients and organic chemicals through the channel network of the watershed to the outlet. In the land phase of hydrological cycle, SWAT simulates the hydrological cycle based on the water balance equation (equation).

Where SWt = the final soil water content (mm),

SWo = the initial soil water content on day i (mm),

t = the time (days),

$$SW_t = SW_o + \sum (R_{day} - Q_{surf} - E_a - W_{seep} - Q_{gw}) \quad \text{.....eq3.7}$$

R_{day} = the amount of precipitation on day i (mm),

Q_{surf} = the amount of surface runoff on day i (mm),

E_a= the amount of evapotranspiration on day i (mm),

W_{seep}= the amount of water entering the vadose zone from the soil profile on day i (mm),

Q_{gw} =the amount of return flow on day i (mm).

A. Surface runoff.

Surface runoff occurs whenever the rate of precipitation exceeds the rate of infiltration. SWAT offers two methods for estimating surface runoff: the SCS curve number procedure (USDA-SCS 1972) or Green &Ampt infiltration method (Green and Ampt, 1911). Using daily or sub daily rainfall, SWAT simulates surface runoff volumes and peak runoff rates for each HRU. In this study, the SCS method was used to estimate surface runoff because of the unavailability of sub daily data for Green &Ampt method. The SCS curve number equation is:

$$Q_{surf} = \frac{(R_{day}-0.2S)^2}{R_{day}-0.8S} \text{.....eq.3.8}$$

In which, Qsurf is the accumulated runoff or rainfall excess (mm), R_{day} is the rainfall depth for the day (in mm), S is the retention parameter (in mm). The retention parameter is defined by

the equation:-

$$S = 25.4 * \left[\frac{100}{CN} - 10\right] \quad \text{.....eq3.9}$$

Where, CN is the curve number for the day and its value is the function of land use practice, soil permeability and soil hydrologic group.

B. Potential evapotranspiration.

Potential Evapo transpiration is a collective term that includes evaporation from the plant (transpiration) and evaporation from the water bodies and soil. There are many methods that are developed to estimate potential evapotranspiration (PET). SWAT provides three options for PET calculation: Penman-Monteith (Monteith, 1965),

Priestley-Taylor (Priestley and Taylor, 1972), and Hargreaves (Hargreaves et al., 1985) methods. The methods have various data needs of climate variables.

For this study, the Penman-Monteith method was selected as the method is widely used and all climatic variables required by the model are available for the three stations in and around the study watershed area.

C. Groundwater flow

To simulate the ground water, SWAT partitions groundwater into two aquifer systems: a shallow, unconfined aquifer which contributes return flow to streams within the watershed and a deep, confined aquifer which contributes return flow to streams outside the watershed (Arnold et al., 1993).

$$aqsh_i = aqsh_{i-1} + W_{rchrg} - Q_{gw} - W_{revap} - W_{deep} - W_{pump,sh} \quad \text{.....eq3.10}$$

Where, aq $sh_{,i}$ is the amount of water stored in the shallow aquifer on day i (mm),

$aqsh_{,i\_1}$ is the amount of water stored in the shallow aquifer on day i-1 (mm),

W_{rchrg} is the amount of recharge entering the aquifer on day i (mm),

Q_{gw} is the ground water flow, or base flow, or return flow, into the main channel on day i (mm),

W_{revap} is the amount of water moving in to the soil zone in response to water deficiencies on day i (mm),

W_{deep} is the amount of water percolating from the shallow aquifer in to the deep aquifer on day i (mm), and

$W_{pump,sh}$ is the amount of water removed from the shallow aquifer by pumping on day i (mm).

SWAT simulates two aquifers for individual sub basin: a shallow unconfined aquifer that donates water to the main stream or reaches of the subbasin and a confined deep aquifer (Arnold et al., 1993). The total recharge is computed using the following equation in SWAT model.

$$W_{rch,i} = \left(1 - e^{-\frac{1}{\lambda_{gw}}}\right) W_{seep} + e^{-\frac{1}{\lambda_{gw}}} W_{rch,i-1} \quad \text{.....eq3.11}$$

where $W_{rch,i}$ and $W_{rch,i-1}$ are water inflowing to the aquifer on day i and day i-1, $б_{gw}$ the drainage delay time of the top formation (days), and W_{seep} is the water leaving from the soil profile at the bottom (day i) which can be calculated using the following relation.

$$W_{seep} = W_{perc} + W_{crk,btm} \quad \text{.....eqq3.12}$$

where W_{perc} is the water escaping from the second layer (mm/ day), and $W_{crk,btm}$ is the bypass flow from the soil profile at the lower boundary (day i).

The deep aquifer obtains some portion of the total recharge approximated with the following formula: $W_{deep} = \beta_{deep} \times W_{rch}$ eq3.13

where W_{deep} is the water moving from shallow to the deep aquifer (day i),

β_{deep} is the percolation coefficient, and W_{rch} is as defined in eq3.11.

3.3.2.3 SWAT model set up

I. Watershed delineation

In the SWAT project, configure the project name and file location of the project speci fied. Then the next step is to delineate the watersheds. The DEM data is projected to t he UTM in region 37. After loading the DEM, the next step is to define the stream. T he watershed demarcation has been further refined in this section by defining the outle t point for the entire basin. The location of the Deme river outlet has been manually

added to the defined flow.

II. Hydrologic response unit analysis

After watershed demarcation, LULC, soil, and watershed slope characterization was performed using commands from the HRU analysis menu on the Arc SWAT toolbar. These tools are used to load LULCs and soil layers from the Deme River basin into the current project. Thus, the LULC/soil/slope combination and distribution for the delimited Deme basin was determined in the HRU analysis. Finally, the watershed is divided into HRUs with similar combinations of soil and LULC.

The LULC composite map and prepared soil map are provided as input to the model at this stage. A lookup table containing the various SWAT LULC class codes has

been prepared. This prepared lookup table is linked to the SWAT LULC database. To link the prepared LULC data to the SWAT database, a lookup table was first prepared. This lookup table has two columns named value and name. The value in the lookup table corresponds to the value of the LULC layer in the attribute table for the classified image, and the name corresponds to the name of the LULC layer corresponding to the name in the SWAT database. This prepared lookup table is then invoked when determining the LULC/Soil during HRU formation.

Similarly, the physical properties of the soil are initially stored in the SWAT database through an interface, the relevant information required for hydrological modeling. This Arc SWAT soil database and the study area soil data are linked by a lookup table. To determine the HRU distribution, the multiple HRU option, which generates multiple HRUs in each sub-basin, was selected. The number of HRUs in the catchment is controlled by the threshold value given when determining the HRU (Melese, 2008) given that 10% LULC, 20% soil, and 10% slope allow a better estimate of replenishment.

III. Write input table

After HRU analysis the weather data to be used in watershed simulation was imported using the first command in the write input table menu item on the Arc SWAT toolbar. This tool helps to load weather stations location in to the current project and assign weather data to the sub watershed. The weather data definition is divided in to six tabs weather generator data, rainfall data, temperature data, solar radiation data, wind speed data and relative humidity data. Arc SWAT reads weather data from the WEGEN users database in which relevant information about climate required for hydrologic modelling was stored. SWAT weather database, which was designed to be friendly to store and process daily weather data to be used with SWAT project, is used to create WEGEN users. Then this prepared WEGEN users was imported to SWAT database to use for this study. Then for weather data definition, the weather generator data file WGEN user, rainfall data, temperature data, relative humidity data, solar radiation data and wind speed data were selected and added to the model respectively. SWAT simulation was the final step which includes running the model and reading SWAT output.

3.3.2.4. Sensitivity analysis, calibration and validation of the model.

I. Sensitivity analysis.

SWAT input parameters are process based and must be held within realistic uncertainty range. The first step in calibration and validation process in SWAT is the determination of the most sensitive parameters for a given watershed. The user determines which variables to adjust based on sensitivity analysis. Sensitivity analysis is the process of determining the rate of change in model output with respect to changes in model input parameters. It's necessary to identify key parameters and the parameter precision required for calibration (Ma et al., 2000).

In this research SUFI2 was used to identify the sensitive parameters. There are two kinds sensitivity, One-at-a-time sensitivity analysis and Global sensitivity analysis. One-at-a-time sensitivity analysis shows the sensitivity of one variable to the change in parameter while other parameters are kept constant at some value. The problem here is the value of those other constant parameters is not known. This is an important consideration as the sensitivity of one parameter depends on the value of other parameters. Global sensitivity analysis sees all variables sensitivity at once but it needs large number of simulation. Global sensitivity was used in SUFI2 prior to calibration and the result was examined for this research. In global sensitivity parameter, t-stat and p-value are used to identify the relative significance of each parameter. Larger t-stat in absolute value and p-value close to zero are more sensitive as suggested by SUFI2 user manual.

In the sensitivity process, the SWAT simulated "TxtInout" was copied to the working directory and SWAT CUP SUFI2 was used for performing the sensitivity of selected parameters with default upper and lower parameter bounds. The selection of sensitive parameters was done by reviewing different literatures in ethiopia (Wakjira et al., 2016: Tadele 2007; Webster 2010). Upon completion of sensitivity analysis, a t-stat and p-value was used to identify the relative significance of each parameter.

Table 3-4 Parameters used for sensitivity analysis .

Parameters	**Description**
1:A__CN2.mgt	SCS runoff curve number
2:A__ALPHA_BF.gw	Alpha base flow recession constant
3:V__GW_DELAY.gw	Groundwater delay
4:V__GW_REVAP.gw	Groundwater revap coefficient
5:R__OV_N.hru	Manning's "n" value for overland flow.
6:R__SOL_BD(..).sol	Moist bulk density.
V__SOL_AWC(..).sol	Available water content of soil
8:R__GWQMN.gw	Threshold depth of water in the shallow aquifer for return flow to occur
9:R__RCHRG_DP.gw	Deep aquifer percolation fraction
10:R__HRU_SLP.hru	Average slope steepness
11:R__CANMX.hru	Maximum canopy storage
12:R__ESCO.hru	soil evaporation compensation factor
13:R__SLSUBBSN.hru	Average slope length.
14:R__CH_N2.rte	Mannings n value for the main channel
15:R__SOL_Z(..).sol	Soil depth (for each layer)
16:R__SOL_K(..).sol	Saturated hydraulic conductivity
17:R__REVAPMN.gw	Percolation to deep aquifer to occur

II.Calibration

After sensitivity analysis, the sensitive parameters were used for model calibration. Calibration was done to better parameterize a SWAT model to a given set local conditions, there by reducing prediction uncertainty. Storm(1996) differentiated three types of calibration procedure such as Manual trial and error,automatic calibration (numerical parameter optimization) and combination of the two. Yenealem (2018) recommended that combination of the manual and auto calibration. For this study, first manual calibration was done and some parameters were adjusted in the SWAT model. Then auto calibration was applied for the calibration of SWAT model. In the SWAT-CUP calibration procedure the SWAT simulation was specified for

performing the calibration and the location of the sub-watershed where the observed flow could be compared against simulated output. Then, the desired parameters for optimization, observed data and methods of calibration were selected. Two third of the total data (1989 to 2001) was used for calibration.

Table 4-5 Sensitive parameters used during calibration accordingly.

Parameter_Name	Fitted_Value	Min_value	Max_value
1:R__OV_N.hru	0.0067	0.0	0.015
2:R__REVAPMN.gw	0.95	0.100000	1
3:V__GW_REVAP.gw	0.0315	0.029	0.032
4:R__RCHRG_DP.gw	1.022500	0.830000	1.180000
5:A__CN2.mgt	0.3	0	6
6:R__ESCO.hru	0.185000	0.05	0.35
7:R__CANMX.hru	1.404550	0	4.013
8:R__HRU_SLP.hru	0.106	0.083	0.54
9:V__SOL_AWC(..).sol	0.087	0.016	0.30

III. Validation.

Calibration was used to test the calibrated parameters with an independent set of data without further changes to parameters. For validation one third (2002-2006) of the total data was used. Both calibration and validation was done based on monthly stream flow data.

3.3.2.5. Model performance evaluation

To evaluate SWAT model simulation outputs in relative to the observed data, model performance evaluation is necessary. There is various method to evaluate the model performance during calibration and validation periods. For this study coefficient of determination (R^2), Nash and Sutcliff simulation efficiency (NSE) and PBIAS were used. Determination Coefficient describes the linear relationship between simulated and observed data. Its value ranges between 0 to one. The higher value close to 1

indicates good co-relation, and typically values greater than 0.6 are considered acceptable (Santhi etal., 2001).

$$R^2 = \frac{[\sum (Q_o - meanQ_o)(Q_s - meanQ_s)]^2}{\sum (Q_o - meanQ_o)^2 \sum (Q_s - meanQ_s)^2} \quad \text{.....eq3.14}$$

Where, Q_o is Observed stream flow data in m^3/s

Q_s is Simulated data in m^3/s

The Nash and Sutcaliffe simulation efficiency indicates how well the plots of observed versus simulated data fits the 1:1 line.

$$\text{NSE} = 1 - \left[\frac{(Q_o - Q_s)^2}{\sum (Q_o - \text{mean}Q_o)}\right] \quad \text{.....eq3.15}$$

Where, Q_o is Observed stream flow data in m^3/s.

Q_s is Simulated data in m^3/s.

The proportion of PBIAS describes the tendency of the simulated data to be greater or smaller than the observed data, expressed as percentage. The optimum PBIAS value is zero and low value indicates that the model simulation is satisfactory. Positive values indicate a tendency of the model to underestimate while negative values indicate over estimation.

$$\text{PBIAS} = \left[\frac{\sum (Q_o - Q_s)}{\sum Q_o}\right] \quad \text{.....eq3.16}$$

Where, Q_o is Observed stream flow data in m^3/s

Q_s is Simulated data in m^3/s

3.3.3 Potential Groundwater Zone Identification.

GIS-techniques and MCDA are effective tools for storing, processing, evaluating, and ranking alternatives in the water resources management sector (Tkach and Simonovic, 1997). Analytical hierarchical process (AHP) is a widely used MCDA technique based on the concept of driving ratio scales from the paired comparison (Saaty, 1987) and it is known to be an easy solution for complex decisions (Podvezko, 2009). Studies show that it has superior accuracy in groundwater potential mapping compared to other methods such as the Catastrophe technique (Singh et al., 2018).

In this work, a GIS-based AHP is used to integrate thematic layers, which influence the natural storage and movement of water. Since the pairwise comparison is vital in the AHP application, the association of layers is weighted according to their contribution to groundwater existence based on Saaty's parameter scaling. Saaty's parameter scaling varies from one to nine: "1 − equal importance, 2 − equal to moderate importance, 3 −moderate importance, 4 − moderate to strong importance, 5 −strong importance, 6 − strong to very strong importance, 7 − very strong importance, 8 − very to extremely strong importance, and 9 − extreme importance" (Saaty, 1987).

Therefore, in this GWPZ mapping process, the ranking was done twice. First, each thematic layer of internal attributes was ranked and recoded. Second, all the layers compared and the rank was given based on their influence on groundwater potential occurrence with considering their spatial extent on the study area and reviewing different literature on groundwater potential Zoning. The data processing and ranking were done with the help of a literature survey (Berhanu et al., 2013; Bashe, 2017; Hussein et al., 2017; Mallick et al., 2019), experience, and an acquaintance of the area. Then the matrix of all thematic layers with the assigned weight was constructed in pair wise comparison matrix in AHP process as follow to carry out weighted overlay in GIS.

Table 3-6 pair wise comparison matrix.

Criteria	RF	LULC	Sl	Geo	DD	So	Geom	LD
RF	1	3	5	5	7	7	7	5
LULC	1/3	1	3	3	4	5	6	7
Sl	1/5	1/3	1	3	3	4	3	5
Geo	1/5	1/3	1/3	1	3	3	3	4
DD	1/7	1/4	1/3	1/3	1	3	3	3
So	1/7	1/5	1/4	1/3	1/3	1	3	3
Geom	1/7	1/6	1/3	1/3	1/3	1/3	1	2
LD	1/5	1/7	1/5	1/4	1/3	1/3	1/2	1

Where

RF = Rainfall, Geo = Geology, Geom. = Geomorphology, Slope = Slope, LD = Lineament density, DD = Drainage, and LULC = Landuse Land cover, and So = Soil.

Table 3-7. Ranking and coding of each subclass of factors.

Factors	Class	Groundwater Prospect(rank)	Coding
Rainfall	1293.17-1332.72mm	Very high	5
	1253.62-1293.17mm	High	4
	1214.07-1253.62mm	Moderate	3
	1174.52-1214.07mm	low	2
	1134.97-1174.51mm	Very low	1
LULC	Forest Area	Very High	4
	Water body	Very high	5
	Agricultural Land	high	4
	Grassland	moderate	3
	Bushland	Low	2
	Built-up Area	Very low	1
Slope	0-12.9	Very high	5
	12.9-25.9	High	4
	25.9-38.8	Moderate	3
	38.8-51.75	low	2
	51.75-64.69	very low	1
Geology	NQr	low	5
	Pv	High	4
	Nmn	Very High	5
DD	0-0.68	Very high	1
	0.68-1.32	High	2
	1.32-1.96	Moderate	3
	1.96-2.61	Low	4
	2.61-3.26	Very low	5
Soil	Humic Alisol(Alu)	Very low	1
	Eutric vertisol(VRe)	low	2
	ChromicLuvisol(Lvx)	moderate	3
	Humic Nitosol(NTu)	High	4

	Lithic Leptsol(LPq)	Very high	5
Geomorphology	Bottom	very high	5
	Flat plain	high	4
	Plateaus	low	2
	High slope	low	2
	Summit	Very low	1
LD	0-0.109	Very low	1
	0.109-0.303	low	2
	0.303-0.51	Moderate	3
	0.51-0.76	high	4
	0.76-1.46	Very high	5

Consistency is a measurement of dependency within and between the sets of thematic layers of its structure in AHP (Saaty, 1987). The consistency ratio (CR), principal Eigen value (λmax), and consistency index (CI) were calculated using the following Saaty's equation.

$$CI = \frac{\lambda_{max} - n}{n-1} \quad \text{.....eq3.17}$$

$$CR = \frac{CI}{RCI} \quad \text{.....eq3.18}$$

where n is the number of data considered and RCI is random consistency index value

A CR of 10% or less is satisfactory to proceed with the analysis (Saaty, 1990). However, if the consistency index exceeds 10%, reconsidering the judgment is necessary to identify the sources of inconsistency and adjust it accordingly. A zero value of CR indicates that the pair wise comparison has a perfect consistency.

The normalized weight of all the data was produced from the pair wise comparison matrix and the GWPZ map was produced using weighted linear combination (WLC) technique. WLC is founded on the theory of a weighted averaging where the criteria are standardized to the same numeric bound (Drobne and Lisec, 2009). The method can be applied using the GIS; it can be equated as follows:

$$GWPZI = \sum_{i=1}^{n} (W_i \times r_i) \quad \text{.....eq3.19}$$

$$GWPZI = Rf_w Rf_r + Lulc_w Lulc_r + Sl_w Sl_r + Geol_w Geol_r + DD_w DD_r + Sol_w Sol_r + Geom_w Geom_r + Ld_w Ld_r$$

Where GWPZI -groundwater potential zone index

n-number of factors.

W_i-weights of each factor.

r-rank value of sub classes of main thematic layers.

Rf-rainfall, Geol-geology, Ld-lineament density, Lulc-land use land cover, Sl-slope, Geom-geomorphology, So-soil, DD-drainage density.

3.3.3.1 Sensitivity analysis of groundwater potential influencing factors.

A sensitivity analysis will be performed for each influencing factor to determine which factors have the most influence on the delineation of GWPZs.

Sensitivity analysis helps to understand which inputs are most important for monitoring the presence of groundwater. Sensitivity analysis is a method of determining the most sensitive parameters that have a significant influence on the validity of the study. Sensitivity analysis describes how the output of the model changes over a range of a given input variable.

Sensitivity analysis provides meaningful data on the impact of each influencing factor on the GWPZ analysis. Sensitivity analysis is an effective way to interpret the groundwater potential index. The layer removal technique represents the potential sensitivity of groundwater associated with layer-by-layer removal (lodiwok et al., 1990) according to the following equation.

$$S_x^y = \left(\frac{A_{-x}^y - A_n^y}{A_n^y}\right) \times 100 \quad \text{.....eq3.20.}$$

where x is the factor variable,

y is the zone type (i.e., very good, good, moderate, poor, very poor),

S_x^y refers to the percentage variation in Y^{th}type of groundwater potential zone area owing to the removal of X^{th} factor,

A_{-x}^{y} is the y[th] type of groundwater potential zone area resulting from the removal of the X^{th} factor, and

A_{n}^{y} is the Y^{th} type of groundwater potential zone area using all factor.

3.3.3.2. Groundwater flow direction.

Groundwater flow direction and contour maps were generated from groundwater level data using Surfer 17 software. The ground water level data was organized as XYZ file where, X and Y are plane coordinates of measuring points and Z is a function of elevation of water table. The values of static water level (SWL), elevation of water level in the wells were obtained by subtractions of depth to water level in the wells from ground surface elevation.

Ground water level (static water level) was obtained by:-

$$\mathrm{SWL} = \mathrm{GSE} - \mathrm{DWL} \quad \ldots\ldots\ldots\ldots\ldots\ldots\ldots\ldots\ldots\ldots \text{eq3.21}$$

Where, GSE :- Ground surface elevation.

DWL :-Depth to water level in the well(m).

Finally,groundwater contour line indicated and groundwater flow direction was identified using groundwater level map with Surfer model.

3.3.3.3 Validation of potential groundwater zones.

Validation is considered an essential step in the modeling process (Chung & Fabbri, 2003). Using MCDA techniques, the obtained groundwater potential maps were validated with the existing groundwater well maps of the study area to verify the accuracy of the proposed MCDA techniques. Validation is comparing the outputs of the model with an independent data set without making any adjustments to check if the model can predict the underlying truth over a different time period. The map of wells was projected on the GWPZs map to verify the effectiveness of the RS-GIS and AHP-based method in demarcating GWPZs in the study area (Yousefi, et al., 2018) Verification of delimited groundwater areas is achieved through validation, using existing data on boreholes, wells and streams . Drilling or well data can include: name, location details like coordinates, important yield for classification of groundwater areas, depth of ground water level, source type and location details(shown in Appendix Table-3). These data were prepared in suitable format as input to GIS model to

spatially distribute on delineated GWPZ. The groundwater potential map was validated using data from 46 ground water well inventory data projected on GWPZ map in GIS soft ware.

3.4 Methodological Framework.

The general framework of the study was shown in figure as follow:

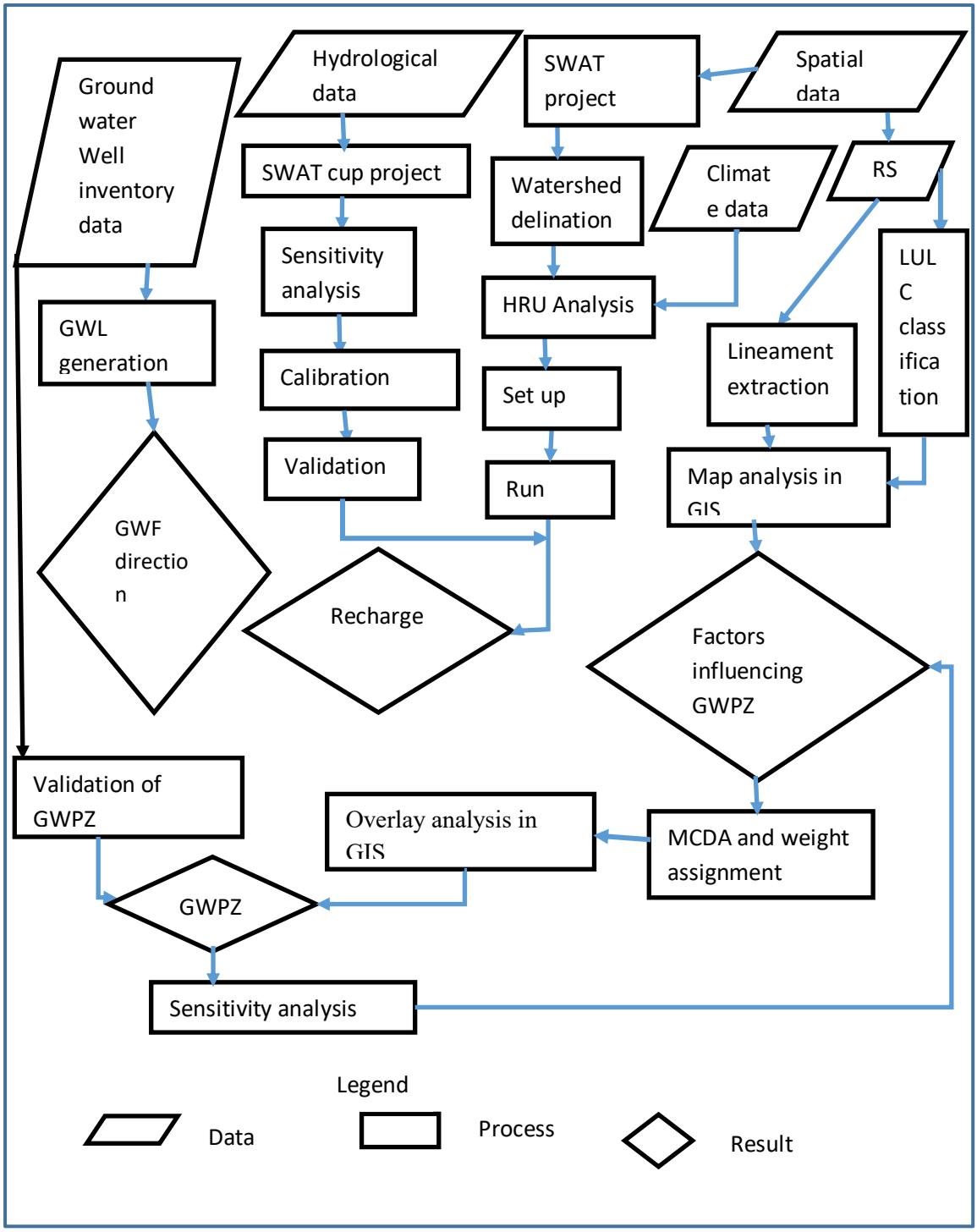

Figure 3-10. Methodological Frame work.

4. RESULTS AND DISCUSSION.

4.1. Factors Affecting Groundwater potential occurrence.

4.1.1 Rainfall.

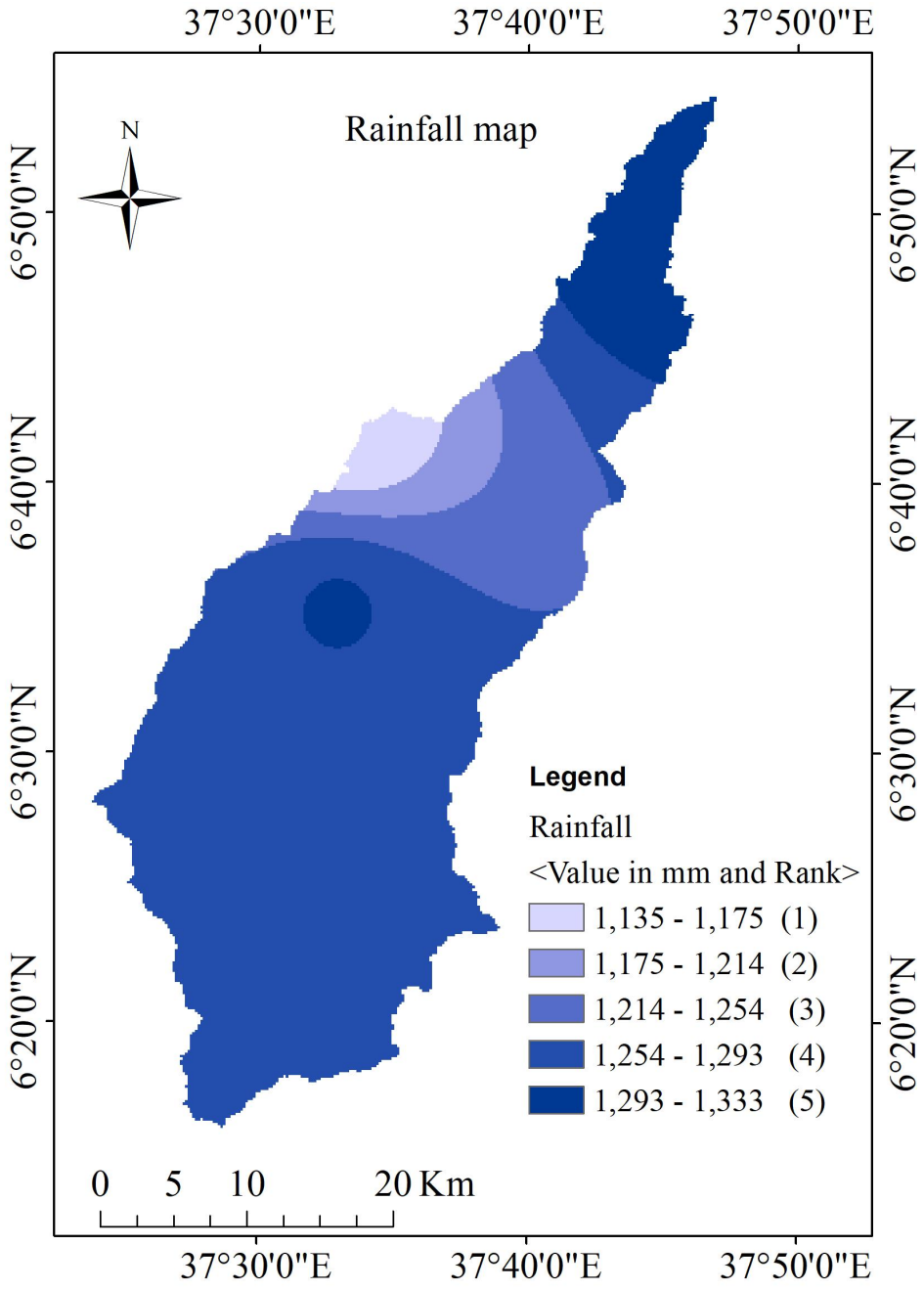

Figure 4-1 Rainfall map.

The classes were developed as per the recommendation by (Tolche, 2021; Zeinolabedinia, and Esmaeily, 2015) .

This figure shows the study area's yearly rainfall, which ranges from 1134 to 1332 millimeters. The northern tip and certain center portions of the watershed get an abundance of rainfall each year, which helps to recharge the groundwater in the western and some portions of the southeastern portions of the watershed. Due to the watershed's northwestern region's insufficient yearly rainfall, the region is regarded as having a water shortage. In areas with high rainfall, there may be more chance for groundwater potential and recharge, but this is not the case in areas with low rainfall . Because of the variable rainfall patterns in the research area's immediate proximity, there are also variations in the groundwater potential. With regard to rainfall spatial map data, the majority of the study area is projected to have high to very high groundwater potential, as shown in table 4-1 below.

Table 4-1. Groundwater Potential Prospect Rainfall Map Information.

Rainfall class(mm)	GWP prospect value	Rank	Count	Area(km^2)	Area (%)
1135-1175	Very low	1	28754	25.8786	2.334
1175-1214	low	2	52842	47.558	4.29
1214-1255	moderate	3	161082	144.9733	13.08
1255-1293	High	4	860001	774.0009	69.835
1293-1333	Very high	5	128787	115.9083	10.458

4.1.2. Geology

According to figure 4-2, the majority of the Deme watershed's geologic formation was divided into two groups: quaternary extrusive and intrusive rock groups (Pv) and tertiary extrusive and intrusive rock groups (NMn).

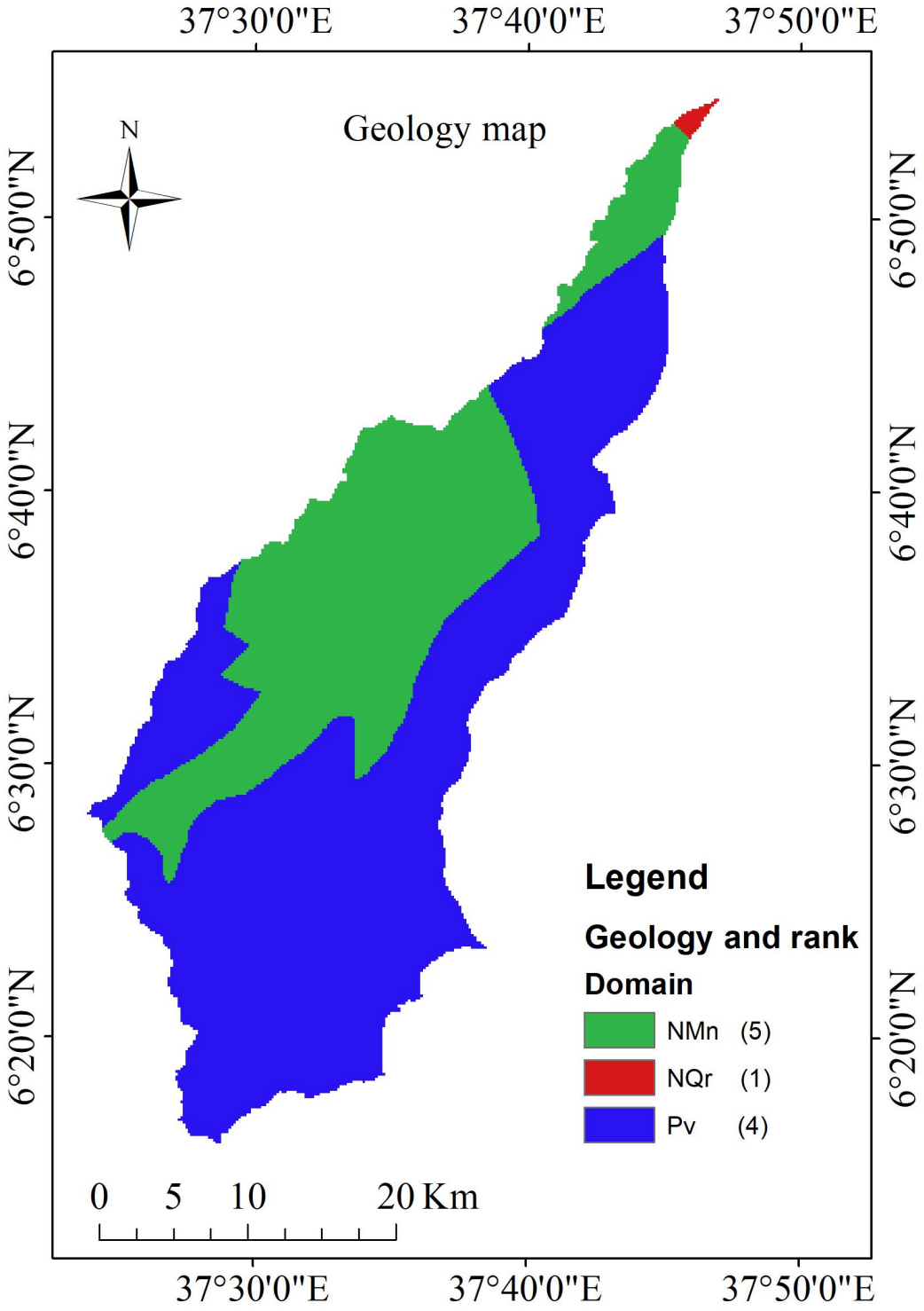

Figure 4-2 Geology map

Geology thematic layer was developed with classes as appropriate for groundwater potential prospective scaling as recommended by (Dainelli et al., 2001).

The weathered basaltic, fractured ignibrite aquifer types, and quaternary terrace deposits with alluvium that characterize the quaternary extrusive and intrussive rock groups make them favorable for the occurrence of groundwater resources. Due to their reduced permeability, metamorphic and igneous rocks were said to have the lowest groundwater potential, whereas alluvium and Quaternary terrace deposits were given the highest GWP rankings (Stefano et al., 2002).

Due to their appropriateness for groundwater occurrence, the majority of the study area's geologic formations have a high or extremely high groundwater potential. Accordingily the extent of geological weathering or geological formations largely determines the presence of groundwater and the size of its reservoir.

Table 4-2. Groundwater Potential Prospect Geology Map Information.

Geology	GWP prospect value	Rank	Count	Area(km^2)	Area(%)
NQr	Low	1	3319	2.9871	0.28
Pv	High	4	753510	678.16	63.6
NMn	Very High	5	427819	385.0371	36.11

4.1.3 Lineament Density.

The lineament map of the study region shows that there are significant amounts of groundwater potential resources in the northern, southern, south-eastern, some sections of the center, and south-western parts of the study area due to the distribution of lineaments in these areas, which ranges from moderate to high. Distribution of high lineament density significantly can increases groundwater potential and recharge.

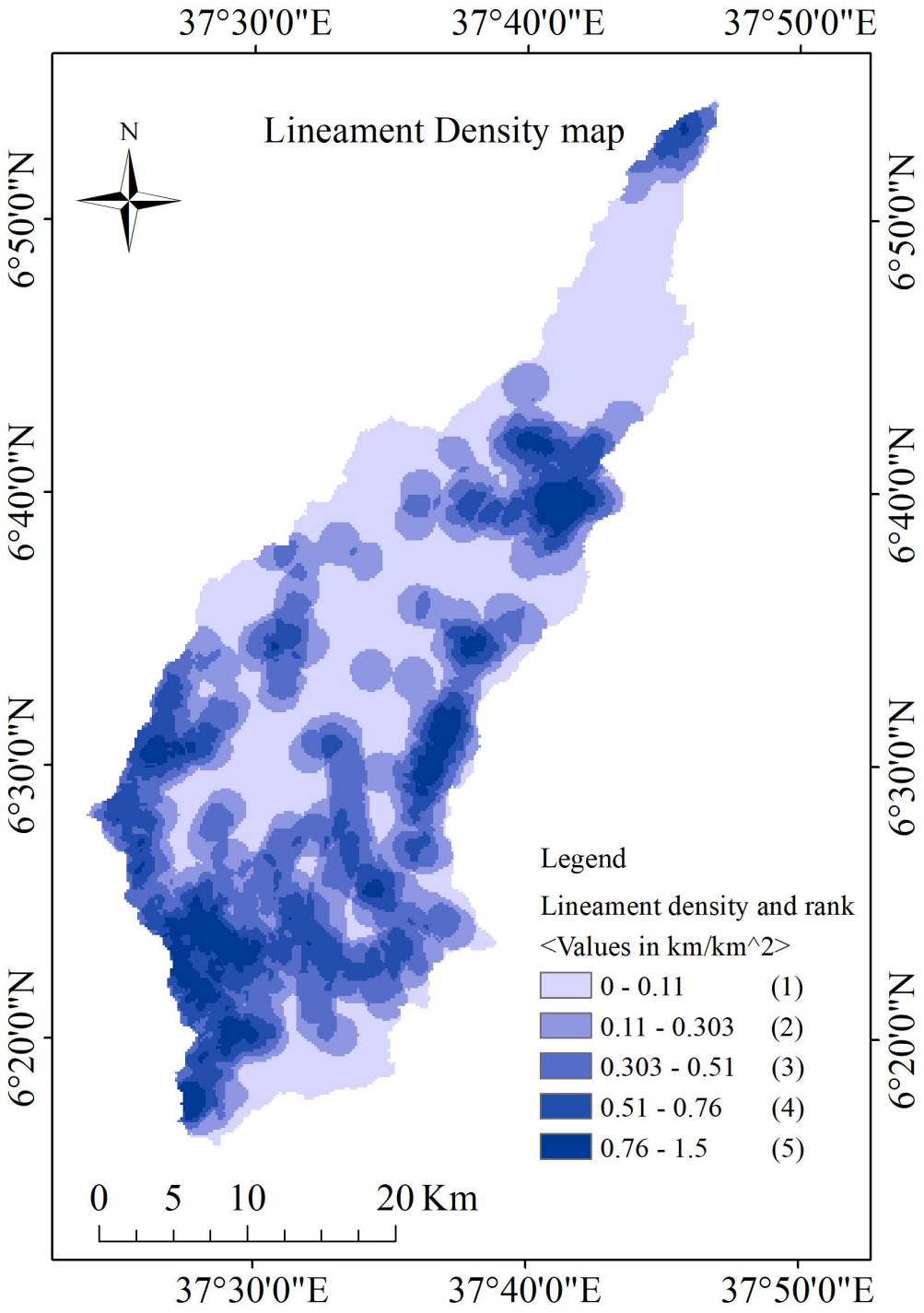

Figure 4-3. Lineament density map.

The classes were developed as per the recommendation by (Waikar and Nilawar, 2014; Tolche, 2021).

According to Figure 4-3, the density of lineaments in the research area varies from 0 to 1.5 km/km^2. The lineament density was divided into five categories: very high

(0.76-1.5 km/km^2), high(0.51-0.76km/km^2), moderate(0.303-0.51km/km^2), low (0.11-0.303 km/km^2), and very low (0-0.11 km/km^2). The highest rank was given to the very high class to determine ground water potential zone. For the purpose of analyzing GWP-prospective and spatial distribution of fault density, a reclassified lineament density (LD) map was created.

Table 4-3.Groundwater Potential Prospect Lineament Density Map Information.

LDclass(Km/Km^2)	GWP prospect value	Rank	Count	Area(km^2)	Area(%)
0-0.11	Very Low	1	460811	414.73	37.47
0.11-0.303	Low	2	274270	246.84	22.3
0.303-0.51	Moderate	3	247618	222.85	20.13
0.51-0.76	High	4	176430	158.79	14.35
0.76-1.46	Very High	5	70375	63.34	5.72

4.1.4 LULC .

Thematic map of Deme's LULC (figures 4-4) reveals that the majority of the study area's LULC is agricultural land, making it suitable for the occurrence of ground water with a wide spatial extent.The remaining LULC is made up of bush land (11.55%), built-up area 1.51%, forest 6.69%, grass land 6.09%, and water bodies 0.4%. Surfaces protected by vegetation, such as agricultural plants, grasses, and forests, have a better chance of groundwater opportunity due to higher infiltration through trapping and protecting the rainwater in the roots of plants and cracks of rocks. Built-up and rocky surfaces have much less opportunity for groundwater potential prevalence through creating runoff during rainfall.

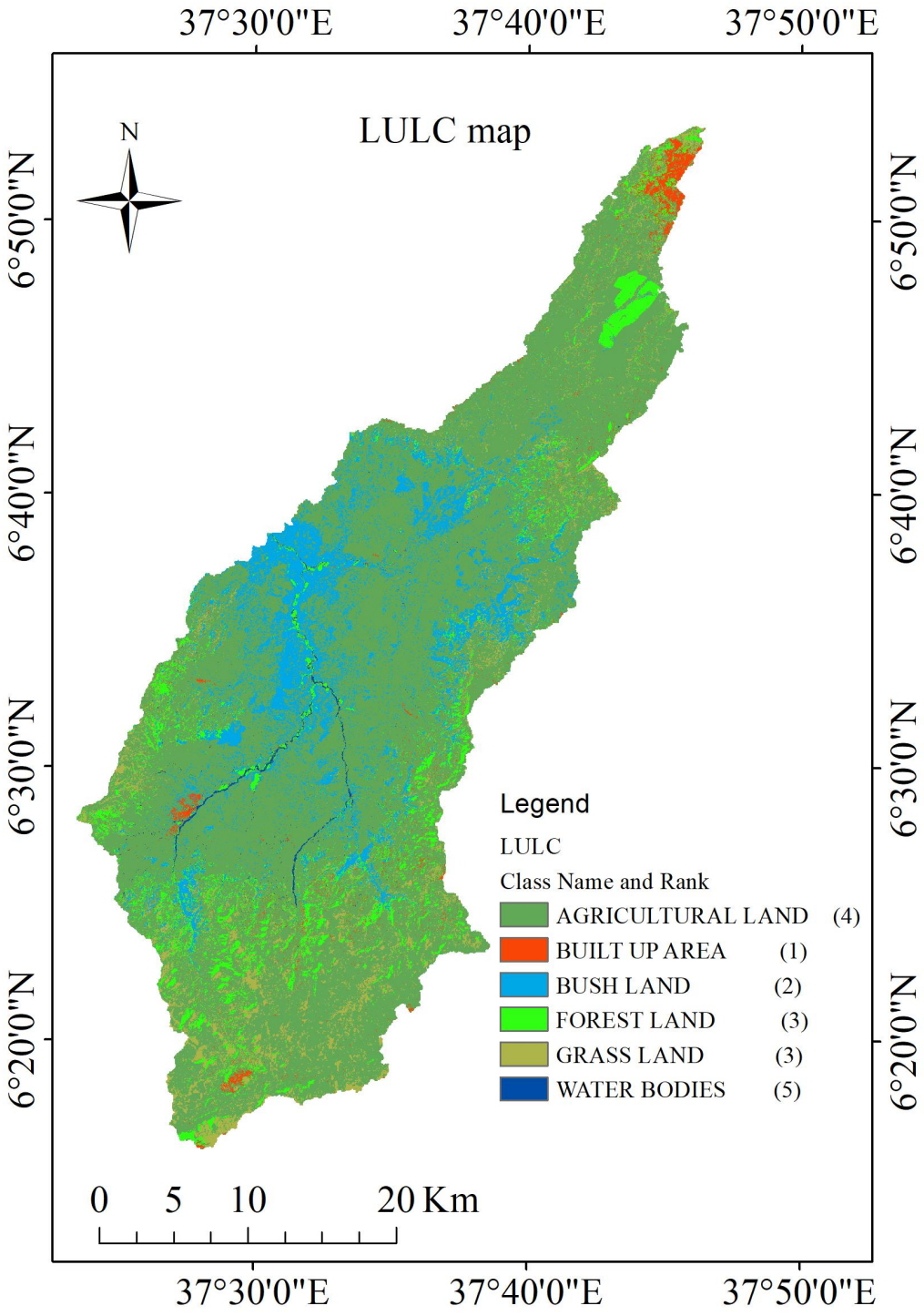

Figure 4-4. LULC map.

The classes were developed as the recommended (Tolche, 2021; Andualem, and Demeke,2019). About 85.4% of a place is predicted to have high groundwater potential with respect to land use/land cover (Table).

Table 4-4.Groundwater Potential Prospect LULC Map Information.

LULC	GWP prospect value	Rank	Count	Area(km^2)	Area(%)
Agricultural land	Very high	4	911277	820.1493	73.77
Built up area	Very low	1	18653	16.7877	1.51
Bush land	Moderate	3	142742	128.4678	11.56
Forest land	High	4	82538	74.2842	6.69
Grass land	High	3	75202	67.6818	6.09
Water bodies	Very high	5	4836	4.3524	0.4

4.1.5 Slope.

In the gentle slope vicinity near the north eastern, north western, and central parts of Watershed, the surface runoff is sluggish, which traps precipitation and allows rainwater to percolate or infiltrate via the soil and is considered a good groundwater potential zone, while steep slope vicinity areas such as the northern tip, south eastern, and south western areas create excessive runoff, permitting much less lag time for rainfall and therefore relatively much less infiltration and a poor groundwater potential occurrence. However, slope classes have been identified based on their degree of significance to groundwater potential and recharge in GIS and reclassified according to groundwater potential prospects (Tables 4-5). From the spatial distribution of slope, about 69.61% of the study area is predicted to have high to very high groundwater potentiality with respect to slope. Thematic slope maps of the Deme watershed are shown below in Figs. 4–5.

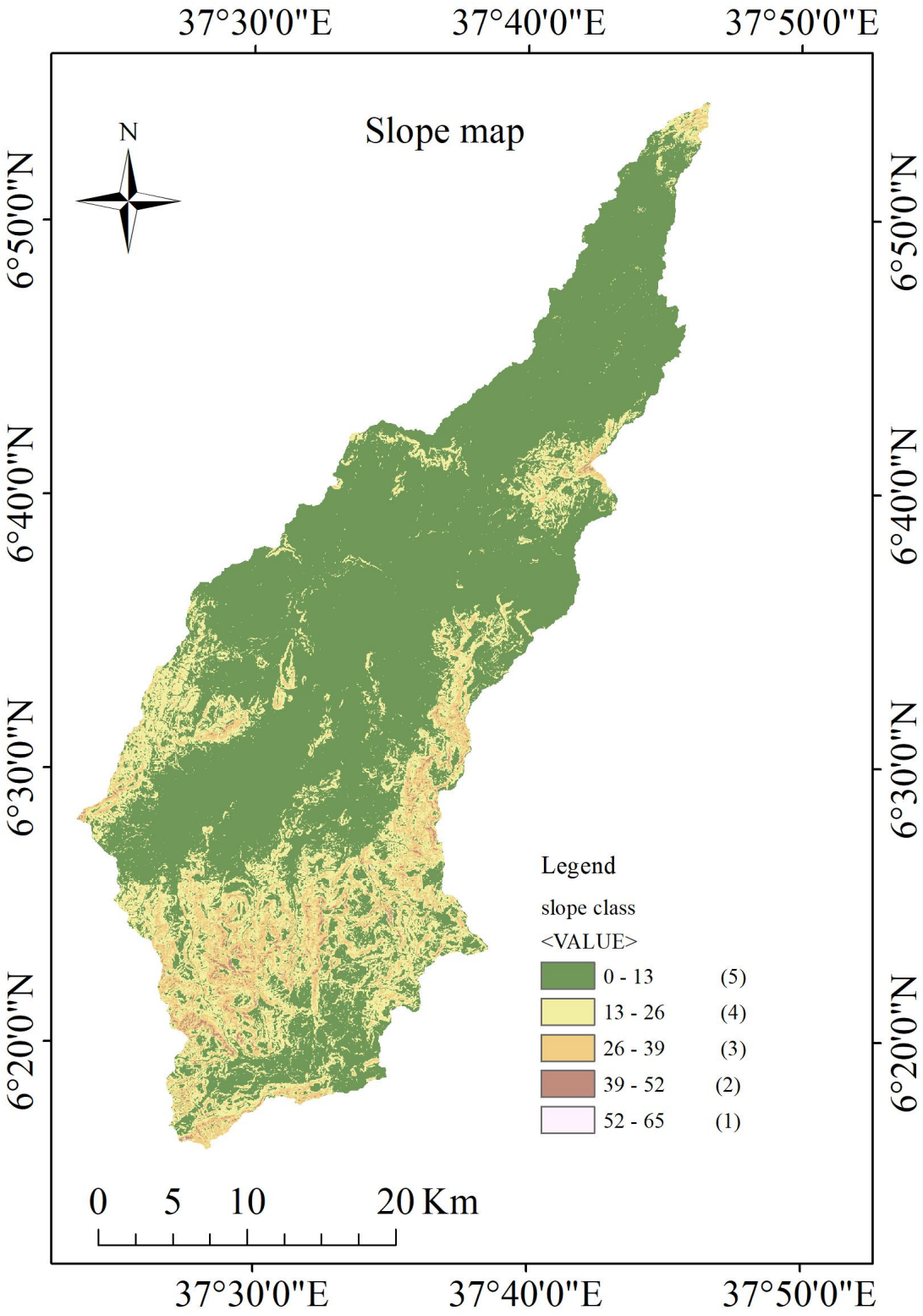

Figure 4-5: Slope map.

The classes were developed as per the recommendation by (Daniel et al., 2018; Waikar and Nilawar, 2014) have reported Slope gradient and category.

Table 4-5: Groundwater Potential Prospect Slope Map Information.

Slope class (degree)	GWP prospect value	Rank	Count	Area(km^2)	Area(%)
0-13	Very high	5	520549	468.4941	42.55
13-26	High	4	331599	298.4391	27.1
26-39	Moderate	3	188575	169.7175	15.41
39-52	Low	2	123007	110.7063	10.05
52-65	Very Low	1	59583	53.6247	4.87

Generally, groundwater resource potential occurs in gentle slope to plain region as water flow is slow and the time is enough available to improve the infiltration of water to the underlying fractured aquifer. Therefore, higher GWPZ prospective rank was given to lower degree of slope map area, but lower GWPZ prospective rank was given to higher degree of slope map area.

4.1.6. Geomorphology.

The hills or bottom surface, coastal plain (flat areas or flood plain), slope facets, and summit are major geomorphic features categorized based on elevation difference in the Deme Watershed area, as shown in Figs. 4–6.

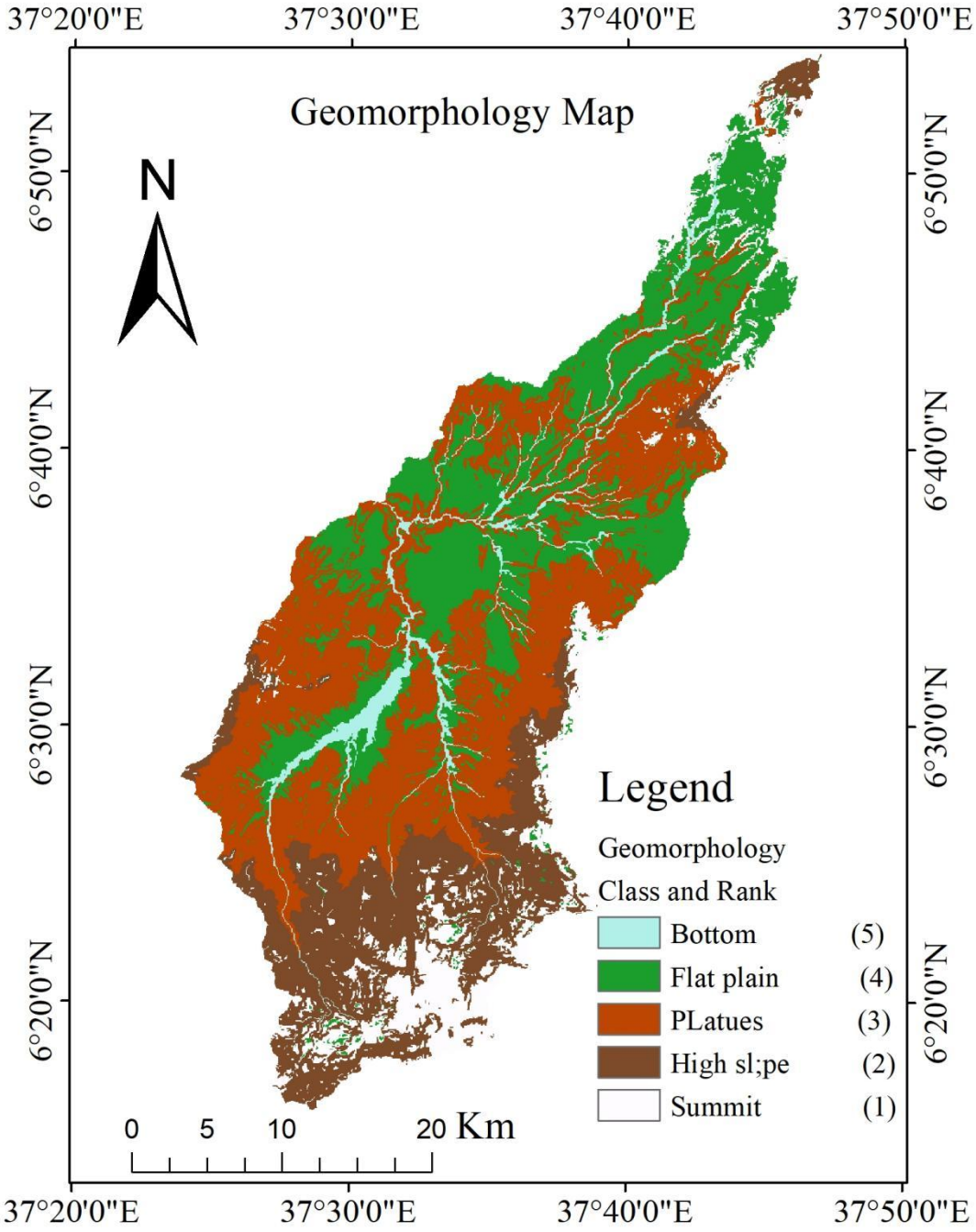

Figure 4-6 Geomorphology map.

The classes were developed as per the recommendation by (On, 1768; Arnot & Grant, 1981) description of landform classification.

The geomorphology of the area is a crucial factor to consider when assessing the prospect and potential zone of groundwater since it regulates how groundwater moves beneath the surface. The Deme watershed has about 31.75 percent of its land in a flat

plain, which is advantageous for the possibility of groundwater resource occurrence in the area. In the northern and southern portions, lava plateaus and steep slope facets are typical. Groundwater prospective rank is given a moderate to very low score for evaluation in Tables 4-6 because places with stony beaches, ridges or hills, lava plateaus, and high slope facets were classified as low groundwater potential areas. The geomorphic classifications contain those suitable sites for the possible occurrence of ground water.

Table 4-6.Groundwater Potential Prospect Geo morphology Map Information.

Geomorphology class	GWP prospect value	Rank	Count	Area(km^2)	Area(%)
Bottom	Very high	5	14917	13.425	1.21
Flat plain	High	4	390541	351.487	31.75
Plateaus	low	2	698725	628.823	56.82
High slope	Low	2	69629	62.67	5.66
Summit	Very Low	1	55888	30.3	4.55

4.1.7. Soil.

It was found that the study area soil type is categorized as humic alisol, lithic leptosols, chromic luvisol, humic nitosol, and eutric vertisol according to FOA soil classification, with the soil texture of each soil type being clay-loam, clay loam, silt-clay-loam, clay, and clay soil type, respectively.

Soil mainly influences the rainfall infiltration and percolation capacity that from long period of time it can affect the groundwater recharge process after which it has impact on groundwater potential of a study area. In Deme Watershed, about 37.96% of the area is expected to have high groundwater potential with respect to soil group and 57% of study area soil type spatial distribution contributes for low ground water potential. The dominant soil types in the study area are depicted in Fig. 4–7, while the spatial information of each soil type is shown in Table 4–7. Soil is a critical factor in controlling the rate of infiltration and runoff, which is important for groundwater

replenishment. Weathered soils (sandy loam) would have high porosity and permeability, which are good for infiltration, whereas clay soils would have low infiltration. Soil types like Vertisol, Alisols, and Nitosols, would have a low affinity for infiltration and hence would lead to rainfall and runoff, while soil types like Leptosols, and Luvisols would lead to high infiltration. .

Soil texture affects rainfall infiltration and percolation capacity, Over a long period of time it can influence the groundwater recharge process, which has an impact on the groundwater potential of a given area. In Deme Watershed, about 37.96% of the area is expected to have high groundwater potential with respect to soil group, and 57% of the study area's soil type spatial distribution contributes to low groundwater potential. A reclassified soil map was developed to analyze the GWP prospective of each soil group with their rank and their spatial extent in the study area.

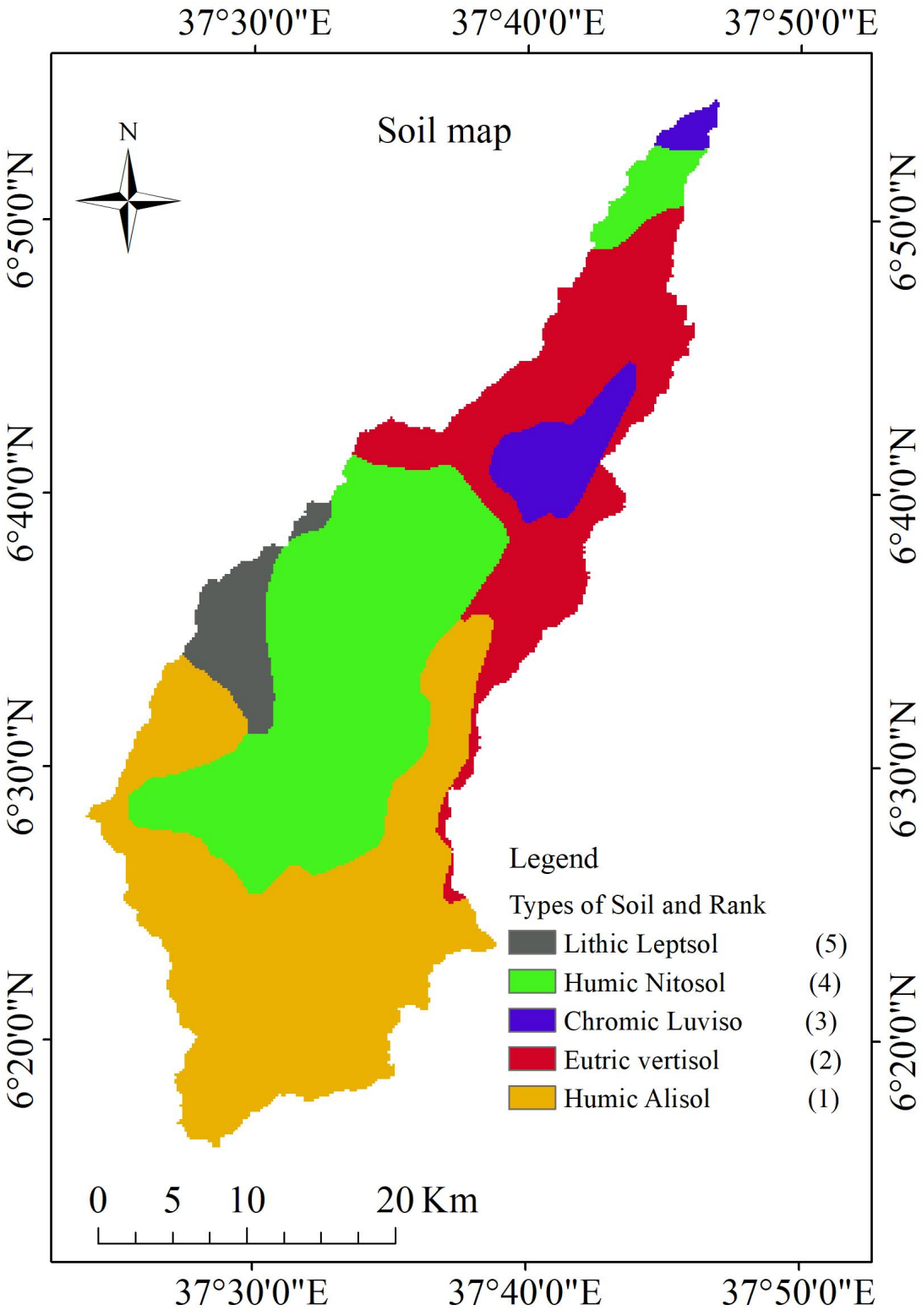

Figure 4-7 Soil map.

Soil thematic layer was developed with classes for groundwater potential prospective as recommended by (Tolche, 2021).

Table 4-7. Groundwater Potential Prospect Soil Group Map Information.

Soil group	GWP prospect value	Rank	Count	Area(km^2)	Area(%)
Humic Alisol(Alu)	Very low	1	14041	410.4	37.09
Eutric vertisol(VRe)	Low	2	7523	219.89	19.87
Chromic Luvisol(Lvx)	Moderate	3	1917	56.03	5.06
Humic Nitosol(NTu)	High	4	12651	369.76	33.41
Lithic Leptsol(LPq)	Very High	5	1725	50.41	4.55

4.1.8. Drainage Density.

Figure 4-8 represents drainage density map and reclassified drainage density map of deme watershed with large area coverage of moderate class (43.73%) spatial distribution of drainage density with perspective of groundwater potential occurrence.

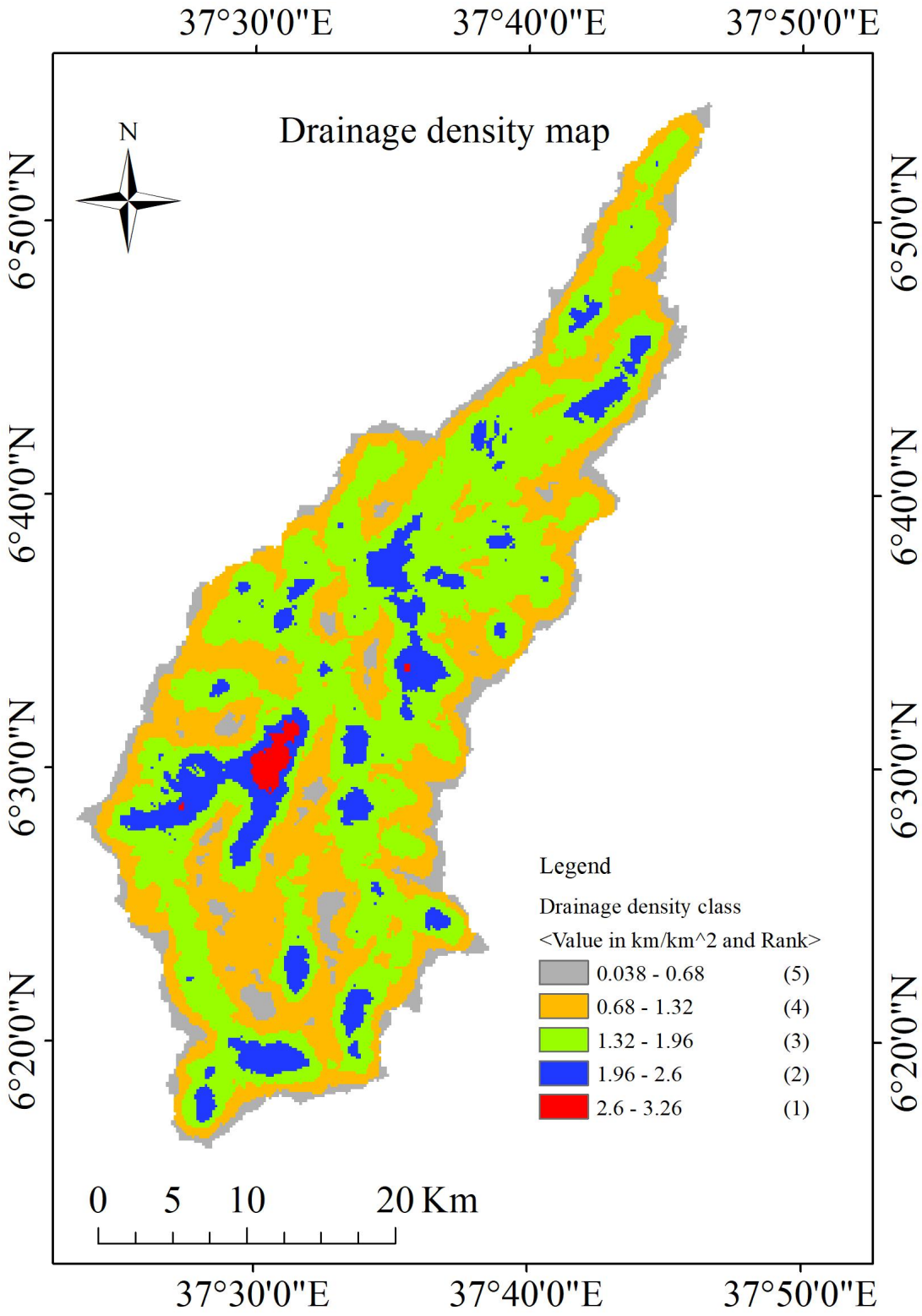

Figure 4-8.Drainage density map.

The classes were developed as per the recommendation by (Tolche, 2021; Waikar, and Nilawar, 2014).

The drainage density in the studied area ranges from 0 to 3.255 km2/km2 and is classified into five distinct classes as shown in Fig. 4-8 and Table 4-8. From the classified drainage density map,very low classes received the highest rank for groundwater potential zonation.

Drainage density has an inverse relationship with the permeability of aquifers and plays an important role in the runoff distribution and degree of infiltration. Drainage density is one of the parameters affecting groundwater potential and recharge and plays an essential role in groundwater potential zoning. Groundwater potential is poor in regions with a very excessive drainage density because it misplaces the majority in the form of runoff, while regions with a low drainage density permit high infiltration to recharge the groundwater and, therefore, have a high value for groundwater potential occurrence. About 45.2% of the study area is predicted to have high groundwater potential with respect to drainage density, as shown in Tables 4–8.

Table 4-8.Groundwater Potential Prospect Drainage Density Map Information .

DDclass(Km/Km^2)	GWP prospect value	Rank	Count	Area(km^2)	Area(%)
0.038-0.68	Very high	5	114181	102.8	9.29
0.68-1.32	high	4	441417	397.3	35.9
1.32-1.96	Moderate	3	537770	483.9	43.73
1.96-2.61	low	2	127537	114.8	10.37
2.61-3.26	Very low	1	8944	8.05	0.73

4.2. Groundwater Recharge.

4.2.1.Model Calibration

The monthly flow of Deme watershed from 1991 to 2001 was used for calibration. The first two years from the recorded data, 1989 and 1990, were used as a model "warm-up" Period to establish proper initial conditions and stabilize the model as suggested by SWAT manual users. Sensitive parameters were varied several times to obtain acceptable value for R2, NSE and PBIAS.

Table 4-9 Most Sensitive parameters used during calibration accordingly.

Parameter_Name	Fitted_Value	Min_value	Max_value
1:R__OV_N.hru	0.0067	0.0	0.015
2:R__REVAPMN.gw	0.95	0.100000	1
3:V__GW_REVAP.gw	0.0315	0.029	0.032
4:R__RCHRG_DP.gw	1.022500	0.830000	1.180000
5:A__CN2.mgt	0.3	0	6
6:R__ESCO.hru	0.185000	0.05	0.35
7:R__CANMX.hru	1.404550	0	4.013
8:R__HRU_SLP.hru	0.106	0.083	0.54
9:V__SOL_AWC(..).sol	0.087	0.016	0.30

The calibration was done until simulated flow closely matched the observed flow. The calibration result showed that the result of R^2, NSE and PBIAS were 0.81, 0.78 and -12.3. This indicated that the model performance assessment indicated a good correlation and agreement between the monthly measured data and simulated flow.

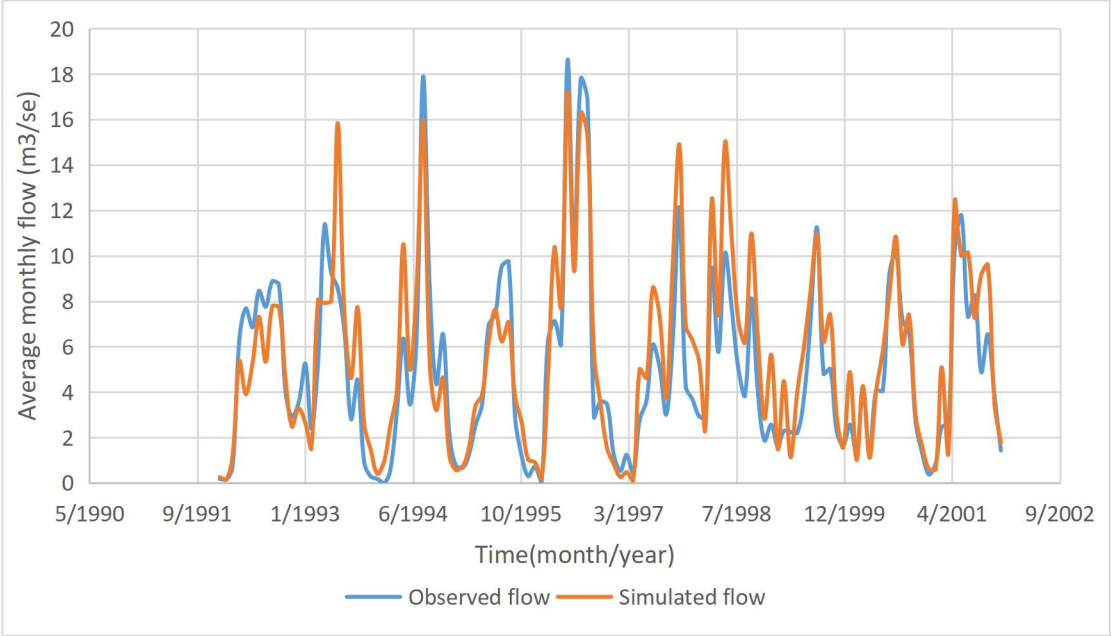

Figure 4- 9. Monthly Stream flow hydrograph during calibration period (1991-2001).

4.2.2.Model Validation.

The model's ability to estimate the watershed stream flow in a realistic manner was demonstrated by the model validation results. The acceptable range was reached by the ENS and R^2 values, which were 0.74 and 0.76, respectively. This is consistent with a study of the nearby Hare River watershed conducted by (Tadele, 2009). For the validation of monthly data, he stated that the R^2 value of 0.72 to 0.85 and the ENS of 0.66 to 0.8 were within an acceptable range. (Muluken, 2021) also did a study on the Deme Watershed and reported that during calibration, the R^2 value was 0.79 and the NSE value was 0.73, and during validation, the R^2 value was 0.75 and the NSE value was 0.67. This indicates that the study's findings are consistent with those of earlier investigations using the SWAT model, indicating a high degree of study accuracy.

Table 4- 10. Monthly time step calibration and validation statics.

This shows Good correlation in between observed and simulated values, So the simulation is good on estimating flow prediction and the result is acceptable.

period	Evaluation criteria			Remark
	R^2	ENS	PBIAS	
Calibration (1991-2001)	0.81	0.78	-12.3	Very good
Validation (2002-2006)	0.76	0.74	9.4	Very good for R^2 and ENS. Good for PBIAS.

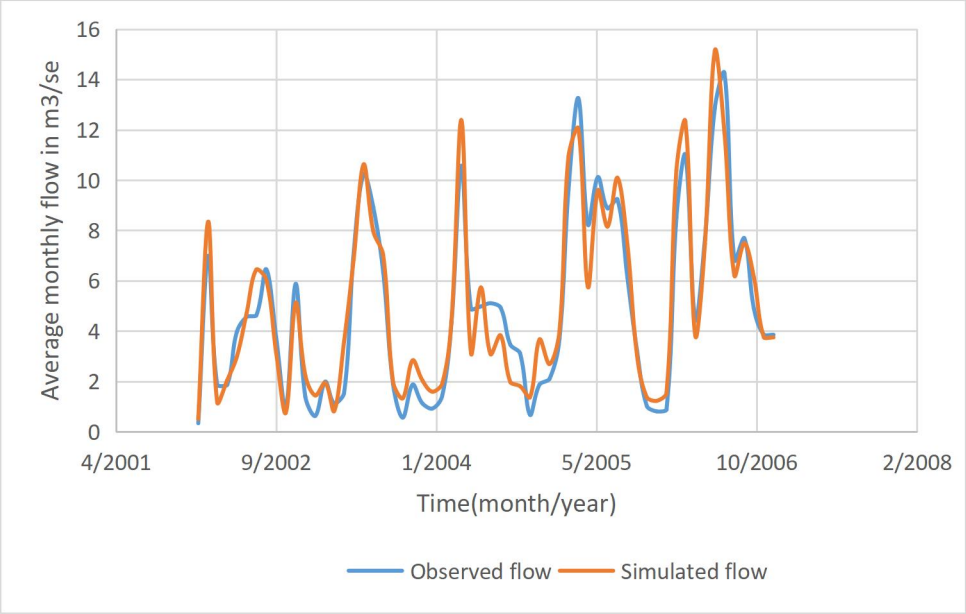

Figure 4- 10. Monthly stream flow hydrograph during validation period (2002-2006).

4.2.3. Spatio temporal variation of recharge in Deme watershed.

The seasonality varaition of the recharge and the principal water balance components are presented figure 4-11.

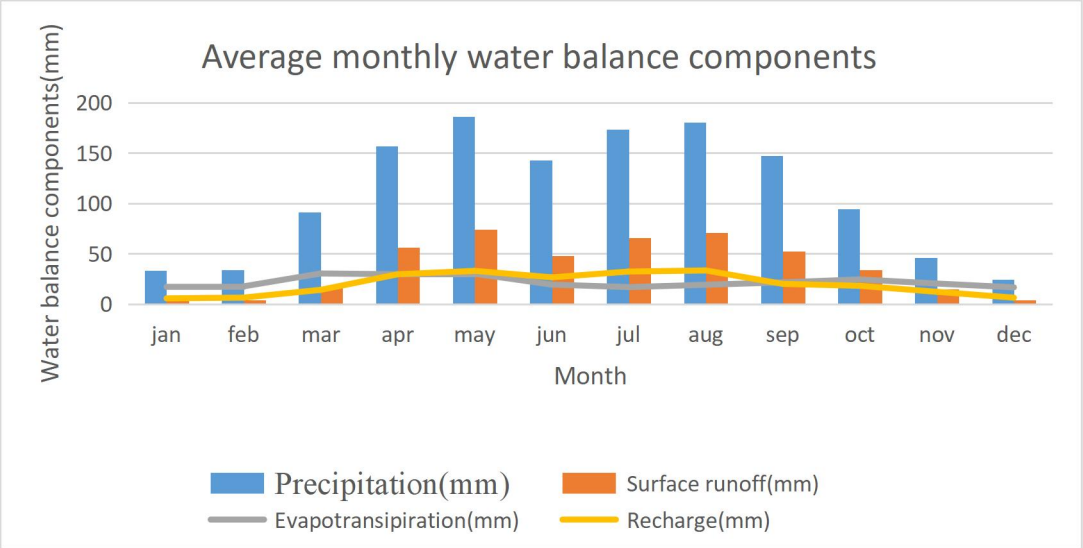

Figure 4-11. Water balance components.

From the overall averaged annual monthly period, the months of December, January, and February have the lowest recharge values because of low precipitation distribution and high evapotranspiration. From the statistical analysis, it was found that the maximum monthly average recharge is 33.27mm in August and the minimum monthly average recharge is 5.53mm in January.

Around 14.08% of the recharge occurs in August, which counts around 2.54% of the area precipitation, which is more than other months values in the watershed. The highest percent of recharge occurs in four months, from May to August. The long-term average annual groundwater recharge is 18.04% of the average annual rainfall. The watershed area shows significantly high surface runoff (SQ), with a maximum monthly average value of 74.09mm in May compared to recharge and evapotranspiration. The maximum monthly average ET is around 30.27 mm in the month of March. when the long time mean monthly rainfall distribution in the watershed increases, the tendency for increase of long time mean monthly recharge distribution is high even though there are other factors which determine temporal variation of recharge.

The long time yearly average spatial variation of recharge in Sub basin of Deme watershed is as shown in figures.

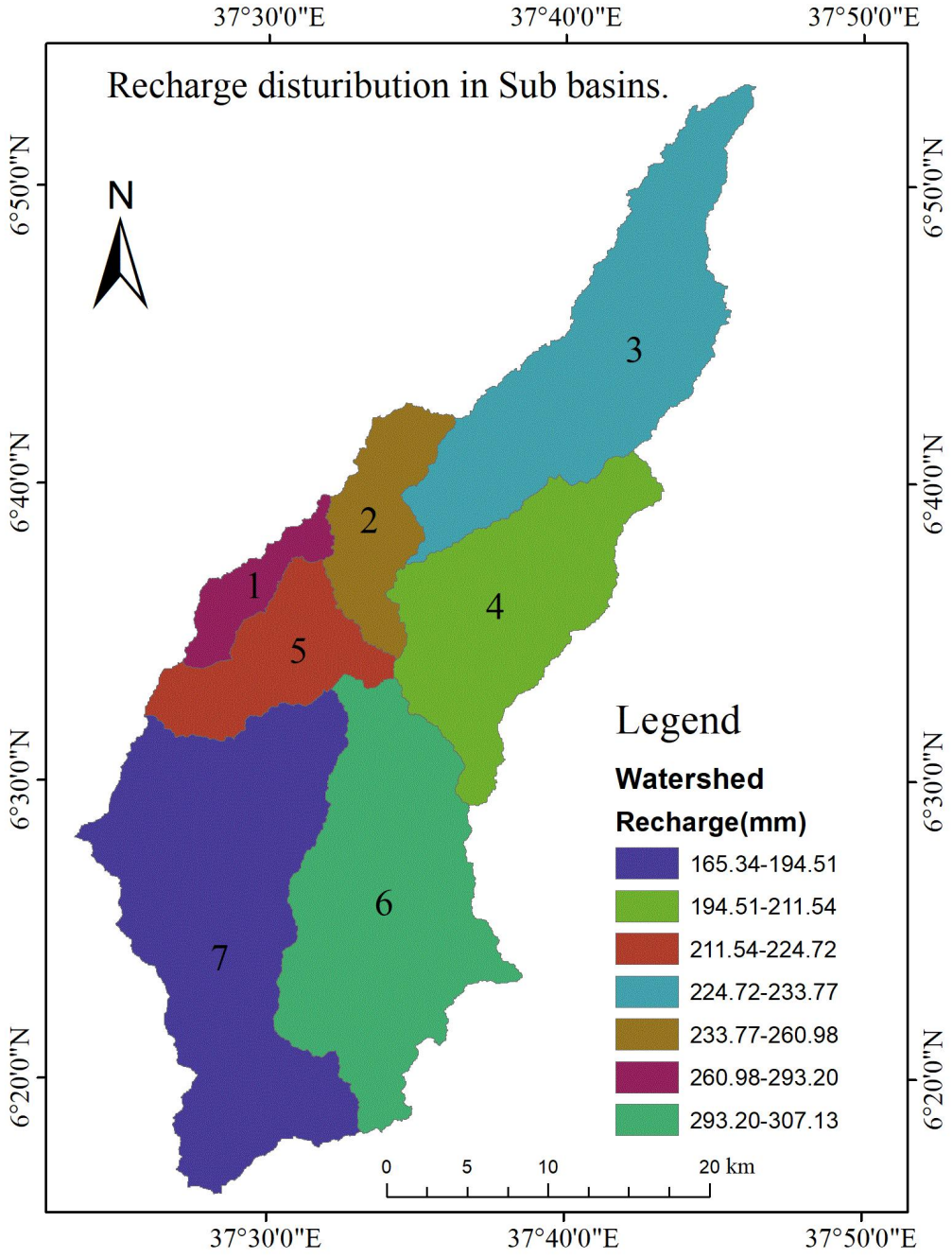

Figure 4-12. Annual average Recharge distribution in sub basin.

From Figure 4–13, the largest recharge spatial distribution amount is observed in subbasin 1, subbasin 2, and subbasin 6, and the minimum recharge spatial distribution amount occurs in subbasin 7, subbasin 4, subbasin 5, and subbasin 3, respectively. The cause for variation in recharge distribution can be the occurrence of different physiographic and hydrologic characteristics such as land use, land cover, soil type, geology, geomorphology, drainage density, rainfall, evapotranspiration, and runoff in

the Deme watershed. High recharge distribution areas are characterized by high rainfall, agricultural land coverage, hilly geomorphology, and sandy soil texture, while low recharge distribution areas are characterized by sumit geomorphology, steep slopes, low rainfall distribution, and low vegetation cover in the Deme watershed.

Table 4-11.Groundwater Potential Prospect Recharge Map Information.

Recharge class(mm)	GWP prospect rank	value	Count	Area(km^2)	Area(%)
194.51-217.03	Very low	1	553844	498.46	14.1
217.03-239.55	Low	2	359672	323.7	46.6
239.55-262.08	Moderate	3	250735	225.67	22.32
262.08-284.6	High	4	47755	42.97	10.17
284.6-307.6	Very high	5	20159	18.14	6.8

The Recharge distribution shows that 46.62% of the area has a recharge value varying from 194.52 -239.55 mm annual coverage, which covers most of the lower elevation area of the watershed with low recharge distribution and the mountain regions with high recharge distribution . A small part of the watershed has a high (262.077 − 307.12 mm) recharge, which is distributed in lower mountain slope of the Southeastern and Southern highland areas and north western areas.

4.3. Groundwater potential areas.

4.3.1. Weighted Overlay Analysis

The selection of criteria for groundwater potential area mapping is a key task in the proposed GIS-based multicriteria selection evaluation, where the criteria choice calls for appropriate site information, the correct weighting of criteria through hydrogeologist experts, and correct cooperation among the decided-upon factors. Pair-wise comparison and a normalized principal eigenvector (NPEV) were established as controlling factors for groundwater occurrence were identified. It was

discovered that rainfall, land use, land cover, slope, and geology are the more influential parameters, with percentages of weight accounting for 37.95%, 21.83%, 13.5%, and 9.48%, respectively. Other characteristics that are regarded as less important features include drainage density, soil, geomorphology, and lineament density; their respective percentage weights are 6.51%, 4.7%, 3.32%, and 2.72 percent, respectively, which are considered less influential parameters for groundwater potential occurrence in the study area.

Table 4-12 Weight of parameters or normalized principal vectors.

Matrix		RF	LULC	Slope	Geology	Drainge density	Soil	Geomorphology	Lineament density	0	0	normalized principal Eigenvector
		1	2	3	4	5	6	7	8	9	10	
RF	1	1	3	5	5	7	7	7	5	-	-	37.95%
LULC	2	1/3	1	3	3	4	5	6	7	-	-	21.83%
Slope	3	1/5	1/3	1	3	3	4	3	5	-	-	13.50%
Geology	4	1/5	1/3	1/3	1	3	3	3	4	-	-	9.48%
Drainge density	5	1/7	1/4	1/3	1/3	1	3	3	3	-	-	6.51%
Soil	6	1/7	1/5	1/4	1/3	1/3	1	3	3	-	-	4.70%
Geomorphology	7	1/7	1/6	1/3	1/3	1/3	1/3	1	2	-	-	3.32%
Lineament density	8	1/5	1/7	1/5	1/4	1/3	1/3	1/2	1	-	-	2.72%

In computing the consistency ratio, the principal eigenvalue (max) of 8.792 was calculated for the eight*eight matrix with AHP. Hence, the principal eigenvalue (max) needs to constantly be greater than or identical to the number of criteria. As stated in the above, the end result of max can lead to the calculation of the consistency index (CI), hence pairwise comparison is reliable due to the fact that the principal eigenvalue (max = 8.792) is greater than the number of criteria investigated (n = 8), and the consistency index (CI) value calculated was 0.081. The random index (RI) for the nine criteria is 1.41. RI relies on the range of the criteria being compared, as shown below in Table 4-13 (Saaty, 1980).

Table 4-13. Ratio index for various n factors.

N	3	4	5	6	7	8	9	10
RI	0.58	0.89	1.12	1.24	1.32	1.41	1.45	1.49

The Consistency Ratio (CR) computed is 0.081, which is much less than 0.1 for large matrices more than 4 × 4 (Saaty, 1995) and, therefore, the CR gained is suitable and the weight or percentage influence assigned for all thematic layer is acceptable.

4.3.2. Groundwater Potential Occurrence Area Map.

The groundwater potential study layer was generated from superimposed thematic layers applying the weighted overlay approach with the help of spatial analysis tools in Arc GIS. In the weighted overlay analysis and groundwater potential layer development, as found in Table 4-12 drainage density is assigned the lowest percentage of influence (weight), while rainfall was assigned the higher weight/percentage influence. As presented on the map, regions of high groundwater potential are concentrated in the central and northern tip of the Wolayta zone because of the presence of high rainfall distribution, water body and agricultural land coverage, alluvial geological formations, sandy loam soil texture, and gentle slope topography, which cover an area of 26.084% (271.9179 Km2). Areas having high groundwater potential are located near the outlet section of the watershed. The spatial distribution of groundwater potential in study area is the sum of the products of factors percentage influence (weight) and the corresponding reclassified parameters rank.

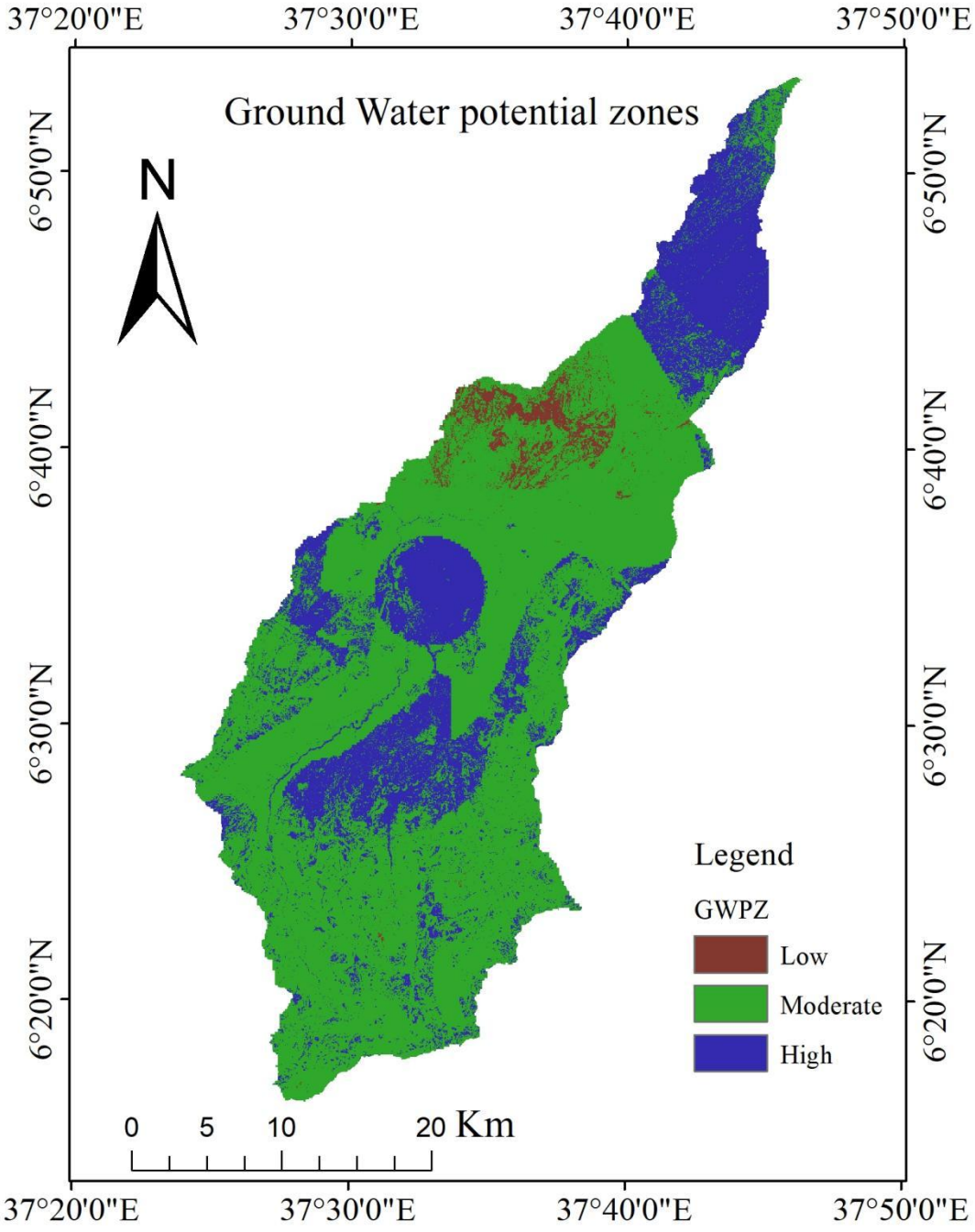

Figure 4-13. Spatial distribution of groundwater potential zones.

Table 4-14 GWPZ Classes.

Groundwater potential Zones in Deme Watershed				
VALUE	GWP prospect rank	Count	Area(km^2)	Area(%)
2	Low	29296	26.3664	2.5292
3	Moderate	826864	744.1776	71.3864
4	High	302131	271.9179	26.084

The remaining part of the study area of 71.386% (744.1776 Km2) is classified as having moderate groundwater potential, in which the distribution is throughout the watershed; however, it is dominant on the southern, south eastern, south western, north eastern, and north western parts of the study location, and 2.529% (26.3664 Km^2) of the watershed is classified as having low groundwater potential due to the distribution of low rainfall, clay texture soil type, and high drainage density. Summit geomorphology, bare land coverage, and low lineament density in the study area.

4.3.3. Groundwater Flow Direction.

The groundwater flow of the study area seems to follow the surface water flow because most of ground water flow vector directions are to wards the outlet section of watershed, and it is dependent on the geomorphology and geological structures. Small intermittent and perennial rivers that feed local aquifers follow those alignment lines, and the groundwater flow also follows such a pattern. The direction of emergency of spring points on the tertiary volcanic and Mesozoic sediments is sometimes structurally controlled, indicating the structural tendency of groundwater flow. Ground water flow direction is concentrated towards the central part of the study area, which is identified as the discharging area, and ground water is flowing outward at the southern tip of the study area. In the study area, groundwater flow direction is from the southern and northern parts to gentle slope areas and hilly areas of the watershed.

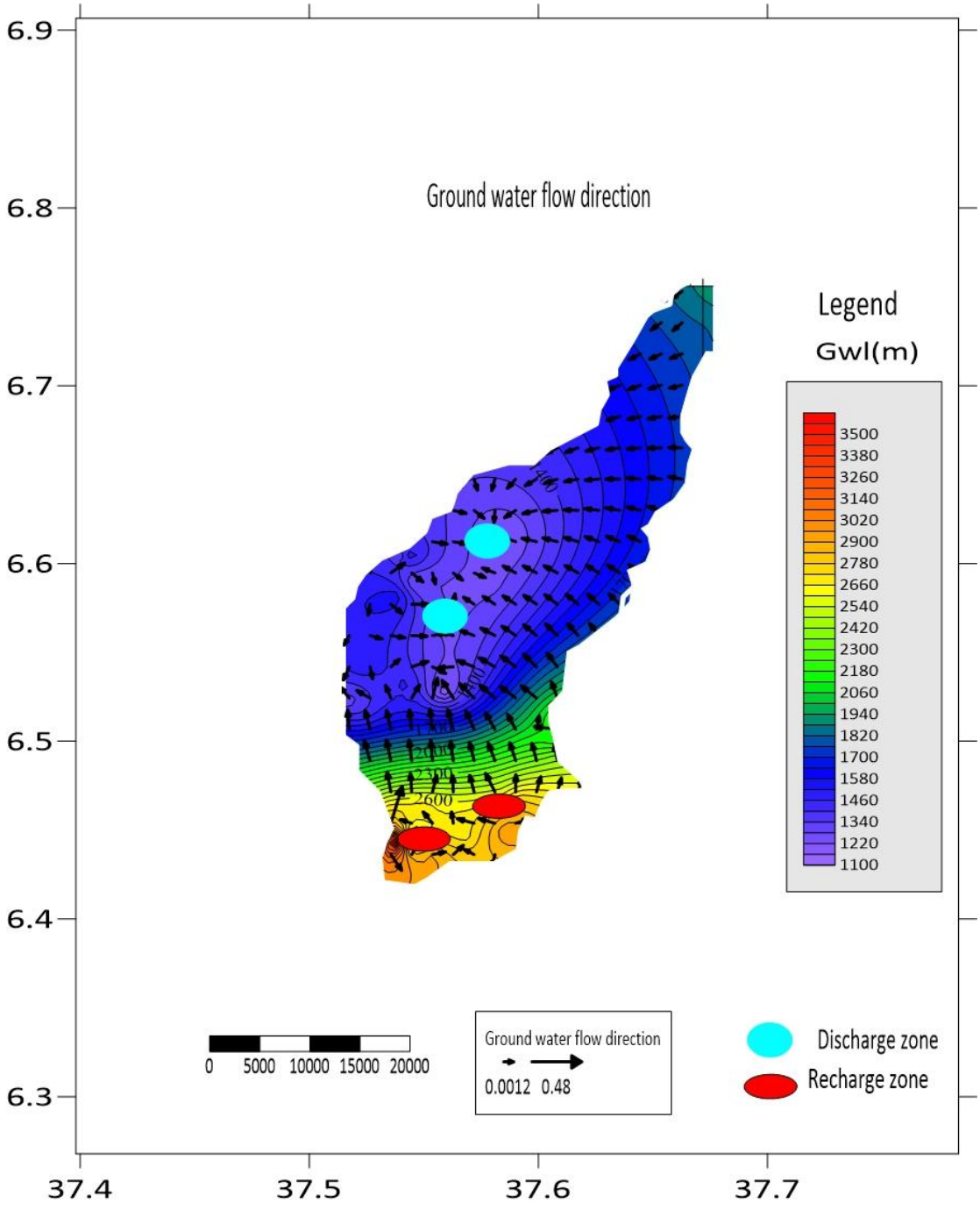

Figure 4-14 Groundwater flow direction.

4.3.4. Sensitivity analysis of Groundwater influencing Factors..

According to the sensitivity analysis (Table 4-15), the Rainfall factor has the largest variation index due to the key role of the rainfall as being an important source of groundwater recharge. Besides its relatively high theoretical weight , Rainfall has high contribution value for GWPZ occurrence in sub classes that occupy most of the watershed area.

Table 4-15. Sensitivity analysis of GWPZ influencing factors.

Thematic layer eliminated	Variation index(Sx)in %
Rainfall	3.73
LULC	1.78
Slope	0.44
Geology	-1.07
DD	-0.89
Soil	-1.2
Geomorphology	-1.34
LD	-1.5

The removal of Rainfall layer influences the GWPZ highly and this is due to that Rainfall area can contribute for the occurrence of ground water potentiality. The impact of LULC on GWPZ assessment can be attributed to the fact that the agricultural land is favorable for recharge, and since it occupies around 73.77% of the total basin area. The removal of the Slope layer also influences the GWPZ as gentle slope land surface trap precipitation and allow rainwater to percolate/infiltrate via the soil and is considered a good groundwater potential zone, while a steep slope vicinity areas creates excessive runoff, permitting much less lag time for rainfall and therefore relatively much less infiltration and poor groundwater potential occurrence. According to sensitivity analysis table Rainfall, LULC, Slope and Geology are the most groundwater occurrence controlling factors.

4.3.5. Groundwater potential zone Validation.

At last, groundwater zones produced are compared against borehole yield data to check the validity of the result.The groundwater potential map is an expectation for the existence of groundwater potential. Therefore, to provide an accurate expectation, the accuracy was estimated based on the agreement and disagreement between

expected potential and actual yield data through overlay. The result of GWPZ in the GIS overlay was classified into three classes, such as low, moderate and high potential zones, based on the hydrogeological map of Ethiopia, which states that optimum yields in liters per second with very low potential (0.05 l/s), low potential (0.05–0.5 l/s), moderate potential (0.5–2 l/s), high potential (2–25 l/s), and very high potential (>25 l/s).

Table 4-16. Verification of identified groundwater potential zones with actual yield.

Expected GWPZ	High	moderate	Low	Total
Total number of actual yeild in each zone	10	17	8	35
Number of agreements with expected GWPZ	4	8	4	16
Number of disagreements with expected GWPZ	6	9	4	19
Prediction accurracy(%)	66.67	88.9	100	84.44

In general, the result indicated high yield (2 to 25 l/s) in the high potential areas, very low yield (0.05 l/s) in the low potential areas, and intermediate values occurred in the zones between these extremes of water points, with yields of (0.5 to 2 l/s) occurring in the moderate GWPZ according to the Ethiopian hydrogeological map (Bereket, 2011; Tesfaye, 2010). As shown in Fig. 4–17, most of the suitable groundwater areas are found in the central, southern, northern, and eastern parts of the study area.

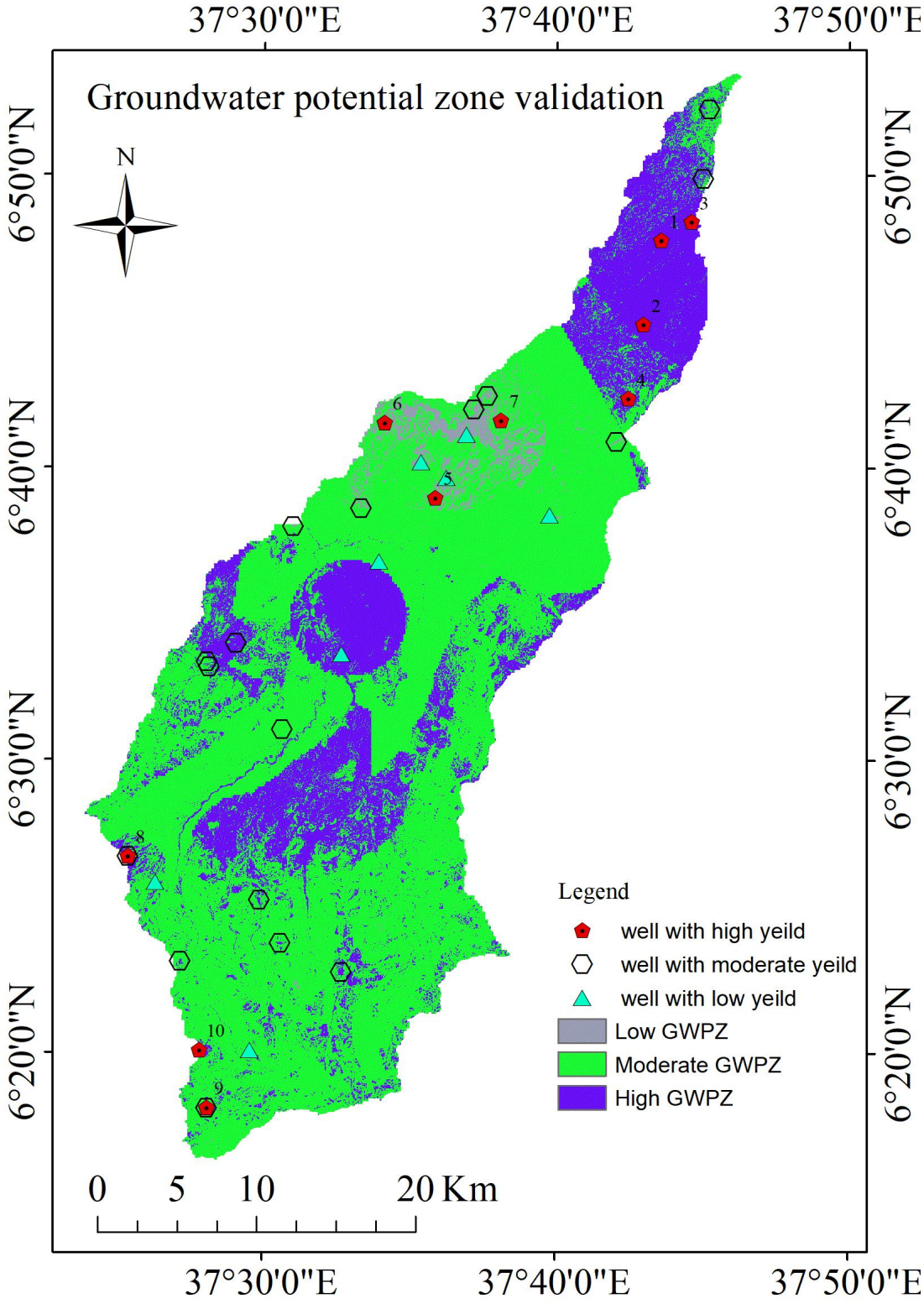

Figure 4-15 Validation of GWPZ in Deme Watershed.

As shown on the figure, the validation analysis revealed that there is good agreement between groundwater point data and groundwater potential zones delineated on the study area.

5. SUMMARY AND CONCLUSION.

SUMMARY.

The study aimed to map the groundwater potential zone in a water-stressed area of Deme River watershed, sub basin of middle Omo-Gibe basin, Ethiopia, using various data sources such as climate, stream flow, and spatial thematic layers including land use maps, soil maps, drainage density maps, geology maps, slope maps, lineament density maps, and geomorphology maps. The Soil and Water Assessment Tool model was utilized to estimate the recharge amount and its spatio-temporal fluctuation in the watershed. Surfer tool model was applied to determine ground water flow direction with ground water well inventory data. The study used several modeling techniques, sensitivity analysis, calibration, and validation to accurately reproduce the stream flow pattern and various hydrograph responses. The study estimated the mean annual recharge rate to be 214.5 mm/y, with the northern top section of the watershed experiencing the highest recharge rate. Analytical Hierarchical Process was used to rank various layers based on a pair-wise comparison matrix. GIS-based Multi-Criteria Decision Analysis was used to map the groundwater potential zones, which identified three zones: low, moderate and high. Around 71.4% of the region has moderate groundwater potential, and 26.084% has a high potential. The groundwater well inventory data for 35wells dispersed around the region were used to validate the Groundwater Potential Zone map, and the validation results confirmed that 84.4% of the study Groundwater Potential Zone matched with groundwater well points in the Deme watershed. The study's results can help in planning, management, and sustainable utilization of the groundwater resources in this water-stressed area.

CONCLUSION.

The study provided preliminary assessment of the groundwater resources in the Deme watershed in a more cost- and time-effective way compared with traditional techniques. The present study demonstrated that GIS, SWAT, remote sensing, and AHP approaches were applied for demarcating GWPZs in the Deme Watershed. The focus of this study was groundwater potential assessment using the SWAT model and GIS-based MCDA in a data-scarce area. The SWAT model was calibrated and validated using SWAT-CUP, and the agreement between the observed and simulated stream flow was measured using NSE, PBIAS, and R^2 values. As the results show, the SWAT model calibration and validation are reasonably acceptable. The estimated recharge shows noticeable spatio temporal variation. Around 46.6% of the area receives a yearly average recharge varying from 217.03 to 239.55 mm of annual coverage. The rainfall, geology, geomorphology, LULC, soil, and DEM-derived major water flow-controlling topographic attributes were analyzed using GIS-based MCDA to map the GWPZ in a data-scarce region. The result is categorized as low, moderate and high GWPZs. The high GWPZ covers 26.08% of the study area, about 71.38% of the area has moderate potential, and 2.53% covers low potential areas. The assessment result was cross-validated with pumping well and spring data in the watershed; the result shows that most of the GWPZ matches water well control points. Important results of the study were produced in an acceptable way using SWAT and GIS-based MCDA. The result provides valuable insight into the groundwater potential in the study area for policymakers and the community toward efficient groundwater resource management practices.

RECOMENDATION

- Information on the delineation of the groundwater potential zone will be useful for effective identification of the suitable locations for extraction of groundwater and planners, engineers, and decision-makers can use it as a guideline for further research.

- The groundwater potential zone maps along with other thematic maps should be used as reconnaissance survey and decision support, and can serve as resource information database which can be updated from time to time by adding new information for efficient and effective decision making, planning, and management.

- SWAT model input data were created using meteorological data with a large number of missing values that were filled with normal ratio method and linear arthematic method, so that the model result can be modified with improved hydrometeorological data analysis and soil, dem and land use land cover input data.

- The groundwater potential map provides first-hand information to investigate groundwater exploration studies and serves as a baseline information input.

- To gain additional insights on the methodology followed and to validate outcomes, geophysical investigations at the potential well drilling sites are recommended and further hydrogeological study should be carried out to know the distribution of groundwater potential quantitatively.

- Inventory data indicates that water supply in the study area is highly dependent on groundwater sources, so a groundwater modeling study and is recommended to determine the sustainable exploitation of this resource. In general, a proper well inventory with all the necessary data is needed to have good water planning and management, which makes tasks easy for further study.

REFERENCES

Abbaspour KC., Yang J., Maximov I., Siber R., Bogner K., Mieleitner J., Zobrist J.,Srinivasan R. (2007). Modelling hydrology and water quality in the pre alpine thur watershed using SWAT. Journal of Hydrology, 413-430.

Abebe., D. (2021). Groundwater potential mapping using geospatial techniques: a case study of Dhungeta-Ramis sub-basin, Ethiopia. Geology, Ecology, and Landscapes, 65-80.

Adimalla N., Taloor A.K. (2020). Hydro geochemical investigation of groundwater quality in the hard rock terrain of South India using Geographic Information System (GIS) and groundwater quality index (GWQI) techniques. Journal of Groundwater for Sustainable Development, 100-288.

Aggarwal M., Saravanan S., JenniferJ., Abijith D. (2019). Delineation of groundwater potential zones for hard rock region in Karnataka using AHP and GIS. Advances in Remote Sensing and Geo Informatics Applications,Springer., 315–317.

Ahmad I, Dar M., Teka A., Teshome M., Andualem T., Teshome A. (2020). GIS and fuzzy logic techniques-based demarcation of groundwater potential zones: A case study from Jemma River basin, Ethiopia. Journal of African Earth Sciences., 103-160.

Al-Abadi A.M., Al-Shamma A. (2014). Groundwater potential mapping of the major aquifer in Northeastern Missan Governorate, South of Iraq by using AHP and GIS. J. Environ. Earth Sci, 125–149.

Aldjazouli M.O., Elmorabiti K., Rahimi A., Amellah O., Fadil O.A.M. (2020). Delineating of groundwater potential zones based on remote sensing, GIS and analytical hierarchical process: a case of Waddai,eastern Chad. GeoJournal, 20., 121–148.

Allafta H., Opp C., Patra S. (2021). Identification of Groundwater Potential Zones Using Remote Sensing and GIS Techniques: A Case Study of the Shatt Al-Arab Basin. Remote Sens.13,, 112.

AlSaud., M. (2018). Mapping potential areas for groundwater storage in Wadi Aurnah Basin,western Arabian Peninsula, using remote sensing and geographic information system techniques. Hydrogeology Journal., 18(6): 1481–1495.

Andualem T.G., D. G. (2019). Groundwater potential assessment using GIS and remote sensing: a case study of Gunatana landscape, upper Blue Nile Basin. Ethiopia Hydrol Reg. Stud., 24, 100-131.

Anuraga T.S., Ruiz L., Mohan Kumar M.S., Sekhar M., Leijnse A. (2006). Estimating groundwater recharge using land use and soil data: A case study in south india. Agric. Water Manege., 84, 65–76.

Arabameri A., Rezaei K., Cerda A., Lombardo L., Rodrigo-Comino J. . (2019.). GIS-based groundwater potential mapping in Shahroud plain, Iran.A comparison among statistical (bivariate and multivariate), data mining and MCDM approaches. Sci.Total Environ., 34, 658.

Arkoprovo B., Adarsa J., Prakash S. (2012.). Delineation of groundwater potential using satellite remote sensing and geographic information system techniques.a case study from ganjam district, Orissa, India. Remote Sens., 46, 160–177. https://doi.org/10.1016/j. scitotenv.2018.12.115.

Arnold JG., Moriasi DN., Gassman PW., Abbaspour KC., White MJ., Srinivasan R.,Santhi C., Harmel RD., Van Griensven A., Van Liew MW., Kannan N., Jha MK. (2012). SWAT Model use, calibration, and validation. Transactions of the ASABE, 55(4):1491-1508. DOI: 10.13031/2013.42256.

Arnold JG., Srinivasan R., Muttiah RS., Williams JR. (1998). Large area hydrologic modeling and assessment part I, Model development. Journal of the American Water Resources Association., 34(1),73-89.

Arora. (2000). Irrigation water power and water resource engineering. Delhi, India: fourth edition,A.K.Jain.

Arulbalaji P., Padmalal D., Sreelash K. (2019). GIS and AHP techniques-based delineation of groundwater potential zones: a case study from the southern Western Ghats, India. Sci Rep, 9(1):2082.

Arunbose, S..Srinivas., Y.Rajkumar., S. Nair., N. C & Kaliraj S. (2021). Remote sensing, GIS and AHP techniques based investigation of groundwater potential zones in the Karumeniyar river basin, Tamil Nadu, southern India. Groundwater of Sustainable Development., 14,586.

Atmaja., Rilo R., Putra., Doni P., Setijadji., Lucas Donny. (2019). Delineation of groundwater potential zones using remote sensing, GIS, and AHP techniques in southern region of Banjarnegara, Central Java, Indonesi. Remote Sens., 19(4), 729-740.

Awan UK., Ismaeel A. (2014). A new technique to map groundwater recharge in irrigated areas using a SWAT model under changing climate. Journal of Hydrology., (519),1368-1382. DOI: 10.1016/ j.jhydrol.2014.08.049.

Ayano H., K.S. Kasiviswanthan, Deepak K. (2021). A spatial-temporal assessment of groundwater development in response to soil erosion. A Case Study of Omo River basin. Ground water for sustainable management.18,, 1081.

Bahiru., E. A., & Woldai T. (2016). Integrated geological mapping approach and gold mineralization in Buhweju area, Uganda. Ore Geology Reviews., 72,777–793.

Barthel R., and Banzhaf S. (2016). Groundwater and surface water interaction at the regional-scale, A review with focus on regional integrated models. Water Resources Management., 30(1), pp.1-32. https://doi.org/10.1007/s11269-015-1163-z.

Bashe, B. (2017). Groundwater potential mapping using Remote Sensing and GIS in rift valley lakes basin, Weito Sub Basin, Ethiopia. International Journal of Scientific & Engineering Research., 8(2),43- 50.

Batelaan O & De Smedt F. (2001). WetSpass: A flexible, GIS based, distributed recharge methodology for regional groundwater modelling. IAHS-AISH Publication., (269), 11–18.

Batelaan., O & De Smedt F. (2001). WetSpass: A flexible, GIS based, distributed recharge methodology for regional groundwater modelling. IAHS-AISH Publication,, (269), 11–18.

Berehanu B., Ayenew T., Azagegn T. (2017). Challenges of groundwater flow model calibration using MODFLOW in Ethiopia, With particular emphasis to the Upper Awash River Basin. Journal of Geoscience and Environment Protection., 5(3):50-66. DOI: 10.4236/gep.2017.53005.

Bisson R., and Lehr J. (2014). Model in Modern Groundwater Exploration ,Case Studies in Sudan. Water Resource management, 1-32.

Bobba A.G., Bukata R.P., Jerome J.H. (1992). Digitally processed satellite data as a tool in detecting potential groundwater flow systems. J.Hydrol, (4),25–62.

Calow RC., MacDonald AM., Nicol AL., Robins NS. (2010). Ground water security and drought in Africa. Ground Water, 48(2),246-256.

Chernet., T. (1993). Hydrogeology of Ethiopia and water resources development. Addis Ababa: Ethiopian institute of geological surveys.

Chowdhury J., Jhan M.K., Chowdary V.M., Mal, B.C. (2010). Integrated Remote Sensing and GIS Based Approach for Assessing Groundwater Potential in West Mendinipur district, West Bengal. Int.J.Remote Sens., 30,231–250.

Das B., Pal S.C. (2019). Assessment of groundwater recharge and its potential zone identification in groundwater stressed Goghat-I block of Hugli District, West Bengal, India. Int. J. Remote Sens., 35, 315–340.

Das N., Mukhopadhyay S. (2018). Application of multi-criteria decision-making. Geosciencefrontiers 4(1), 145– 164.

Das S., G. A. (2017). Exploring groundwater potential zones using MIF technique in semi-arid region: a case study of Hingoli district, Maharashtra. Groundwaterfor Sustainable Dev't, 31, 49–64 DOI: 10.1007/s41324-017-0144-0.

Das., S. (2019). Comparison among influencing factor, frequency ratio, and analytical hierarchy approach process techniques for groundwater potential zonation in Vaitarna basin, Maharashtra, India. Groundwaterfor Sustainable Dev.8, 617–629.

Doke A., Pardeshi S.D., Pardeshi S.S., and Das S. (2018). Identification of morphogenetic regions and respective geomorphic processes: a GIS approach. Arabian J. Geosci., 11,1–13.

Drobne S., Lisec A. (2009). Multi-attribute decision analysis in GIS: Weighted linear combination and ordered weighted averaging. Informatica (Ljubljana), 33(4),459-474.

Eilers A., Miller J., Watson A., Sigidi N. (2017). Groundwater Recharge Quantification from Historical Rainfall Records and Salinity Profiling in the RAMSAR Listed Verlorenvlei Catchment, South Africa. Procedia Earth and Planetary Science, 17, 586–589. https://doi.org/10.1016/j.proeps.2016.12.150.

Elewa H.H., Qaddah A. A., El-Feel A. A. (2012). Determining potential sites for runoff water harvesting using remote sensing and geographic information systems-based modeling in Sinai. American Journal of Environmental Sciences, 8(1), 42–55.

Elmahdy S.I., Mohamed M.M. (2015). Probabilistic frequency ratio model for groundwater potential mapping in Al Jaww plain, Arab. JGeosci (8), 2405–2416. https://doi.org/10.1007/s12517-014-1327-9.

Elmahdy S.I., Mohamed M.M. (2016). Mapping of tecto-lineaments and investigate their association with earthquakes in Egypt: A hybrid approach using remote sensing data. Geomatics,Natural Hazards and Risk., 7(2), 600–619.

Eshtawi T., Evers M., Tischbein B. (2016). Quantifying the impact of urban area expansion on groundwater recharge and surface runoff in barbary, India. Hydrological Sciences Journal 61(5), 826-843. DOI: 10.1080/ 02626667.2014.1000916.

Ettazarini., S. (2007). “Groundwater potentiality index: a strategically conceived tool for water research in fractured aquifers,karsamae, India. Environmental Geology., 52, 477-487.

Falah F., Ghorbani Nejad S., Rahmati O., Daneshfar M., Zeinivand H. (2021). Applicability of generalized additive model in groundwater potential

modelling and comparison its performance by bivariate statistical methods, Turkey. Geosci.

FAO. (2006). World reference base for soil resources: a framework for international. Rome: Agriculture Organization of the United Nations.

FAO/IIASA/ISRIC/ISSCAS/JRC. (2012). Harmonized World Soil Database (version 1.2). Austria: FAO.

Foster., S. (1998.). Groundwater assessing vulnerability and promoting protection of a threatened resource. Proceedings of the eighth Stockholm water (pp. pp79–90). Sweden: Geocarto Int.

Githui F., Selle B., Thayalakumaran T. (2012). Recharge estimation using remotely sensed evapo transpiration in an irrigated catchment in southeast Australia. Hydrological Processes 26(9), 1379-1389. DOI: 10.1002/hyp.8274.

Gogu R., Dassargues A. (2000). Sensitivity analysis for the EPIK method of vulnerability assessment in a small karstic aquifer, southern Belgium. Hydrogeol.J, 8,337–345.

Gogu R.C., Carabin G., Hallet V., Peters V., and Dassargues A. (2001). GIS based hydrogeologicaldatabases and groundwater modeling. Hydrogeol J, 9:555–569.

Goodchild., M. (1993). The state of GIS for environmental problem solving. New York: Oxford University Press.

Gossel W., Ebraheem A.M., Wycisk P. (2004). A very large-scale GIS based groundwater flow model for the Nubian sandstone aquifer in Eastern Sahara. Hydrogeol J, 12(6): 698–713.

Greenbaum., D. (1985). Review of remote sensing applications to groundwater exploration in basement and regolith in British. Nottingham, UK: British geological survey.

Gupta M., Srivastava P. K. (2010). Integrating GIS and remote sensing for identification of groundwater potential zones in the hilly terrain of Pavagarh, Gujarat, India. Water International, 35(2): 233–245.

Guzman J.A., Moriasi D.N., Gowda P.H., Steiner J.L., Starks P.J, Arnold J.G, R. Srinivasan. (2015). A model integration framework for linking SWAT and MODFLOW. Environmental Modelling, 73, 103-116.

Hamdani N., Baali A. (2020). Characterization of groundwater potential zones using analytic hierarchy process and integrated geomatic techniques in Central Middl Atlas. Appl.Geomat, 4, 23–45.

Han L., Liu Z., Ning Y., Zhao Z. (2018). Extraction and analysis of geological lineaments combining a DEM and remote sensing images from the northern Baoji loess area. Advances in Space Research, 62(9), 2480–2493.

Hasanuzzaman M., Song X., Han D., Zhang Y., Hussain S. (2017). Prediction of groundwater dynamics for sustainable water resource management in bogra district,northwest bangladesh. Water(Switzerland), 9(4).

Hussein A.A., Govindu V., Nigusse A.G.M. (2017). Evaluation of groundwater potential using geospatial techniques. Appl. Water Sci., 7 (5): 2447–2461.

Jasmin I., Mallikarjuna P. (2011). Satellite-based remote sensing and geographic information systems and their application in the assessment of groundwater potential, with particular reference to India. Hydrogeology Journal., 19(4): 729-740.

Jha M. K., Chowdhury A., Chowdary V. M., Peiffffer S. (2012). Groundwater management and development by integrated remote sensing and geographic information system. Water Resources Management, 21(2): 427–467.

Jin G., Shimizu Y., Onodera S., Saito M., Matsumori K. (2015). Evaluation of drought impact on groundwater recharge rate using SWAT and Hydrus models on an agricultural island in western Japan. Proceedings of the International Association of Hydrological Sciences, 371:143- 148 DOI: 10.5194/piahs-371-143-2015.

Julla K., Dereje A., Motuma S., Megersa K. (2022). Groundwater Potential Assessment Using GIS and Remote Sensing Techniques: Case Study of West Arsi Zone, Ethiopia. Water.Tech, (14), 1838-1858. https://doi.org/10.3390/w14121838.

Kaliraj S., Chandrasekar N., Magesh N. (2014). Identification of potential groundwater recharge zones in Vaigai upper basin, Tamil Nadu, using GIS-based analytical hierarchical process (AHP) technique. Arab. J. Geosci. 7, 1385–1401.

Kebede., S. (2013). Groundwater in Ethiopia. Features, numbers and opportunities. Springer Hydrogeology, 16, 245-267 doi:10.1007/978-3-642-30391-3.

Kotchoni D.O.V., Vouillamoz J., Lawson F.M.A. (2019). Relationship between rainfall and groundwater recharge in seasonal humid Benin: A comparative analysis of long-term hydrographs in sedimentary and crystalline aquifers. Hydrogeol.J, 27, 447–457.

Krishna R., Kishan D., Sarup J. (2015). Lineament extraction and lineament density assessment of Omkareshwar, M P, India, using GIS Techniques. International Journal of Engineering and Management Research., 5(3), 717–720.

Krishnamurthy J., Srinivas G. (1995). Role of geological and geomorphological factors in ground water exploration: A study using IRS LISS data. Int. J Remote Sense, 16, 2595–2618.

Kumar C., P. (2020). Understanding SWAT-MODFLOW, An Integrated Modelling System for Surface Water and Groundwater Processes. Roorkee, India.: National Institute of Hydrology,247-667.

Kumar P., Herath S., Avtar R., Takeuchi K. (2016). Mapping of groundwater potential zones in Killinochi area, Sri Lanka, using GIS and remote sensing techniques. Water Resour. Manag, 2, 419–430.

Kumar V., Mondal N,, Ahmed S. (2020). Identifification of Groundwater Potential Zones Using RS, GIS and AHP Techniques: A Case Study in a Part of Deccan Volcanic Province (DVP) Maharashtra, India. Indian Soc. Remote Sens., (48) 497–511.

Kuriqi A., Ali R., Pham Q.B., Gambini J.M., Gupta V., Malik A., Linh N.T.T., Joshi Y., Anh D.T., Nam V.T., Dong X. (2020). Seasonality shift and stream flow variability trends in central India. International Journal of Engineering, 48, 487–521 DOI:10.1007/s11600-020-00475-4.

Kuriqi A., Pinheiro A.N., Sordo-Ward A., Garrote L. (2020). Ground water potential mapping with GIS and Remote Sensing. Energy Convers, 223, 113267.

Lee S., Hyun Y., Lee M. J. (2019). Groundwater potential mapping using data mining models of big data analysis in Goyang-si, South Korea. Sustainable Water Res., 11(6):1678 https://doi.org/10.3390/su11061678.

Libasse., S. (2007). Application of Remote Sensing and GIS for Groundwater Potential zone Mapping in Northen Ada, Mojo Cachment. Addis Ababa: GeoSci.

Liu W., Bailey R.T., Andersen H.E., Jeppesen E., Nielsen A., Peng K., MolinaNavarro E., Park S., Thodsen H., Trolle D. (2020). Quantifying the effects of climate change on hydrological regime and stream biota in a groundwater dominated catchment: amodelling approach combining SWAT–MODFLOW with flow-biota empirical models. Sci.Total Environ, 745, 1–13.

Liu W., Bailey R.T., Andersen H.E., Jeppesen E., Park S., Thodsen H., Nielsen A., Molina-Navarro E., Trolle D. (2020). Assessing the impacts of groundwater abstractions on flow regime and stream biota: Combining SWAT–MODFLOW with flow-biota empirical models. Sci. Total Environ, 706, 1–11.

Liu W., Park S., Bailey R.T., Molina-Navarro E., Andersen H.E., Thodsen H. (2020). Quantifying the stream flow response to groundwater abstractions for irrigation or drinking water at catchment scale using SWAT and SWAT–MODFLOW. Environ. Sci. Eur, 32 (1), 1–25.

Loague K., Corwin D.L. (1998). Regional-scale assessment of non-point source groundwater contamination. Hydrol Process ., 12(6):957–966.

Machiwal D., Madan K., Jha M., Bimal C., Mal B. (2011). Assessment of groundwater potential in a semi-arid region of India using remote sensing, GIS and MCDM techniques. Water Resour. Manag., (25): 1359–1386.

Magesh N, Chandrasekar N, and Soundranayagam, J . (2014). Delineation of groundwater potential zones in Theni district, Tamil Nadu, using remote sensing, GIS and MIF techniques. Geosci. Front , 14(4): 45-56.

Magesh N. S., Chandrasekar N., Soundranayagam J. P. (2012). Delineation of groundwater potential zones in Theni district, Tamil Nadu, using remote sensing, GIS and MIF techniques. Geoscience Frontiers, 3(2):189–196.

Magesh N., Chandrasekar N., Soundranayagam J. (2014). Delineation of groundwater potential zones in Theni district, Tamil Nadu, using remote sensing, GIS and MIF techniques. Geosci. Front, 14(4);43-54.

Mageshkumar P., Subbaiyan A., Lakshmanan E., Thirumoorthy P. (2019). Application of geospatial techniques in delineating groundwater potential zones: a case study from South India Arab. Geosci, 12(5): 151.

Maity D.K., Mandal S. (2019). Identification of groundwater potential zones of the Kumari river basin, India: an RS & GIS based semi-quantitative approach. Environ.Sustain Dev, 21, 1013–1034 https://doi.org/10.1007/s10668-017-0072-0.

Malczewski., J. (2006). GIS-based multicriteria decision analysis: A survey of the literature. Int. J. Geogr. Inf. Sci., 20: 703–726.

Mallick J., Khan R., Ahmed M., Alqadhi S., Alsubih M., Falqi I., Abul Hasan M. (2019). Modeling Groundwater Potential Zone in a Semi-Arid Region of Aser Using Fuzzy-AHP and Geoinformation Techniques. Water Techno, 11, 2656.

Masetti M., Poli S., Sterlacchini S. (2007). The use of the weights-of evidence modeling technique to estimate the vulnerability of groundwater to nitrate contamination. Nat Resource, 16,109– 119. https://doi.org/10.1007/s11053-007-9045-6.

Mehra M., Oinam B., Singh C. (2016). Integrated Assessment of Groundwater for Agricultural Use in Mewat District of Haryana, India Using Geographical Information System (GIS). Geoscience Frontiers, 3(2),189–196 DOI:10.1007/s12524-015-0541-6.

Meijerink A.M.J., Schultz G.A., Engman E.T. (2000). Remote sensing in hydrology and water management. Springer, pp 305–325.

Melloul A.J., Collin M.L. (2001). A hierarchy of groundwater management, land-use,and social needs integrated for sustainable resource development. Environ.Sci Dev. Sustain, 3: 45–59 https://doi.org/10.1023/A:1011420206575.

Moriasi DN., Arnold JG., Van Liew MW., Bingner RL., Harmel RD., Veith TL. (2007). Model evaluation guidelines for systematic quantification of accuracy in watershed simulations. Transactions of the ASABE, 50(3):885-900.

Mukherje A., Fryar A. E. (2008). Deeper groundwater chemistry and geochemical modeling of the arsenic affected western Bengal basin, West Bengal, India. Applied Geochemistry, 23(4), 863- 894.

Muluken., E. (2021). Impact of land use land cover change on stream flow,The case of Deme river,Middle Omo Gibe Sub-basin, Ethiopia.

Murthy K., Mamo A. (2009). Multi-criteria decision evaluation in groundwater zones identification in Moyale-Teltele subbasin, South Ethiopia. International Journal of Remote Sensing, 30(11), 2729- 2740 https://doi.org/10.1080/01431160802468255.

Naghibi S., Pourghasemi H., Pourtaghi Z., Rezaei A. (2015). Groundwater potential mapping using frequency ratio and Shannon's entropy models in the Moghan watershed, Iran. Earth Sci. Inf, 8, 171–186.

Nampak H., Pradhan B., Manap M. A. (2014). Application of GIS based data driven evidential belief function model to predict groundwater potential zonation. Journal of Hydrology, 513, 283–300.

Nasir M., Khan S., Zahid H., Khan A. (2018). Delineation of groundwater potential zones using GIS and multi influence factor (MIF) techniques: A study of district Swat, Khyber Pakhtunkhwa, Pakistan. Environ. Earth Sci., 77, 367.

Nata T., Bheemalingeswara K., Abdulaziz M. (2010). Hydrogeological Investigation and Groundwater Potential Assessment in Haromaya Watershed Eastern Ethiopia.

Olutoyin A., Fashae MN., Tijani AO., Talabi OI. (2014). Delineation of groundwater potential zones in the crystalline basement terrain of SW-Nigeria: an integrated GIS and remote sensing approach. Appl Water Sci, 4,19–38 doi:10.1007/s13201-013-0127-9.

Pande C.B., Moharir K.N., Singh S.K., Varade A.M. (2019). An integrated approach to delineate the groundwater potential zones in Devdari watershed area of Akola district, Maharashtra, Central India. Environ.Dev.Sustainability, 22, 4867–4887 https://doi.org/10.1007/s10668-019-00409-1.

Parameswari K., Padmini T.K. (2018). Assessment of groundwater potential in Tirukalukundram block Of Southern Chennai Metropolitan Area. Environ.Dev. Sustain., 20(9), 45-64.

Patil S.G., Mohite N.M. (2014). Identification of groundwater recharge potential zones for a watershed using remote sensing and GIS. International Journal of Geomatics and Geosciences, 4(3), 485-498.

Podvezko., V. (2009). Application of AHP technique. Journal of Business Economics and Management, 10(2):181-189 DOI: 10.3846/1611- 1699.2009.10.181-189.

Prosper a,b,c., Ebenezer E., Abdul G ., Bernard N ., Vincent K ., Benjamin W. (2022). Spatial assessment of groundwater potential using Quantum GIS and multi-criteria decision analysis (QGIS-AHP) in the Sawala Tuna Kalba district of Ghana. Environ. Dev. Sustain., 16(7), 23-41.

Putthividhya A., Laonamsai J. (2017,May 21-25). SWAT and MODFLOW modeling of spatio-temporal runoff and groundwater recharge distribution. Proceedings of world environmental and water resources congress, (pp. 51-65). Sacramento, CA, USA DOI: 10.1061/ 9780784480618.006.

Rahaman S., Ajeez S., Aruchamy S., Jegankumar R. (2015). Prioritization of Sub Watershed Based on Morphometric Characteristics Using Fuzzy. Analytical Hierarchy Process and Geographical Information System. A Study of Kallar Watershed, Tamil Nadu. Aquat. Procedi, 4, 1322–1330.

Rajaveni S. P., Brindha K., Elango, L. (2015). Geological and geomorphological controls on groundwater occurrence in a hard rock region. Appl Water Sci, 7(3):1377–1389.

Ramu M. B., Vinay M. (2014). Identification of ground water potential zones using GIS and Remote Sensing Techniques : A case study of Mysore taluk Karnataka Karnataka. International Journal of Geomatics and Geosciences, 5(3), 393–403.

RMurasingh., S. (2014). Analysis of Groundwater Potential Zones Using Electrical esistivity: Remote Sensing and GIS Techniques in a Typical Mine Area of Odisha; National Institute of Technology: Rourkela, India.

Roy S., Hazra S., Chanda A., Das S. (2020). Assessment of groundwater potential zones using multi criteria decision-making technique: a micro-level case study from red and lateritic zone (RLZ) of West Bengal, India. Sustain .Water Resource Manag, 6,445 https://doi.org/10. 1007/s40899-020- 00373-z.

Rukundo E., Dogan A. (2019). Dominant influencing factors of groundwater recharge spatial patterns in Ergene river catchment, Turkey. WaterTech, 11, 653.

Rushton, K. R. (1991). Groundwater support of stream flows in the Cambridge area, UK. 202, 367–376 .

Saaty, T. (1980). Group decision making and the AHP in Berlin/Heidelberg, Germany. Springer, 56, 467-485.

Saaty., T. (1980). The Analytic Hierarchy Process. New York, NY, USA: McGraw-Hill International 12th ed Book.

Saaty., T. (2014). Decision Making for Leaders: The Analytic Hierarchy Process for Decisions in a Complex World. Pittsburgh, PA, USA: RWS Publications.

Saghebian S M., Sattari M T., Mirabbasi R., Pal M. (2014). Groundwater quality classification by decision tree method in Ardebil region, Iran Arab. J.Geosci, (7), 4767–4777. https://doi.org/10.1007/s12517-013-1042-y.

Salwa., F. (2015). An overview of integrated remote sensing and GIS for groundwater mapping in Egypt. Shams Engineering Journal, 6(1), 1-15.

Saraf A., Choudhury P. (1998). Integrated remote sensing and GIS for groundwater exploration and identification of artificial recharge sites. Int. J. Remote Sens, 19, 1825–1841.

Saranya T., Saravanan S. (2020). Groundwater potential zone mapping using analytical hierarchy process (AHP) and GIS for Kancheepuram District, Tamilnadu, India. Model Earth Syst Environ, 6,1–18 https://doi.org/10.1007/s40808-020-00744-7.

Sashikkumar M., Selvam S., Kalyanasundaram V., Johnny J. (2017). GIS based groundwater-modeling study to assess the effect of artificial recharge: A case study from Kodaganar river basin, Dindigul district, Tamil Nadu. J. Geol, (89),57–64.

Sashikkumar S., Selvam S., Kalyanasundaram V., Johnny J. (2017). GIS based groundwater-modeling study to assess the effect of artificial recharge: A case study from Kodaganar river basin, Dindigul district, Tamil Nadu. J. Geol.Soc, (89), 57–64.

Schillaci C., Braun A., Kropacek J. (2015). Terrain Analysis and Landform Recognition with Geomorphological Techniques. London: British Society for Geomorphology.

Selvam S., Magesh N., Chidambaram S., Rajamanickam M., Sashikkumar M. (2015). GIS based identification of ground water recharge potential zones using RS and IF technique: A case study in Ottapidaram taluk, Tuticorin district, Tamil Nadu. Environ. Senanayake, (7), 85-96.

Semere., S. (2003). Remote sensing and GIS: applications for groundwater potential assessment in Eritrea. (Doctoral dissertation, Byggvetenskap).

Sener, E., Davraz, A., & Ozcelik, M. (2005). An integration of GIS and remote sensing in groundwater investigations: A case study in Burdur, Turkey. Hydrogeology Journal, 13 (5–6), 826–834.

Singh LK., Jha MK., Chowdary VM. (2018). Assessing the accuracy of GIS-based multi-criteria decision analysis approaches for mapping groundwater potential. EcologicalIndicators, 91,24-37. DOI:10.1016/j.ecolind.2018.03.070.

Singh Sk C.K., Mukherjee, S. (2010). Impact of land use and land cover change on groundwater quality in the lower Shiwalik hills: A remote sensing and GIS based approach. Cent. Eur. J. Geosci. , (2), 124–131.

Singh, A. K., & Prakash, S. R. (2002). An integrated approach of remote sensing geophysics and GIS to evaluation of groundwater potentiality of Ojhala subwatershed, Mirzapur district, India. Conference on GIS, GPS, Aerial Photography and Remote Sensing. Asia: Proceedings of the First Asian.

Sophocleous, M., S.P. Parkins. (2000). Methodology and application of combined watershed and ground-water models in Kansas . J. Hydrol. , 236(3–4), 185–201.

Souissi, D., Msaddek, M., Zouhri, L., Chenini, I., El May, M., Dlala., M. . (2018). Mapping groundwater recharge potential zones in arid region using GIS and Landsat approaches, southeast Tunisia. Hydrol. Sci. J. , 63:251–268.

Soumen., D. (2014). Delineation of ground water prospect zones using remote sensing,GIS techniques a case study of Baghmundi development block of Puruliya district, West Benga. Int Geol Earth Environ Sci, 4(2),62–72 http://www.cibtech.org/ jgee.htm.

Stafford, K.W., Rosales-Lagarde, L., Boston, P.J. (2008). Castile evaporite karst potential map of the Gypsum Plain, Eddy County, New Mexico and Culberson County, Texas. GIS methodological comparison. J Cave Karst , 70(1),35–46.

Stumpp, C., Żurek, A.J., Wachniew, .P, Gargini, A., Gemitzi, A., Filipini, M., Witczak, S. (2016). A decision tree tool supporting the assessment of groundwater vulnerability. Environ Earth Sci., (75),1057 https://doi. org/10.1007/s12665-016-5859-z.

Tahmassebipoor, N., Rahmati, O., Noormohamadi, F., Lee, S. (2016). Spatial analysis of groundwater potential using weights of evidence and evidential belief function models and remote sensing. Arab J Geosci., 9,79 https://doi.org/10.1007/s12517-015-2166-z.

Tamiru., P. O. (2014). Impact of Land Use/ Land Cover Change on Catchment Hydrology (A case Study of Awassa Catchment). Masters of Science. Arba Minch University, Ethiopia. .

Teklebirhan, A., Dessie, N., & Tesfamichael, G. . (2012). Groundwater Recharge Evapotranspiration and Surface Runoff Estimation Using WetSpass Modeling Method in Illala Catchment, Northern Ethiopia. Ethiopian Journal of Science, 4(2), 96 https://doi.org/10.4314/mejs.v4i2.80119.

Tesfaye., T. (2015). Ground Water Potential Evaluation Based on Integrated GIS and Remote Sensing Techniques in Bilate River Catchment, South Rift Valley of Ethiopia. American Scientific Research journal For Engineering.

Todd DK., Mays LW. . (200). Groundwater hydrology. Wiley,New york.

Tolche., A. D. (2021). Groundwater potential mapping using geospatial techniques case study of Dhungeta-Ramis sub basin, Ethiopia. Geology, Ecology, and Landscapes. , 45, 65-80.

Tsakiris., G. (2004). Water resources management trends, prospects and limitations. Proceedings of the EWRA symposium on water resources management : risks and challenges for the 21st century,2–4 September 2004 (pp. pp 1–6). Izmir.

Vaux., H. (2011). Groundwater under stress and the importance of management. Environmental Earth Sciences, 62(1), 19–23.

Wan ., N. (2019). Estimation of rainfall and stream flow missing data for Terengganu,Malaysia by using interpolation technique methods. Malaysia: School of Mathematical Sciences, Faculty of Science and Technology, University Kebangsaan.

Wang, J., Huo, A., Zhang, X. (2020). Prediction of the response of groundwater recharge to climate changes in Heihe river basin, China. Environ.Earth Sci, 79, 1–16.

Watkins, B., LU, Y.C., Hart, G., Daughtry, C. (1997). The current state of precision farming . Food Rev Inte , 13(2), 141–162.

Yeh, H. F., Cheng, Y. S., Lin, H. I., & Lee, C. H. (2016). Mapping groundwater recharge potential zone using a GIS approach in Hualian River, Taiwan. Sustainable Environment Research , 26(1), 33–43.

Yousefi, H., Haghizadeh, A., Yarahmadi, Y., Hasanpour, P., Noormohamadi, P. (2018). Groundwater pollution potential evaluation in Khorramabad-Lorestan Plain, western Iran . J. Afr. Earth. Sci. , 647–656.

Yusof, N., Ramli, M. F., Pirasteh, S., & Shafri, H. Z. M. . (2011). Landslides and lineament mapping along the Simpang Pulai to Kg Raja highway, Malaysia . International Journal of Remote Sensing, 32(14), 4089–4105.

Zandi, J., Ghazvinei, P.T., Hashim, R., Yusof, K.B.W., Ariffin, J., Motamedi, S. (2016). Mapping of regional potential groundwater springs using logistic regression statistical method Water Resource . GeoSci., 43, 48– 57 https://doi.org/10.1134/S0097807816010097.

Zomlot, Z., Verbeiren, B., Huysmans, M., Batelaan. . (2015). Spatial distribution of groundwater recharge and base flow: Assessment of controlling factors. J.Hydrol. , 4,349–368.

Kumar C, P. (2020). Understanding SWAT-MODFLOW, An Integrated Modelling System for Surface Water and Groundwater Processes. Roorkee, India.: National Institute of Hydrology,247-667.

APPENDICES.

APPENDIX-A.

Appendix Table-1 Mean annual Rainfall data for each station.

Year	Gesuba	Danna 2	Dinke	Wolayta
1989	1311.97	1408.79	1198.75	1532.34
1990	1167.98	1153.45	1148.89	1076.87
1991	1100.67	1072.75	1035.46	1243.45
1992	1278.46	1043.78	1403,56	1056.34
1993	1356.78	1376.89	1384.36	1794.23
1994	1397.74	1226.89	978.67	1628.56
1995	1176.87	926.56	1213.45	1325.67
1996	1362.98	1725.58	1218.19	1220.50
1997	1336.67	1345.67	1485.78	1456.89
1998	1287.75	1645.08	1411.57	1065.12
1999	1160.22	1167.83	1035.76	1480.40
2000	1456.34	1213.67	1056.73	1712.45
2001	802.28	1382.70	1319.84	1436.20
2002	698.23	1103.35	1354.47	1619.79
2003	1188.70	1086.98	1269.74	1326.40
2004	917.73	1004.64	1268.26	1283.00
2005	880.58	1745.75	1331.07	1045.70
2006	1378.01	1860.29	1275.70	1583.42

2007	1142.52	1840.31	1317.55	1362.20
2008	1216.92	1687.95	1287.11	938.20
2009	1031.05	1018.73	1386.13	1343.89
2010	1033.96	2060.02	1228.71	1458.30
2011	1665.30	1238.20	1164.35	1551.32
2012	1010.49	1134.30	1040.13	1080.20
2013	1486.62	1612.28	1196.01	1204.25
2014	1384.60	1741.17	1565.21	1443.50
2015	808.25	1375.98	838.95	1316.90
2016	962.14	780.79	1379.02	1112.70
2017	1417.36	1344.01	1184.93	1072.20
2018	1567.91	1751.72	1602.37	1275.90
2019	1188.599611	1606.245959	1303.35	1599.1
2020	1723.469586	2770.169421	1658.1	1888.6

Appendix Table-2 Mean monthly stream flow data for Orata alem station(in m3/sec).

Year	jan	feb	mar	apr	may	jun	jul	aug	sep	oct	nov	dec
1989	0.721	0.069	6.17	7.123	6.1016	18.6077	10.1423	17.7829	18.8547	2.9116	3.5893	3.4613
1990	0.923	1.423	4.321	10.567	4.875	4.983	5.1074	4.943	3.456	3.123	0.678	1.8819
1991	1.56	2.545	4.13	1.954	4.213	5.13	5.7439	4.0039	6.952	2.852	0.1777	0.1277
1992	0.1765	0.1455	0.765	6.3363	7.679	7.854	9.456	9.753	10.876	9.7474	4.0107	2.9139
1993	3.546	5.245	2.3881	5.3313	11.345	9.2397	8.564	6.653	2.8063	4.543	0.8993	0.2861
1994	0.1739	0	0.535	3.123	6.345	3.456	6.253	17.875	8.456	4.354	6.543	2.136
1995	0.735	0.672	1.234	2.543	3.4445	6.943	7.4303	9.543	9.745	2.9381	1.1813	0.3
1996	0.721	0.069	6.17	7.123	6.1016	18.6077	10.1423	17.7829	18.8547	2.9116	3.5893	3.4613
1997	1.245	0.534	1.231	0.457	2.7839	3.5937	6.0845	5.1187	3.0157	6.234	12.123	4.232
1998	3.664	2.935	2.8368	9.454	5.768	10.12	7.756	5.0706	3.8477	8.123	3.875	1.8681
1999	2.564	1.585	2.2948	2.239	2.1955	3.7127	6.975	11.234	4.8003	5.023	2.244	1.6487
2000	2.567	1.2072	4.245	1.254	4.0658	4.0433	9.135	10.132	7.145	6.667	2.6513	1.3065
2001	0.3785	0.8389	2.456	2.6323	10.321	11.756	7.324	8.254	4.8797	6.543	3.875	1.4342
2002	0.3404	6.985	1.86	1.865	3.952	4.564	4.6245	6.456	3.754	0.9397	5.875	1.3924
2003	0.6332	1.9913	1.132	1.543	7.123	10.23	8.9223	6.345	1.875	0.565	1.875	1.135
2004	0.923	1.423	4.321	10.567	4.875	4.983	5.1074	4.943	3.456	3.123	0.678	1.8819
2005	2.1014	3.689	9.5787	16.2516	8.235	12.1148	8.8774	9.234	6.134	3.231	1.0161	0.8129
2006	0.8807	8.512	10.9875	4.4619	7.678	12.875	14.24	6.8103	7.6887	4.8853	3.8571	3.8571

Appendix Table-3.Groundwater well inventory data.

Id	longitude	latitude	elevation(m)	Gwl(m)	Water source type	Q(l/s)
1	359460	756647	1867	1820	HDW	31.5
2	361868	755320	1877	1826	spring	1.6
3	362263	759693	2057	1930	spring	0.8
4	327081	716489	1518	1503	Borehole	33
5	334997	720252	1302	1277	spring	3.2
6	335320	720642	1308	1275	spring	1.12
7	341437	731200	1262	1207	spring	0.023
8	339092	725377	1285	1267	spring	0.045
9	340167	730065	1266	1240	HDW	26
10	339358	727318	1277	1272	HDW	9.8
11	339602	729130	1295	1255	HDW	28.3
12	339577	726000	1264	1240	HDW	13.7
13	332455	726084	1285	1260	HDW	1.89
14	330612	724893	1553	1533	spring	0.9
15	330733	724604	1565	1540	spring	1.35
16	330942	724161	1567	1530	Borehole	35
17	332081	729159	1519	1500	Borehole	30
18	331035	729236	1398	1370	HDW	25.6
19	327357	711012	1473	1423	spring	0.47
20	325611	712647	1347	1300	spring	1.75
21	335315	713666	1218	1175	spring	4.56
22	332038	714729	1512	1470	Borehole	37
23	332144	713138	1481	1440	Borehole	34

24	332768	712807	1490	1453	Borehole	31
25	329038	713566	1475	1430	spring	3.33
26	333284	700425	2739	2728	spring	0.2
27	330552	696785	3635	3624	HDW	1.78
28	330097	700423	2747	2730	spring	0.8
29	328844	697298	2775	2765	spring	1.3
30	331969	695699	2837	2825	HDW	5.7
31	332161	697488	2612	2600	HDW	7.23
32	332137	697600	2498	2485	HDW	26.8
33	334312	695623	2920	2910	spring	0.6
34	336902	700575	2659	2646	spring	0.9
35	337440	697320	2700	2688	spring	1.4
36	341575	697979	2971	2956	spring	1.6
37	342526	690294	2685	2674	spring	1.9
38	341208	702376	2586	2570	spring	2.6
39	342930	701527	2791	2788	spring	3.4
40	349634	689510	2829	2819	spring	0.4
41	343338	701486	2782	2770	spring	0.5
42	346465	706633	2379	2358	spring	0.67
43	346934	708489	2092	2072	Borehole	6
44	348595	708313	2356	2340	spring	1.67
45	346971	710564	2303	2288	spring	0.35
46	348219	710225	2240	2220	spring	0.4

Appendix Figure-1. Calibration statics summary

Iter37extension18 - Summary_Stat.txt

This file has the statistics comparing observed data with the simulation band through p-factor and r-factor and the best simulation of the current iteration by using R2, NS, bR2, MSE, and SSQR.

```
Goal_type= R2    No_sims= 500    Best_sim_no= 318    Best_goal = 8.073788e-001

Variable          p-factor  r-factor  R2    NS    bR2     MSE      SSQR      PBIAS  KGE   RSR   MNS   VOL_FR  ---  Mean_sim(Mean_obs)   StdDev_sim(StdD
FLOW_OUT_1        0.56      0.51      0.81  0.78  0.7074  3.4e+000 6.3e-001  -12.3  0.84  0.47  0.53  0.89          5.52(4.91)           3.79(3.88)


---- Results for behavioral parameters ---
Behavioral threshold= 0.500000
Number of behavioral simulations = 500

Variable          p-factor  r-factor  R2    NS    bR2     MSE      SSQR      PBIAS  KGE   RSR   MNS   VOL_FR  ---  Mean_sim(Mean_obs)   StdDev_sim(StdD
FLOW_OUT_1        0.56      0.51      0.81  0.78  0.7074  3.4e+000 6.3e-001  -12.3  0.84  0.47  0.00  0.89          5.52(4.91)           3.79(3.88)
```

Appendix Figure-2.Calibration hydrograph from SWAT CUP

Iter37extension18 - 95ppu plot

The 95ppu of all variables. Also shown are observations and best simulation of the current iteration.

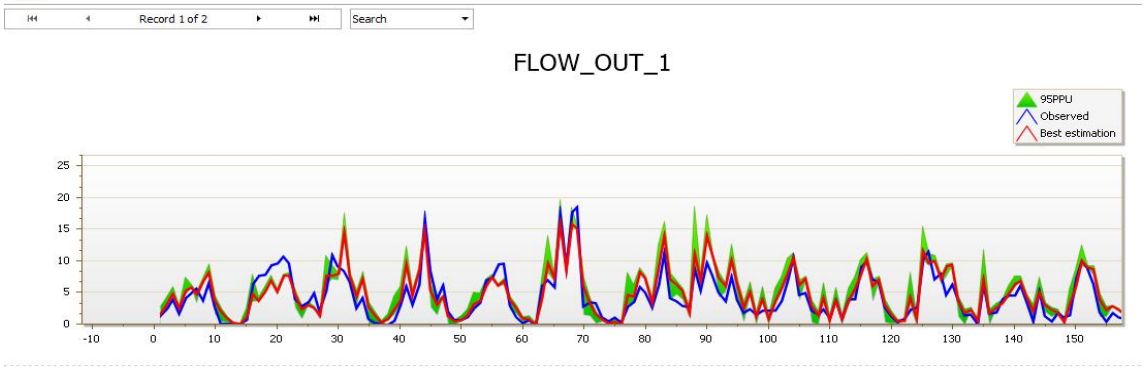

Appendix Figure-3. Validation statics summary.

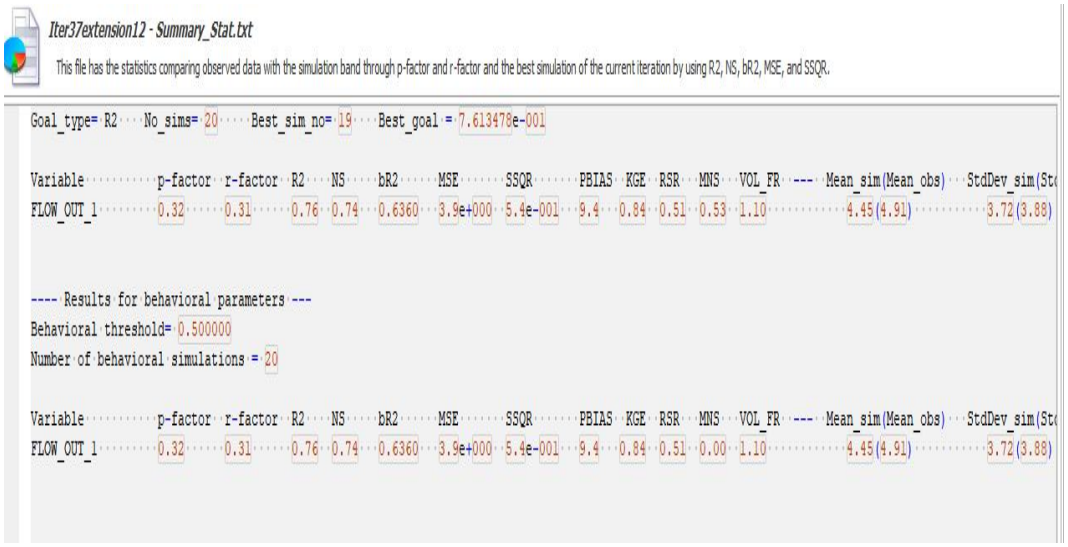

Iter37extension12 - Summary_Stat.txt

This file has the statistics comparing observed data with the simulation band through p-factor and r-factor and the best simulation of the current iteration by using R2, NS, bR2, MSE, and SSQR.

Goal_type= R2 No_sims= 20 Best_sim_no= 19 Best_goal = 7.613478e-001

Variable	p-factor	r-factor	R2	NS	bR2	MSE	SSQR	PBIAS	KGE	RSR	MNS	VOL_FR	---	Mean_sim(Mean_obs)	StdDev_sim(St
FLOW_OUT_1	0.32	0.31	0.76	0.74	0.6360	3.9e+000	5.4e-001	9.4	0.84	0.51	0.53	1.10		4.45(4.91)	3.72(3.88)

---- Results for behavioral parameters ---

Behavioral threshold= 0.500000

Number of behavioral simulations = 20

Variable	p-factor	r-factor	R2	NS	bR2	MSE	SSQR	PBIAS	KGE	RSR	MNS	VOL_FR	---	Mean_sim(Mean_obs)	StdDev_sim(St
FLOW_OUT_1	0.32	0.31	0.76	0.74	0.6360	3.9e+000	5.4e-001	9.4	0.84	0.51	0.00	1.10		4.45(4.91)	3.72(3.88)

Appendix Figure-4.Validation hydrograph from SWAT CUP